CARBON MONOXIDE GENERATION IN A COMPARTMENT WITH A DOORWAY DURING A FIRE

By

Christopher McKay

Thesis submitted to the Faculty of the
Virginia Polytechnic Institute and State University
in partial fulfillment of the requirements for the degree of

MASTER OF SCIENCE
In
Mechanical Engineering

Graduate Committee:

Dr. Uri Vandsburger (Chairman)
Virginia Polytechnic Institute and State University

Dr. Kozo Saito
University of Kentucky

Dr. Brian Lattimer
Hughes Associates

Defended: February 4, 2002 in Blacksburg, Virginia

Keywords:

Carbon Monoxide, Building Fire, Heat Flux, Doorway Flow

CARBON MONOXIDE GENERATION IN A COMPARTMENT WITH A DOORWAY DURING A FIRE

By

Christopher McKay

Abstract

The study of the products of combustion continues to have real-world relevance since the primary cause of death in building fires is smoke inhalation, with the majority of deaths from carbon monoxide, CO, poisoning. An experimental study was conducted to examine upper-layer structure plus provide an initial characterization of a new compartment with a doorway. An additional study of the relationship between heat flux from external burning in a hallway and levels of carbon monoxide is also reported.

Tests were conducted in a new ½scale ISO compartment with a fully scaled doorway, using n-hexane pool fires within the center of the compartment. Upper-layer sampling at eight locations in the compartment has shown that the compartment upper-layer is relatively uniform in species mole fractions, yields, and temperature. Sampling in the front upper-layer of the compartment was performed for a series of experiments where the equivalence ratio was varied. Temperatures, species mole fractions, species yields, and doorway flows were found to have definite trends, which agreed with previous studies.

The heat flux study utilized a reduced scale compartment with a separate inlet and an exit vent, which connected into the side of an attached hallway, forming an L-shape. For two cases of a deep and shallow hallway upper-layer a direct relationship between flames in the upper-layer and total heat flux was measured. High heat flux was found to only denote those areas were flames are present and is not related to the levels of CO present or oxidized in the hallway.

Dedication

This work is dedicated to my mother, Freda Shaffer McKay, whose strength and love throughout her life I will always remember. I know you will always be with me.

Acknowledgements

I would first like to thank Dr. Uri Vandsburger for having faith in an average undergraduate student and taking me on for graduate studies in his lab. His guidance has opened a world of opportunities to me through the knowledge and experience that graduate studies have allowed.

I would also like to thank my fellow graduate students who I have had the honor to work with in the Virginia Tech Building Fire Research Laboratory. I first started working as an undergraduate with Brian Lattimer (no Dr. at that time), who introduced me to the techniques of fire research, which I would use throughout my research. He also graciously agreed to serve on my graduate committee and help guide me through my own graduate work. I would also like to thank Alex Marshakov, my friend, co-worker, and one time roommate with whom I had the chance to work with during his short time spent pursuing his Ph.D. Finally I would like to thank Chris Wieczorek, who I worked the longest with at the Fire Research Laboratory. His dedication and thoroughness helped me complete my experiments and have been an invaluable reference during the writing of my thesis. Also the excellent undergraduate assistants, Jillcha Wakjira and Huang Nguyen ensured the progress of experimentation at the lab.

Much appreciation is due to the other graduate students in the Reacting Flows Laboratory with whom I have worked with over the years. Especially Steve Lepera, Randy Hibshman, Yiqing Yuan, and Ludwig Haber. The help and friendship of my former professors Dr. Bala Ganeshan and Dr. Dennis Jaasma have also meant a great deal to me in my studies at Virginia Tech.

My family deserves a special thanks for all the support and help they have given me throughout college and my life in general. My parents, Doug and Freda McKay, have always inspired me to strive for excellence in both my learning and my personnel life.

Table of Contents

List of Figures

List of Tables

1 Introduction

1.1 Overview

The work described in this document covers two distinct periods. Therefore, the document is separated into two distinct sections. First, the experimental studies verifying compartment instrumentation methods and the upper-layer structure plus the initial characterization of a new compartment with a doorway is presented. The second part reports a study of the relationship between heat transfer from external burning in the hallway and levels of carbon monoxide.

The characterization started with the design and instrumentation of a reduced scale compartment with a doorway, instead of inlet and exit vents as was the case in previous studies of Gottuk et al. (1992), Ewens (1994), and Lattimer (1996). The compartment was designed to be ½scale in its dimensions ($^1/_8$ scale in volume) of a standard ISO 9705 compartment (ISO, 1993). A detailed description of compartment scaling, design, and construction is described in Sections 3.1 and 3.2. Instrumentation techniques from earlier studies at the Virginia Tech Building Fire Research Laboratory were also adapted to this new configuration to measure the flows through the compartment doorway. These techniques and their implementation are described in Section 3.4. This part of the study was divided into two phases. The first was a compartment upper-layer mapping to determine the uniformity of the compartment upper-layer species mole fractions and compare the results to previous published work. Temperature and species were measured at eight locations in the upper-layer. This data was used to determine the species sampling location in the compartment for the next phase of work. In the next phase measurements were made to characterize the species mole fractions in the upper-layer near the doorway, and doorway flows for a series of equivalence ratios.

The heat transfer study used the same compartment/hallway configuration previously reported in the work of Lattimer (1996) and Lattimer et al (1996 a, b), which consisted of a vented compartment attached to the side of a hallway. Experimental conditions were chosen to mirror the conditions studied by Lattimer so that heat transfer data could be

compared to species mole fraction data measured in those studies. Two cases were examined: first the heat transfer in a hallway with a thin upper-layer and second a case with a thick hallway upper-layer. In both cases conditions were used which produced burning external to the compartment in the hallway and were setup identical to those reported in Lattimer's study. The heat transfer was measured and mapped along the ceiling of the hallway, on the sidewall of the hallway opposite the compartment, and along the floor of the hallway. The data is presented as contour maps and compared to mapping performed previously by Lattimer of the species mole fractions for the same conditions.

1.2 Background/Motivation

The goal of the studies performed at the Virginia Tech Building Fire Research Lab has been to provide engineering tools for fire safety professionals and building designers to enable them to predict the transport of CO through various structures. For this purpose non-dimensional correlations were sought. Key parameters which control the evolution of CO in compartment exhaust gases, inside an adjacent hallway were found to be fire exhaust gas momentum, hallway entry inlet geometrical parameters, and hallway upper-layer thickness determined by the hallway exit soffit (Ewens, 1994, Lattimer, 1996).

The study of the products of combustion continues to have real-world relevance since the primary cause of death in building fires is smoke inhalation. According to Hall and Harwood (1995) 76% of deaths in building fires in 1990 were from smoke inhalation. Cases of these deaths and the impact of carbon monoxide inhalation have been documented by Nelson and Tu (1991) and Nelson (1988) for two elderly care facilities.

1.3 Objectives

The main objective of my work was to provide an initial characterization of a scaled compartment with doorway. This characterization included instrumentation design and testing, upper-layer species and temperature mapping, and an upper-layer global equivalence ratio study including flows through the compartment doorway. Results of

this characterization were compared to previous research and will be used to plan further studies at the Virginia Tech Building Fire Research Laboratory.

The objective of the study of heat flux to the surfaces of a hallway attached to a burning compartment was to augment a series of compartment/hallway experiments documented by Lattimer (1996) by examining the relationship between carbon monoxide mole fractions in the hallway and heat flux. These relationships would allow a more thorough understanding of the evolution of CO in burning gases exiting a compartment into a hallway. The attainment of both of these objectives was pursued using the methodologies outlined in Section 3.

2 Previous Work

Two layer fire environments were first investigated utilizing a fume hood mounted above a fire. This work by Beyler (1983), Zukoski (1985, 1991), Toner (1987), and Morehart (1990) simulated a room fire upper-layer in their hoods. They varied the global equivalence ratio (GER) by adjusting the distance between the hood and the fire. If the fire plume extended into the upper-layer in the hood, underventilated (GER >1) room fire conditions could be simulated. The GER decreased as the fire was moved away from the upper-layer. Beyler's upper-layer temperatures were much lower than those reported in compartment studies, for n-hexane temperatures were in the mid 500K range while fires of similar equivalence ratio in compartments had an upper-layer temperature of about 1000K (Gottuk, et al., 1992). Hood experiments also had lower fuel volatilization rates due to less radiant heat transfer from the cooler upper-layer to the fuel surface. A schematic of Beyler's hood experiments is shown in Figure 2.1.

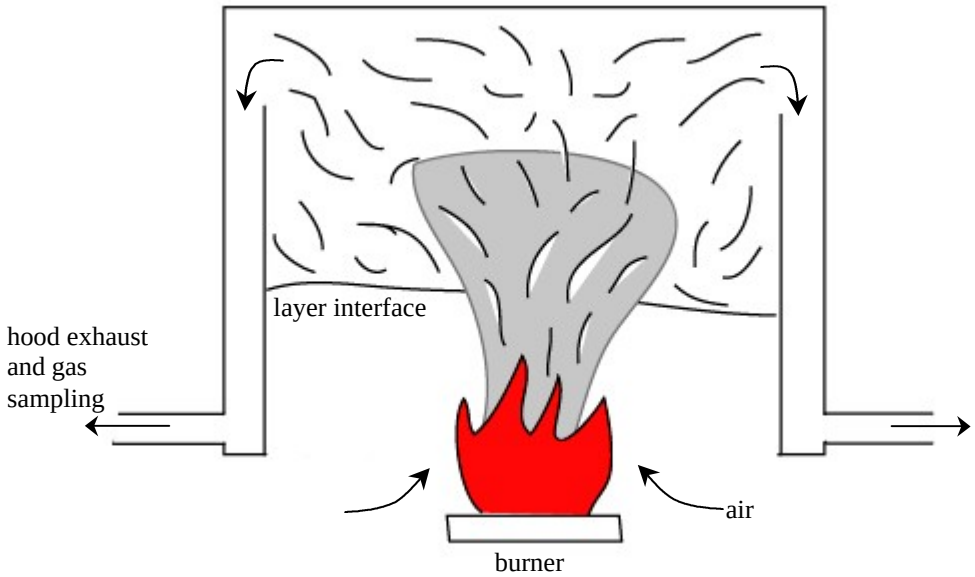

Figure 2.1 Schematic of Beyler's hood experiments

The concepts learned from hood experiments were extended by Gottuk et al. (1992), Bryner et al. (1994), and Lattimer (1996). Gottuk used a compartment setup where air was naturally drawn into the compartment through a plenum below the compartment as

needed, while the combustion gases exited the compartment through a vent. The fire size and airflow into the compartment could be controlled to vary the GER. This work was extended to a more realistic geometry by Bryner, who used a compartment with a doorway for both an air inlet and exit for combustion gases from the upper-layer. Lattimer, utilizing the same compartment as Gottuk, extended his work to examine how the burning combustion gases from the compartment were transported along an attached hallway.

Full scale studies by Chow and Ng (1994-95) examined pre-flashover fires of a compartment with a vent air supply and ceiling exhaust vents. Both natural and forced ventilation situations were examined. Their conclusions examined the effect of ventilation on species mole fractions and heat release rates of their fires. They reported that for pre-flashover fires over-ventilation would lower heat release rates, upper-layer temperatures, and carbon monoxide mole fractions.

Numerous studies have been preformed to examine the toxicity aspects of building fires. Kuhn, et al. (1978) performed studies of smoke toxicity from polyethylene foam fires in full scale room using rats, which examined whether acrolein or carbon monoxide was the fatal component of the smoke. They concluded that carbon monoxide was the dominant factor, with acrolein not playing an important role. Other studies examined the toxicity of gases that have exited the burning room to other parts of a structure. Grand, et al. (1985) examined movement of combustion gases from one room down a hallway to another room (target room) on the same side of the hall. Rats were located in the target room for a series of tests where flashover occurred in the burn room. It was reported that the primary cause of death in the target room was carbon monoxide inhalation by the rats. Morikawa, et al. examined toxic gas movement in a two story structure with a burning room on the first story and mice located in the burn room and stairway, plus rabbits in a separate container to which fire combustion gases were piped from two locations. This study concluded that carbon monoxide is the primary contributor to both incapacitation and death in the subject animals.

3 Experimental Methods

Numerous experimental methods were used to design, instrument, and capture the data required for these studies. These included the development of a scaling procedure used to construct a reduced scale fire compartment to simulate a full-scale facility. Data collection and reduction routines were also developed to capture the experimental data.

3.1 Design - Scaling Procedure for Compartment

The goal was to design a new compartment to simulate more closely hospice, office, and hotel type fires. Emphasis was put on replacing the specially designed test apparatus previously used at Virginia Tech Building Fire Research Laboratory with a new compartment containing prototypical building features. The original test apparatus provided the means for direct measurement of the airflow into the compartment; however, it did not contain realistic building features, which contribute to important fire phenomena such as doorway flows and species production in a burning compartment. The original apparatus was used for the heat flux study reported in Chapter 5 and is described in detail there and in Gottuk et al. (1992), Ewens (1994), and Lattimer (1996). To ensure that similarity, both static and dynamic, was maintained in when scaling the new compartment to ½scale of the ISO 9705 test compartment (ISO, 1993), the design involved two scaling criteria, residence time scaling and ventilation scaling based on Froude number. This scaling allowed the compartment doorway to be specified based on the above criteria.

Listed below are the internal dimensions of the full and half scale compartments:

F.S. = Full Scale (ISO 9705)
Room: 2.4*3.6*2.4 m
Door: 2.0*0.8 m

R.S. = Reduced Scale (1/2 ISO)
Room: 1.15*1.76*1.15 m - (measured)

(Note these room dimensions below are not exactly half of the ISO full scale dimensions, but are the measured final dimensions of the completed compartment. The frame of the new compartment was built to exact half scale dimensions, but when the Fireboard lining and sheet metal skin were added the dimensions were reduced by the thickness of the materials.)

3.1.1 Residence Time Scaling

Since the temperatures in the compartments are high enough to ensure fast chemical kinetics, i.e., $T_{\text{chem}} << T_{\text{res}}$, a characteristic residence time is being used to ensure thermal history similarity. In other words, the residence time for both the full scale and reduced scale compartments was equated. For that purpose the volume of the compartment is divided by the volumetric flow rate of gases, mostly air. Since equality of the thermal environment is desired, the densities are assumed equal.

$$t_{res} = \frac{V}{\dot{V}} \tag{1}$$

and:

$$\dot{V} \propto \frac{A\sqrt{H}}{r} \tag{2}$$

so:

$$\left(\frac{V}{\frac{A\sqrt{H}}{r}} \right)_{F.S.} = \left(\frac{V}{\frac{A\sqrt{H}}{r}} \right)_{R.S.} \tag{3}$$

where:

t_{res} – residence time

$\dot{V}$ - volumetric flow rate

V – volume

r - density (assume $r_{F.S.} = r_{R.S.}$)

A – door area

H – door height

Substitution of numerical values from the compartment dimensions into equation (3) results in one equation for the R.S. door resulted in:

$$A_{R.S.}\sqrt{H_{R.S.}} = 0.254 \quad [\mathrm{m}^{3/2}] \tag{4}$$

3.1.2 Ventilation – Froude Scaling

The definition of the froude number is a nondimensional ratio of inertia forces to gravity forces shown in equation 5. This number was used to scale the ventilation of the doorway and find the height to width ratio for the reduced scale compartment doorway that is scaled to the ventilation characteristics of the full-scale compartment doorway.

$$Fr = \frac{U^2}{gl} \tag{5}$$

where:

$$\dot{m}_{flow} \propto UAr \tag{6}$$

while:

$$\dot{m} \propto A\sqrt{H} \tag{7}$$

therefore:

$$UAr \propto A\sqrt{H} \tag{8}$$

$$U \propto \frac{\sqrt{H}}{r} \tag{9}$$

For length scale (l in equation 5) the width of door, W, can be used:

$$(Fr)_{F.S.} = (Fr)_{R.S.} \tag{10}$$

$$\left(\frac{\sqrt{H}^2}{W}\right)_{F.S.} = \left(\frac{\sqrt{H}^2}{W}\right)_{R.S.} \tag{11}$$

Substitution of values from full scale room dimensions yields:

$$\frac{H_{R.S.}}{W_{R.S.}} = \frac{2}{0.8} = 2.5 \tag{12}$$

$$H_{R.S.} = 2.5 W_{R.S.} \tag{13}$$

$$A_{R.S.} = H_{R.S.} W_{R.S.} = \frac{H_{R.S.}^2}{2.5} \tag{14}$$

Equations (4) and (14) can be combined to obtain:

$H_{R.S.}$ = 0.83 [m]
$W_{R.S.}$ = 0.33 [m]

The standard (full scale) and scaled room dimensions are shown in Table 3.1 with a dimensioned diagram of the compartment shown in Figure 3.1.

Table 3.1 Full and reduced scale room dimensions

	Full Scale Room	Reduced Scale Room
Door Area	1.6 [m^2]	0.28 [m^2]
Door Height	2.0 [m]	0.83 [m]
Interior Surface Area	44.48 [m^2]	10.47 [m^2]
Interior Lining	Gypsum board	3M Firemaster® board
Wall Conduction Coefficient	0.17 [W/m°K]	0.143 [W/m°K]
Wall Material Thickness	0.016 [m]	0.0254 [m]

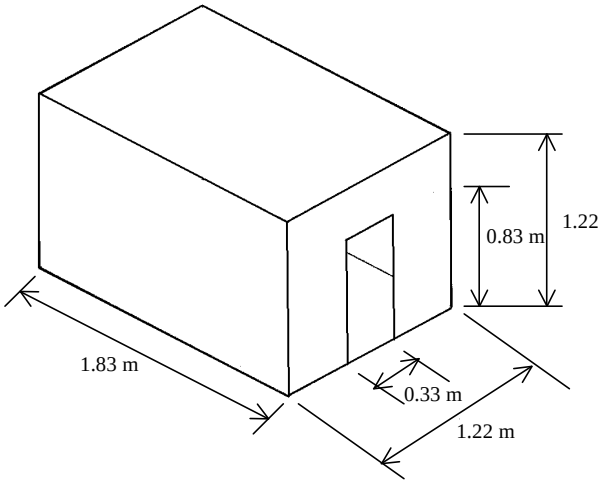

Figure 3.1 Dimensioned drawing of burning compartment

These scaling laws have not been fully explored, especially when comparing data to difference geometric configurations. No attempt was made to prove scaling similarity to the ISO 9705 compartment, but further study of these issues should be pursued. Suggestions for starting similarity comparisons are contained in Section 6.2.

3.2 Construction

The compartment frame was constructed from 3.81 cm x 3.81 cm x 0.3175 cm thick angle iron stock, and was lined on the interior with 0.16 cm thick steel sheet metal which was attached to the frame using machine screws. The compartment was originally designed to rest on a concrete slab at the Virginia Tech Fire Research Lab, so no floor was added to the compartment. The edges of the sheet metal were sealed internally using high temperature fireplace sealant to prevent the escape of gases from the compartment. The compartment was installed in place with the door located under the fume hood and the floor perimeter was sealed to the concrete using a profiled rubber seal. The walls, ceiling and floor of the compartment were lined with 2.54 cm thick sheets of 3M Firemaster® fireboard, which is a common ceramic heat barrier product. This lining was attached using bolts and washers as needed for support. The holes required in the "skin" of the compartment for these bolts were each sealed using the high temperature fireplace

sealant. Removable fireboard front walls form the door entrance to the compartment; therefore, the width of the door could be varied if needed.

With the aid of fireboard blocks, the compartment floor was sloped from the walls to location of the load cell at the compartment center. An A&D load cell (15 kg maximum) measured the weight of fuel in the fuel pan. A load cell is a very precise weight scale, which can be read by a computer data collection system. The gaps in this arrangement were sealed using Fiberfrax® high temperature paper. The load cell and fuel pan configuration can be seen schematically in Figure 3.2 and 3.3. A photograph of the compartment can be seen in Figure 3.4. The load cell was calibrated before each fire to ensure accurate mass measurements of the fuel contained in the fuel pan.

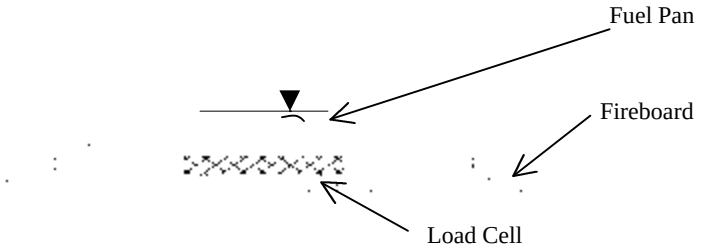

Figure 3.2 Load cell configuration

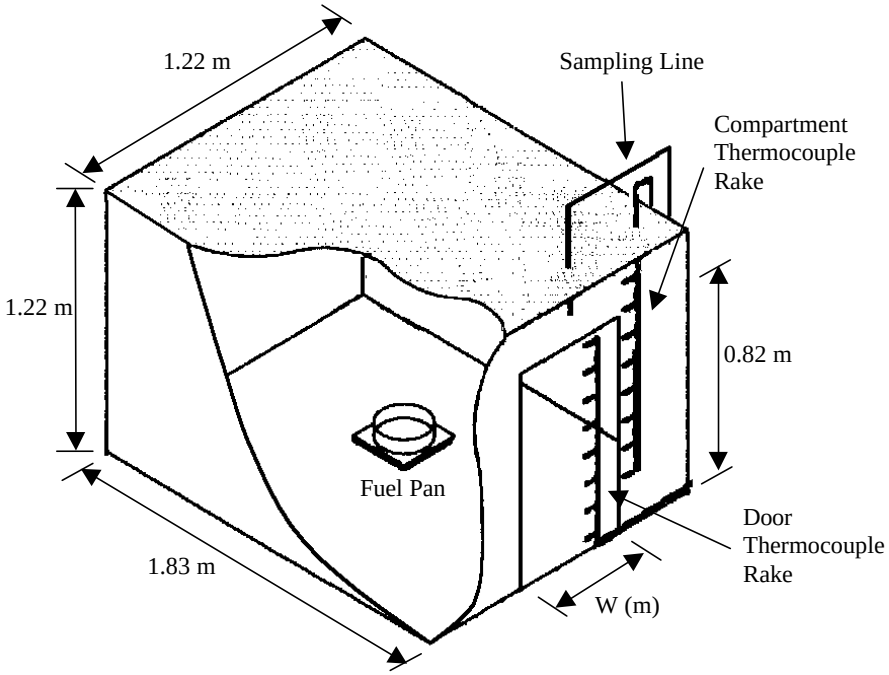

Figure 3.3 New compartment (dimensioned) with instrumentation

Figure 3.4 Assembled compartment with instrumentation

The derivative of the load cell data with respect to time was used to determine the fuel volatilization rate. After a series of initial tests, variations in load cell performance on the

order of 100 grams were noticed and a thermocouple was mounted to the load cell frame to determine if there was a significant temperature change inside the load cell during a fire. These variations were manifested in load cell readings that dropped below the calibrated zero level at the end of the tests. It was determined that the temperature increased enough in the load cell to affect its performance and thus the location of the load cell had to be changed. The entire compartment was raised off the lab floor by 20 cm and supported on concrete blocks at each of the compartment corners so the load cell could be mounted in the ambient air under the compartment. Angle iron supports 5.08 cm x 5.08 cm x 0.3175 cm thick were then installed in the floor of the compartment and a 0.3175 cm thick piece of sheet steel was installed as a floor for the compartment. This was sealed on all sides and the ceramic fireboard was re-installed over it. A 2.54 cm hole was then drilled into the center of the compartment floor and the load cell was placed underneath the compartment with the shaft penetrating through the floor. A schematic of the new compartment and load cell positioning is shown in Figure 3.5. A photograph of the new arrangement is shown in Figure 3.6. To keep the airflow into the compartment as before a false floor was added in front of the compartment, which can also be seen in Figure 3.6.

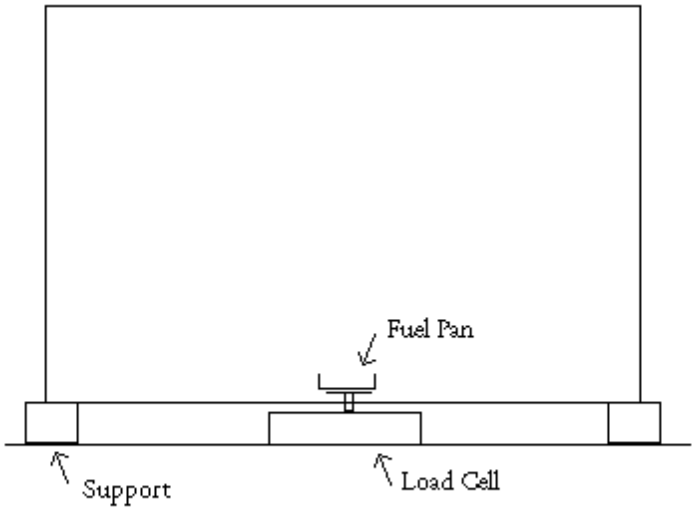

Figure 3.5 Revised compartment and load cell configuration (side view)

Figure 3.6 Photograph of revised compartment configuration

3.3 Exhaust System

The compartment door was positioned directly under the center of a 1.5 m by 1.5 m fume hood, which collects the combustion products. This hood can be seen at the top of Figure 3.6. These products then travel through a 0.46 m diameter duct and are exhausted to the atmosphere through a 142 m^3/min (5000 cfm) blower. A diagram of this system is shown in Figure 3.7*.

* Figures 3.7, 3.10, 3.11 are from Lattimer (1996), who also used the same equipment in the same facility

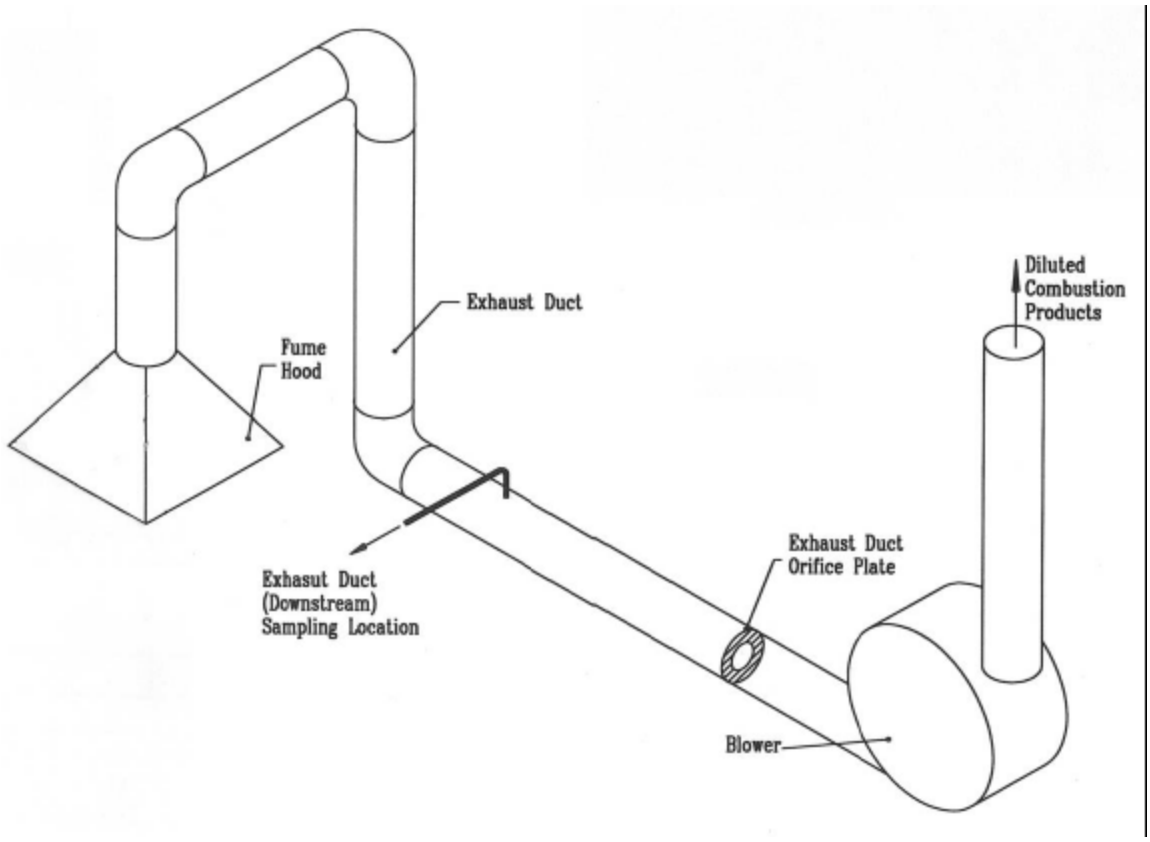

Figure 3.7 Hood exhaust system for fire research facility

3.4 Instrumentation

Instrumentation at the Virginia Tech Building Fire Research Laboratory was extensive to measure the various facets of a compartment fire. This instrumentation included thermocouples, gas sampling and analysis equipment, a load cell to measure fuel mass loss, and a computerized data collection system to monitor and store the data collected.

3.4.1 Thermocouples

Thermocouples were utilized to monitor the temperature of the load cell, and to measure temperatures at sampling locations in the compartment. Two shielded and aspirated thermocouple rakes were also used; one positioned in the in the doorway and one in the front corner of the compartment as shown in Figure 3.3. The front corner rake was positioned 20 cm from either compartment sidewall. These rakes consisted of eight type

K (chromel-alumel) thermocouples mounted in the center of 0.635 cm diameter stainless steel tubing, as shown in Figure 3.8. Shielding and aspiration were used to reduce the temperature error from radiative heating and increase temperature accuracy by increasing the convective heat transfer (Pitts, et al, 1998). Use of a bare thermocouple for temperature measurements in a fire increases error in the gas temperature measurement because the thermocouple bead exchanges radiation with the surrounding structure and gases. The aspiration also reduces the soot buildup on the thermocouples.

Temperature error was not eliminated because the pumps used could only produce an aspiration velocity of just less than 10 m/s, while higher velocities, on the order of 20+ m/s, were recommended by Blevins (1999) to further reduce gas temperature measurement errors. The velocities were not measured, but calculated from the pump rate and thermocouple probe opening areas. This calculated aspiration velocity was further reduced to account for pressure losses in the piping, particulate filter and water trap. Calculations were necessary because the actual system used for aspiration was modified after testing before measurements of flow velocities could be taken. Blevins (1999) also reported that the measurement error would be the greatest for lower gas temperatures (i.e. smaller fires and in the compartment lower layer). This was due to the often high temperatures of the surroundings compared to the relatively low gas temperatures being measured.

Also, since the pump were attached to one end of the thermocouple rake the aspiration velocity would be slightly higher than calculated for the thermocouples on that end and slightly lower than calculated for those on the opposite end. Actual velocity measurements were not performed on each thermocouple in the rakes so individual thermocouple error cannot be calculated.

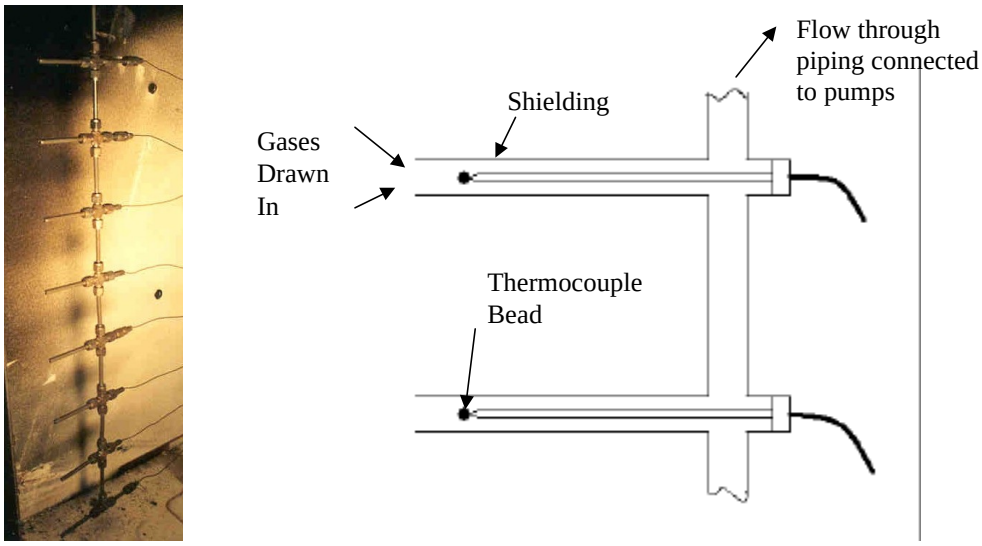

Figure 3.8 Picture and diagram of aspirated thermocouple rakes

3.4.2 Sampling Probe

Figure 3.9 shows the special gas sampling probe which was constructed to enable the measurement of local mole fractions and temperature simultaneously. This probe consisted of a stainless steel "T" connector attached to one end of the 0.635 cm diameter stainless steel sampling line. A type K thermocouple is mounted inside the "T" connector (tip of the sampling probe), and was aspirated by action of the sampling pumps. This probe was located in the upper-layer at a position in the center of the doorway opening 10cm from the ceiling and 20cm from the front wall of the compartment. This probe was introduced into the compartment through a hole in the ceiling and the hole was sealed with ceramic gauze.

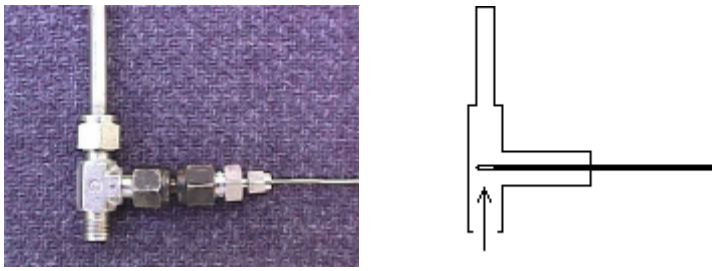

Figure 3.9 Sample probe with integral thermocouple (photo and diagram)

3.4.3 Sampling Lines

The sample probe was connected to 0.635 cm diameter stainless steel tubing which extended 0.35 m to a Balston 915A, DX grade, glass fiber particulate filter. The gas then traveled through heated Teflon tubing for 3 meters and heated stainless steel tubing for another 3 meters. The Teflon tubing section was used to allow the position of the sample probe to be adjusted as needed and for ease of routing through the lab. Next in the sample line an in-line Gelman glass fiber filter type A/E (47mm) was installed to trap any remaining particulates and then the line was split with one half flowing through heated stainless steel tubing directly to the FID total hydrocarbon analyzer and the balance flowing to the other analyzers. The second stream of sample was first directed through a Fisher model #910 refrigerated circulating bath to condense any water from the sample. From there it was passed to the paramagnetic O_2 analyzer, and non-dispersive infrared CO and CO_2 analyzers. A series of valves and bypasses were used to maintain required flow rates and pressures for each analyzer. A diagram of this setup is included as Figure 3.10. The "downstream sampling" location was not used in these studies, but is included for completeness. This "downstream sampling" location was used in previous studies to sample average species mole fractions in the exhaust gas collected by the fume hood.

The sample line system was leak tested before use and at several times over the course of the experiments. This leak check was performed by introducing gas from a cylinder, which contained 100% nitrogen, at the sample probe and verifying on the O_2 analyzer that the reading fell to zero.

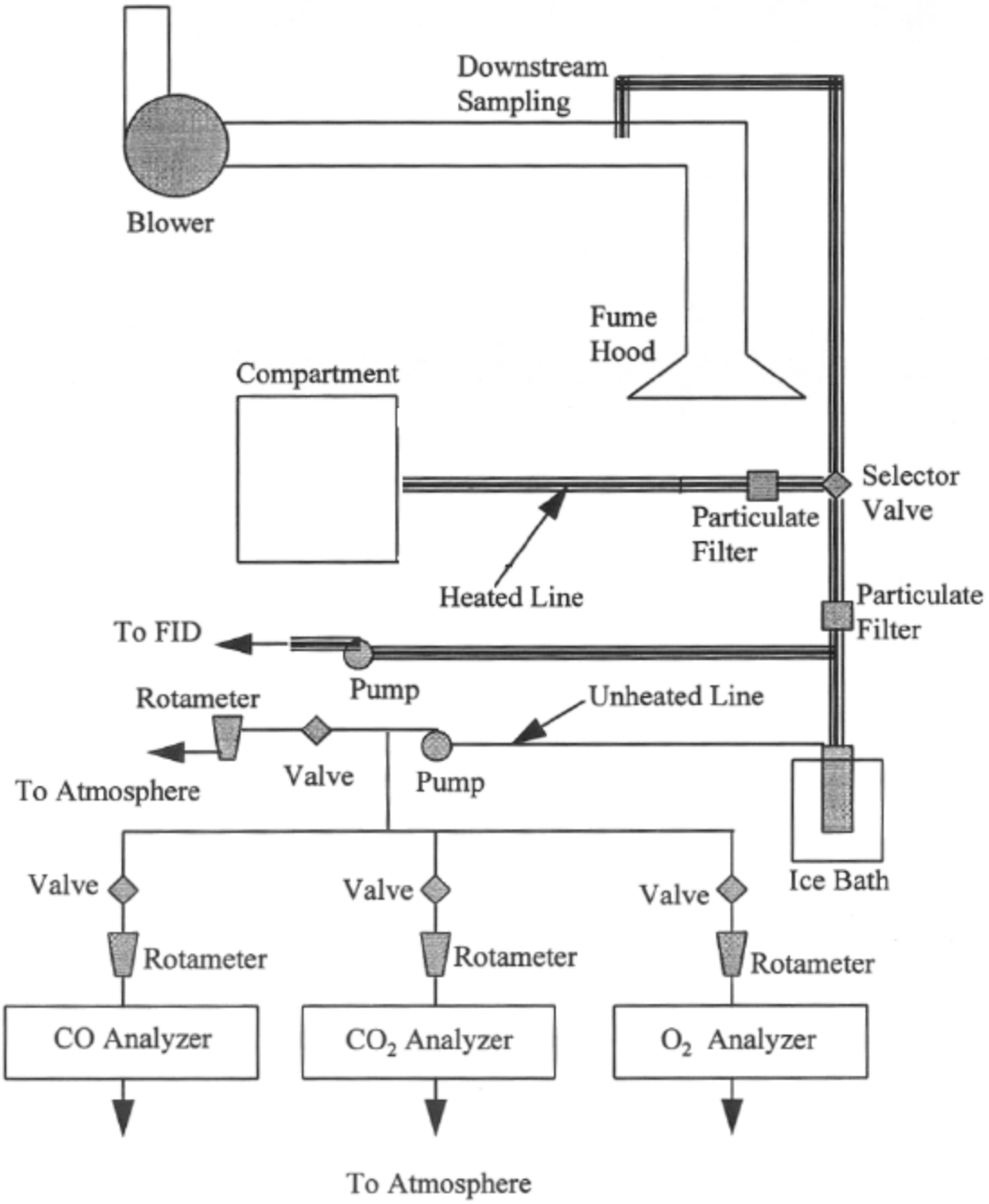

Figure 3.10 Sample line routing from compartment to analyzers

3.4.4 Gas Analyzers

3.4.4.1 Unburned Hydrocarbon measurements

The UHC wet mole fractions were measured using a bench mounted Gow-Mac model #12-800 FID attached to a Gow-Mac model #40-900 electrometer which provided FID signal conditioning. The FID was contained inside an oven maintained at 105° C and used a hydrogen flame produced by a mixture of 40% hydrogen and 60% helium as the fuel and purified air as the oxidant.

In the flame ionization detector, the gas sample is mixed with hydrogen and burned in air. As ions and free electrons are formed in the flame, they enter the gap between two electrodes across which a potential exists. This lowers the resistance across the gap and causes a current to flow. This current is then amplified by the electrometer to produce a signal for data collection. The FID is insensitive to certain gases including air and water.

The hydrogen flame products were vented from the top of the oven into a cooling chamber, which also contained a hydrogen detector. The cooling chamber was kept cool using a cooling coil at –10° C which ran from the refrigerated circulating bath also used to cool the water trap in the sampling line. The hydrogen detector determined if the FID flame has been extinguished and high levels of hydrogen were being vented to the outside. If high levels were detected then the hydrogen detector would shut off the flow of hydrogen using a solenoid valve. A diagram of the system is shown in Figure 3.11.

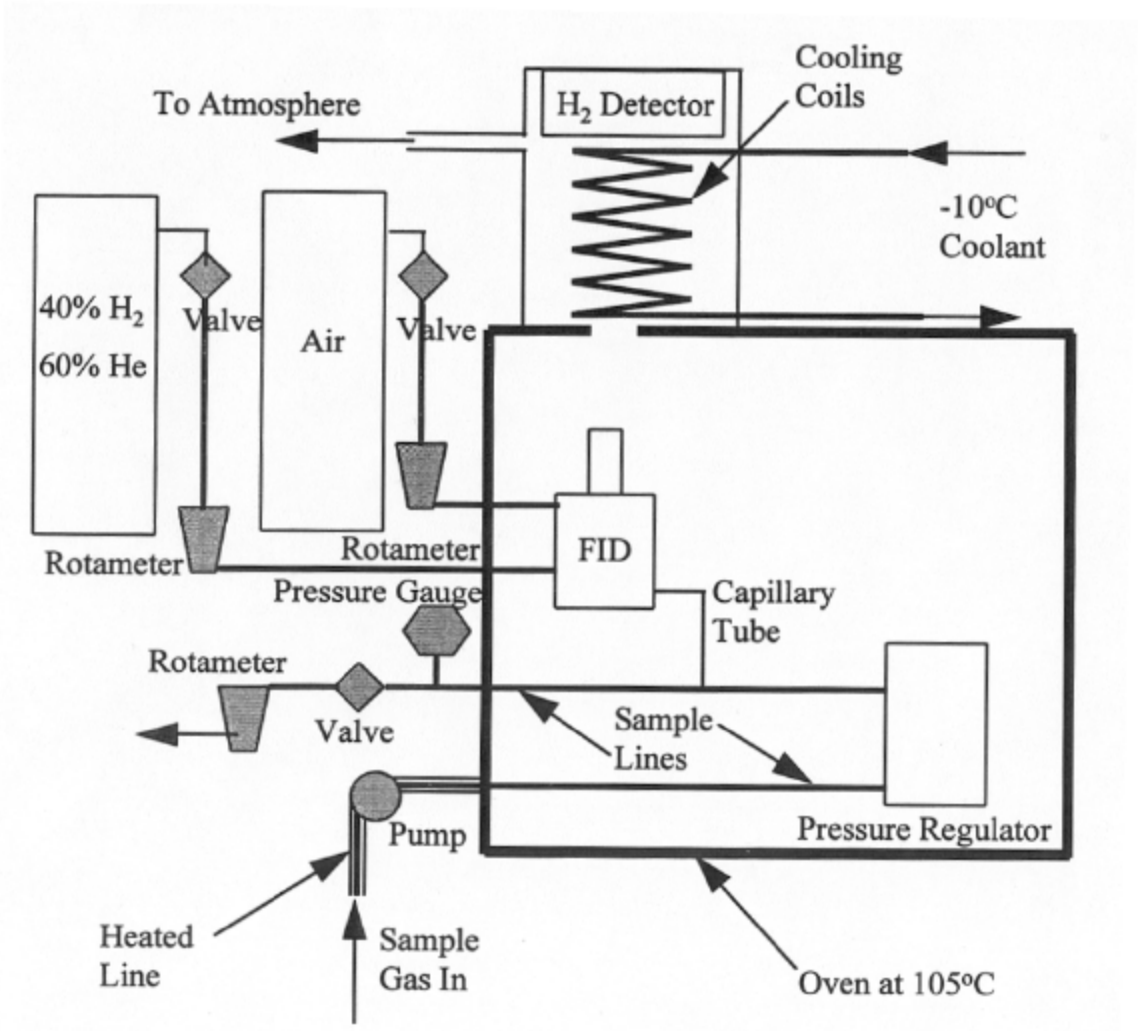

Figure 3.11 FID system schematic

The FID electrometer had four possible sensitivity ranges for signal amplification, though only two were used during the experiments reported in this paper. Before each test the FID was calibrated using a zero and span gas to determine the zero and span points. The span gases are various mole fractions of ethylene (C_2H_4) in a nitrogen makeup gas. The mole fractions of ethylene were 4.71% and 5466 ppm for the two sensitivity ranges used. Ethylene was used as a calibration gas because higher order hydrocarbons tend to pyrolize to ethylene (Westbrook and Dryer, 1984).

3.4.4.2 CO, CO_2 and O_2 Measurements

The CO_2 mole fraction was measured using a Rosemont Analytical model 880 NDIR analyzer. The output of the instrument is 0-5 volts, which was linearized with respect to the mole fraction. This linearization was performed internally using a software calibration and two gas calibration points, zero and an appropriate CO_2 containing span gas. The analyzer had four ranges for measurement (0 to 5000 ppm, 2%, 15%, and 20%). Only the 0-20% range was used for the experiments described in this paper.

The CO mole fractions were measured using two separate Horiba PIR 2000 analyzers, one for the higher mole fractions (0-5%) and the other for lower mole fractions (0-5000ppm). These analyzers were also calibrated with nitrogen for the zero point and an appropriate span gas. They produced a 0-5 volt output linearly scaled to the analysis range chosen.

The O_2 mole fractions were measured using a Siemens paramagnetic Oxymat 5E analyzer. This analyzer produced a 4-20 mA output, which was converted to a 0-5 volt by putting a 250 ohm resistor across the output leads. Since O_2 mole fractions less than ambient (~21%) were expected in the samples the analyzer range of 0-22% was utilized. This analyzer was also zeroed using a nitrogen gas and a span gas of 4.71% O_2 was used to establish a calibration point. This span mole fraction in the low end of the analyzer range was used to ensure that the low levels of oxygen, expected in the measurements, were measured accurately.

3.4.5 Data Acquisition System

Three Data Translation DT 2801-A data acquisition boards were used to perform analog-to-digital conversion of the data from the instruments. These internal boards were connected to external screw termination boards mounted in the facility. Two of these boards were DT 756-Y thermocouple amplifier boards, to which all the thermocouples used within the facility were attached. These boards provided cold junction

compensation for the thermocouples and multiplexing, which allowed 16 thermocouples to be attached per board. The other terminal board was a DT 707 direct input board, which accepted the voltage differential inputs from the analyzers, and the load cell.

LabTech Notebook Pro data acquisition software was used to monitor, acquire, and store the measurement data. The software allowed a visual interface to monitor conditions and outputs of all the sensors and analyzers. Once the sampling run was started the program recorded measurements from all of the instruments into a text data file in 1 second increments. This type of data output allowed easy importation into Microsoft Excel for data reduction.

3.5 Data Reduction

3.5.1 Overview

Each set of data was imported into an Excel workbook specially developed to reduce the data for reporting. The raw data was copied/pasted into the Excel workbook and the test conditions were entered manually into predefined spaces on the sheet. Using a visual basic macro some of the data was exported to a text file to be used in a Fortran subroutine to determine door mass flow rates into and out of the compartment and the doorway neutral plane height using the procedure of Janssens and Tran (1992). This process is explained in detail in Section 3.5.6 and in Appendix B. A copy of the Fortran code is also included in Appendix A. Dr. Brian Lattimer authored this Fortran routine for use in his research and for these compartment studies. After the Fortran routine was complete the output results were imported back into the master Excel workbook.

This workbook also produced automatic graphs of the data for immediate review. The fuel volatilization rate, mass flow, CO and CO_2 yields, and the CO wet gas mole fractions were examined to determine the period of the fire when the levels appear to be the steadiest. This time period of steadiest values was then chosen as the “quasi steady state” period and used to calculate the average values of temperature, mole fraction, fire size,

species yields, and global equivalence ratio for that fire. This "quasi-steady state" period lasted between 25 and 40 seconds depending on the test. An example of the graphs used to visually determine this "quasi-steady state" is shown in Figure 3.12. The graph with door flow rates and fuel vaporization rate is first examined to find the general time period in which fuel vaporization and doorway flows appear constant. A box is used to provide a visual reference during the steady state determination process. Then the same period is examined for CO mole fractions and yields, plus the CO_2 yields. Then a composite time period in which all these levels are the most constant is used as the "quasi-steady state" period over which the data for that test is averaged. This procedure is repeated for each test throughout the study. The tests at lower equivalence ratios tended to have a longer "quasi-steady state" period than the larger fires.

Gottuk, et al. (1992) used a similar method of centering their "quasi-steady-state" period for a 20 second interval about the time at which the equivalence ratio peaked or leveled out during most of their tests using n-hexane as a fuel. Lattimer (1996) used a calculated factor termed the fire growth parameter (G), which was defined as the fuel volatilization rate normalized by the residence time in the compartment. This also was similar to the definition of "quasi-steady state" used in this study as one of the key factors in determining this time period was fuel volatilization rate.

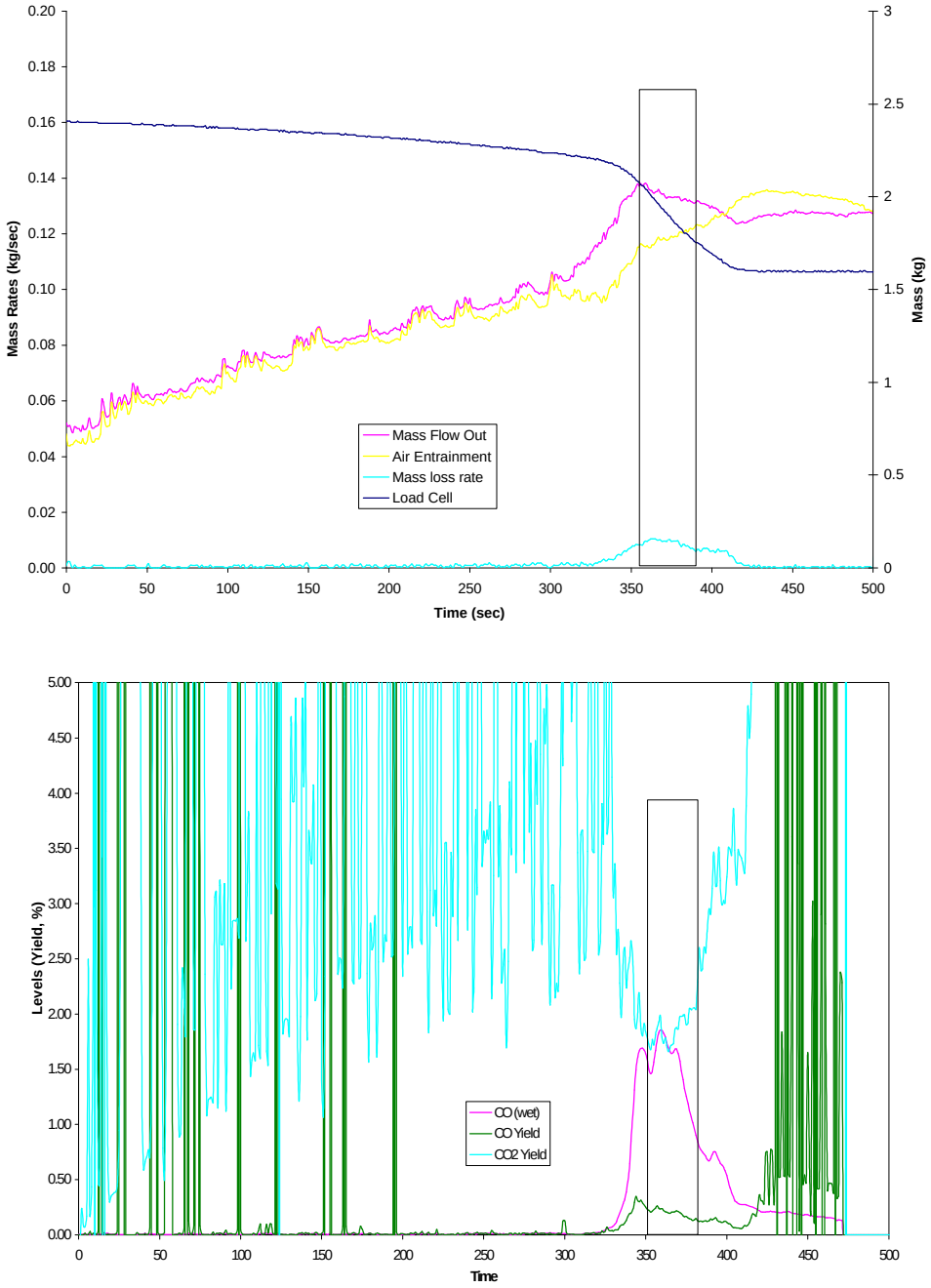

Figure 3.12 Excel charts used to determine the steady state period for a typical $\phi = 1.28$ fire

3.5.2 Temperature Data

The temperature data was examined for inconsistencies, such as spikes or zero values that might indicate that a thermocouple is not working properly. This was done by examining a graph of recorded temperature versus time to look from abnormalities. Incorrect readings were only found for two thermocouples during the entire study, both in the compartment upper-layer. The compartment upper-layer was usually well mixed during quasi-steady state and approximately the same temperature was recorded on the thermocouples above and below the malfunctioning one. The average of the readings of the thermocouples above and below was used to approximate the temperature data for those two thermocouples.

3.5.3 Mole Fraction Data

The mole fraction data, expressed as a percentage, was first time aligned to correct for the time delay that is caused by the sample transport time. This allowed the gas mole fractions to be time matched with the instantaneous temperature readings. This delay was measured to be 35 seconds by immersing the sample probe in a 100% nitrogen gas and timing how long it took the O_2 analyzers to drop by 90% of ambient mole fractions. Therefore, the time it took the O_2 mole fraction to drop from 20% to 2% was defined as the transport time. The CO, CO_2, and O_2 data was corrected to "wet" mole fraction format by using the assumption that all H_2O in the sample gas was produced from the combustion process. The UHC data does not require correction, as the water was not removed from the gas flow to the FID. For the stoichiometric combustion of n-hexane, 6 moles of CO_2 and 7 moles of H_2O are produced. This allows the dry mole fraction of the other species to be converted to wet mole fractions using the following equations with the dry mole fraction of the species and the dry mole fraction of CO_2 as shown in equations 15-17 below. This assumption was also used by Bryner et al. (1994) and Lattimer (1996) when they presented their gas mole fractions on a wet basis.

$$CO_{wet} = \left[\frac{\frac{CO_{dry}}{100}}{1 + 7/6\left(\frac{CO_{2,dry}}{100}\right)} \right] 100 \qquad [\%] \qquad (15)$$

$$O_{2,wet} = \left[\frac{\frac{O_{2,dry}}{100}}{1 + 7/6\left(\frac{CO_{2,dry}}{100}\right)} \right] 100 \qquad [\%] \qquad (16)$$

$$CO_{2,wet} = \left[\frac{\frac{CO_{2,dry}}{100}}{1 + 7/6\left(\frac{CO_{2,dry}}{100}\right)} \right] 100 \qquad [\%] \qquad (17)$$

3.5.4 Fuel Volatilization Rates

The fuel volatilization rate was determined by dividing the change of mass of fuel in the fuel pan over a seven second period of time ($\Delta M/\Delta t$). To ensure that the Fortran routine runs smoothly, the fuel volatilization rate must be very smooth data with no large changes so it was averaged over a rolling 7-second interval.

3.5.5 Species Yields

The species yields in the compartment upper-layer were calculated in the Excel spreadsheet using the expressions in equations 18-21 for products CO, CO_2, UHC, and reactant, O_2, respectively. For all species other than O_2, the yields represent the species production in the compartment relative to the fuel volatilization rate, $\dot{m}_{fuel}$. For O_2 the yield instead represents the oxygen consumption relative to the fuel volatilization rate.

This method of reporting species yields was used by several researchers including Lattimer (1996) and Gottuk et al. (1992). The molecular weight of the upper-layer, MW_{UL}, was assumed to be equivalent to that of air.

$$Y_{CO} = \frac{X_{CO} MW_{CO} (\dot{m}_{fuel} + \dot{m}_{air})}{\dot{m}_{fuel} MW_{UL}} \tag{18}$$

$$Y_{CO_2} = \frac{X_{CO_2} MW_{CO_2} (\dot{m}_{fuel} + \dot{m}_{air})}{\dot{m}_{fuel} MW_{UL}} \tag{19}$$

$$Y_{UHC} = \frac{X_{UHC} MW_{UHC} (\dot{m}_{fuel} + \dot{m}_{air})}{\dot{m}_{fuel} MW_{UL}} \tag{20}$$

$$Y_{O_2} = \frac{MW_{O_2} (X_{O_2,amb} \dot{m}_{air} - X_{O_2} \dot{m}_{out})}{\dot{m}_{fuel} MW_{UL}} \tag{21}$$

A normalized yield, f_i, was calculated by dividing the yield of each species by the maximum theoretical yield of each species for a given fuel, k_{fuel}, as shown in Equation 22. The normalization of the yields removes the variability between studies, which is introduced by different fuel compositions. Normalized yields are most applicable to the species CO_2 and O_2, as these are the major components related to complete combustion of a fuel, i.e. for complete combustion the yields of both CO_2 and O_2 are 1 and decrease as a fire burns more inefficiently. Normalized yields are not as effective on products of incomplete combustion, CO and UHC, for which the theoretical maximum yield varies depending on fire conditions. The parameters that can affect combustion efficiency include temperature, which for temperatures lower than about 900K can quench the conversion of CO to CO_2 (Gottuk, et al., 1992). Compartment geometry can affect the residence time of the gases, which could limit the amount of time in a region with high enough temperatures to support CO oxidation. For this reason, only the CO_2 and O_2 yields will be reported normalized.

$$f_i = \frac{Y_i}{k_{fuel}} \qquad (22)$$

Beyler (1986) suggested that the correlations for maximum normalized yield of both CO_2 and O_2 could be represented with a single simple model. This model assumes complete combustion of a fuel and indicated maximum theoretical yields for CO_2 production and O_2 consumption. These correlations are:

$$f_{CO_2} = f_{O_2} = 1 \qquad \text{for} \qquad f < 1 \qquad (23)$$

$$f_{CO_2} = f_{O_2} = \frac{1}{f} \qquad \text{for} \qquad f > 1 \qquad (24)$$

3.5.6 Door Flow Rates

The air inflow and exhaust outflow were calculated using the iterative process documented by Janssens and Tran (1992), which uses two thermocouple rakes, placed as shown in Figure 3.3. Dr. Brian Lattimer coded this process into a Fortran routine. The routine took input in the form of tabular text files exported from the master Excel workbook and returned a tabular text output file of results. The full text of this routine is shown in appendix A. One input file contained the temperature readings from the thermocouple rakes on the interior and at the door of the compartment, while another contained the fuel mass loss data generated by differentiating the load cell mass readings. The last input file contained all the environmental readings such as ambient temperature and pressure and the height from the compartment floor of each thermocouple. The outputs of this routine included the air entrained through the door, the mass flow exiting the compartment through the door, the neutral plane height (where the incoming and exiting flows met) of the door, and the plume equivalence ratio.

Limitations exist using this method to calculate doorway flows because it is based on thermocouple response time. The thermocouples used in this study had a typical response time of 1.9 seconds (Vandsburger, 2001). This response time could be improved with the use of smaller thermocouple beads or the use of direct pressure measurements. One alternate method would be to use a series of bi-directional probes along the doorway height attached to differential pressure transducers. This method would improve the response time to about 0.050 seconds.

This technique has been used by other researchers in their reported work (Bryner et al., 1994, Dembsey et al., 1995) and is widely accepted as a valid flow estimation procedure. A summary of this approach is detailed in Appendix B. It can reduce significantly the equipment, such as bi-directional pressure probes, required to measure doorway flow by researchers such as Nakaya (1986). Visual observations and photographs on multiple runs verified the neutral plane height calculated by this technique.

3.5.7 Fire Size

A fire size was estimated using equation 25 by estimating the ideal heat release of the n-hexane fuel. This value was calculated by multiplying the fuel volatilization rate ($\dot{m}_v$) by the heat of combustion of n-hexane (ΔH_c = 44,735 kJ/Kg) as shown below. The fuel volatilization rate was calculated as shown in Section 3.5.4. This calculation determines an "ideal" fire size, which assumes that all the fuel that is volatilized is consumed in the fire. Later sections will show that some fuel remains as unburned hydrocarbons in fires with equivalence ratios greater than 0.6. A "real" fire size would require knowledge of the actual amount of fuel that is volatilized and oxidized.

$$Q = \dot{m}_v \Delta H_c \qquad \text{[kW]} \qquad (25)$$

3.5.8 Carbon Error

The data is checked to see if all species present in the gas sample are accounted for using a carbon balance (Lattimer, 1998). The carbon balance was done by comparing the molar flow rate of elemental carbon in the gas sample, $\dot{n}_{c,s}$, with the molar flow rate of carbon from the fuel vaporization, $\dot{n}_{c,f}$. The gas sample, excluding soot, contains three components that contribute to moles of carbon: CO, CO_2, and unburned hydrocarbons (UHC). The general formula to calculate the molar flow rate of a chemical is shown in equation 26.

$$\dot{n}_{gas} = \frac{\dot{m}_o}{MW_{air}} x_{gas} \tag{26}$$

Where $\dot{m}_o$ is the mass flow from the door of the compartment, MW_{air} is the molecular weight of air, x_{gas} and is the mole fraction of the gas. To calculate the total molar flow rate of carbon in the sample, $\dot{n}_{c,s}$, the three components are simply added up as shown in equation 27.

$$\dot{n}_{c,s} = \frac{\dot{m}_o}{MW_{air}} (x_{CO} + x_{CO_2} + 2x_{UHC}) \tag{27}$$

In this equation the UHC value is multiplied by two to account for the two carbon atoms in the span gas used to calibrate the FID, ethylene (C_2H_4), which the FID reported UHC as. The molar flow rate of fuel, $\dot{n}_{c,f}$, is calculated in the same manner, taking into account the six carbon atoms in n-hexane (C_6H_{14}).

$$\dot{n}_{c,f} = 6\frac{\dot{m}_f}{MW_f} \tag{28}$$

The carbon error is computed as a percent, as shown below in equation 29. For these fires the carbon error should range from 0-30%, primarily due to measurement error in the species mole fraction measurements, discussed in the next section and the lack of soot measurements, which are solid carbon particles.

$$C_{ERROR} = \left(\frac{\dot{n}_{c,s} - \dot{n}_{c,f}}{\dot{n}_{c,f}}\right)100 \qquad (29)$$

3.5.9 Experimental Error

Experimental error was not separately calculated for this study. Because the equipment used to take the measurements was identical to that used by Lattimer (1996) in his work, the error is assumed also to be identical to his reported values. The values he calculated are tabulated in Table 3.2, below.

Table 3.2 Calculated experimental error of measurements

PARAMETER	ERROR (+/-)
UHC_{wet}	10.2%
CO_{wet}	11.9%
CO_{2wet}	9.5%
O_{2wet}	8.0%
Compartment Temperatures	3.2%
Fuel volatilization rate	6.0%
ϕ	7.3%
Fire Size	6.0%

4 Compartment Results and Discussion

4.1 Upper-layer Mapping

The upper-layer mapping tests were conducted with n-hexane fuel burning in an 8-inch pan. The calculated global equivalence ratio for all tests was approximately 1.28, which insured underventilated conditions in the compartment and external burning of exiting compartment gases. The ideal fire size averaged 514 kW for all tests, but variations between the individual tests resulted in a standard deviation for the fire sizes of 53.4 kW. In each test flames extended from the burning compartment upper-layer, out the doorway and up into the fume hood. Tests averaged approximately 400 seconds in duration. The sampling probe was placed at eight (8) locations as shown in Figure 4.1, chosen as characteristic for different zones of the upper-layer and to avoid sampling the vertically rising fire plume from the center of the compartment. The location of the fume hood, positioned over the compartment door is also shown with a dashed outline.

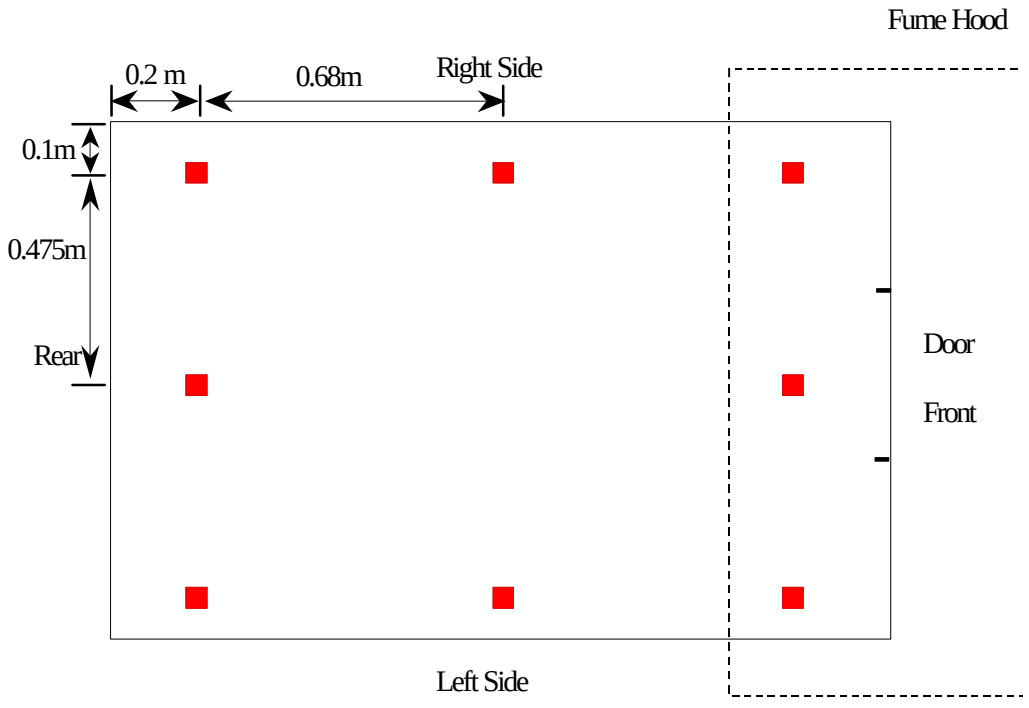

Figure 4.1 Sampling locations for upper-layer mapping

The sampling probe was located 0.10m from the compartment ceiling in all positions ensuring its placement in the upper-layer, the focus of this series of tests. The positions were located 0.2m from the front and back walls of the compartment and 0.1m from the sidewalls. All experiments were conducted in the new compartment with a door height of 0.82m and door width of 0.33m.

4.1.1 Species Mole Fractions

The averaged wet mole fractions of CO, UHC, CO_2, and O_2 in the upper-layer of the compartment, for eight (8) locations are shown in Figure 4.2. A typical plot of these mole fractions over the duration of the test is shown in Figure 4.3 for the right center position. This shows the gradual decrease in oxygen and increase in carbon dioxide as the fire progresses. Oxygen levels rapidly decrease to zero as flashover occurs in the compartment, while the carbon monoxide, carbon dioxide, and unburned hydrocarbon levels rapidly increase. After the fuel is depleted the combustion product levels drop while oxygen again rises toward ambient levels. A composite plot of the CO mole fraction tests for five of the sampling locations is shown in Figure 4.4 and indicates very consistent CO levels between the tests and good agreement on the steady state period of the tests. The time plots on Figure 4.4 have been adjusted in time to start rising at the same point.

Various definitions of flashover have been used in previous research. Peacock, et al. (1999) performed an extensive review of the various definitions and concluded that upper-layer temperatures ≥873K or a heat flux at the floor of ≥20kW/m^2 is consistent with flashover for a broad range of experimental data. A simpler visual definition is the transition from a single fuel source burning to total involvement of all fuel sources in a room.

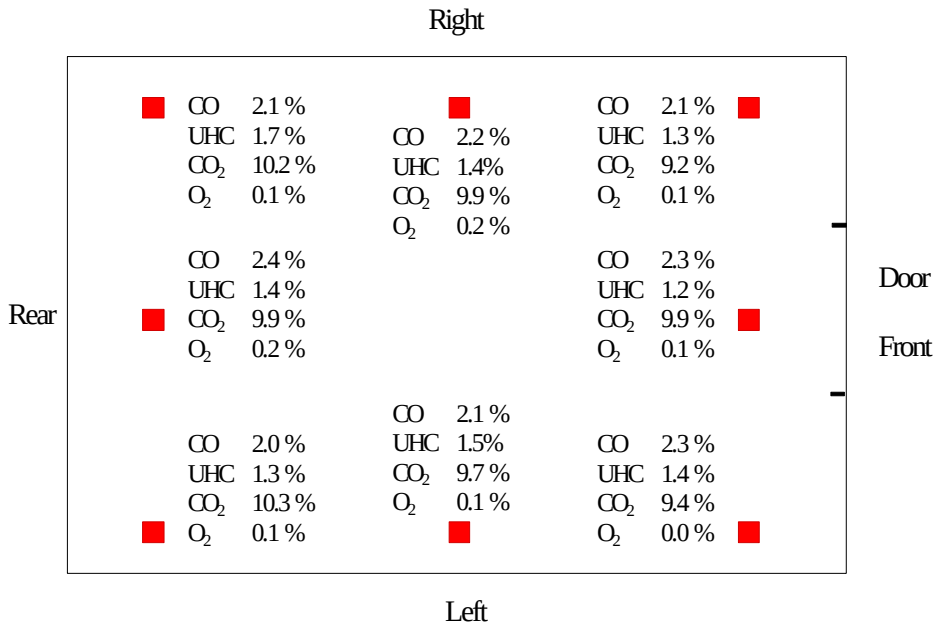

Figure 4.2 Wet mole fractions of CO, CO_2, O_2 and UHC in upper-layer; ϕ =1.28, 514 kW fire.

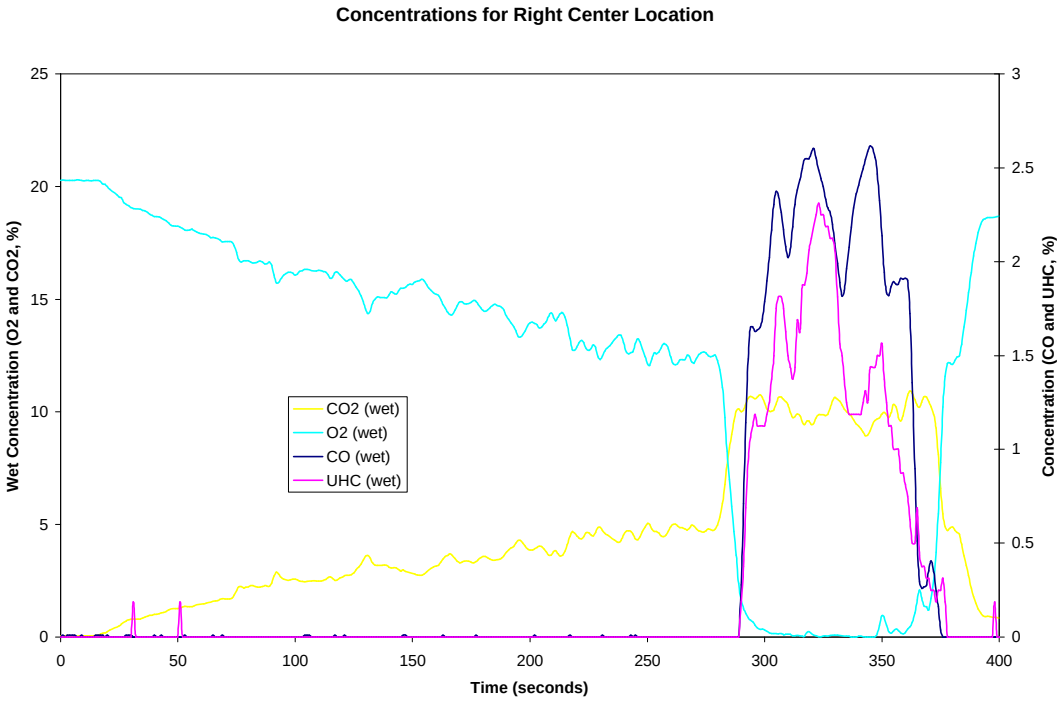

Figure 4.3 Species mole fraction for typical compartment test

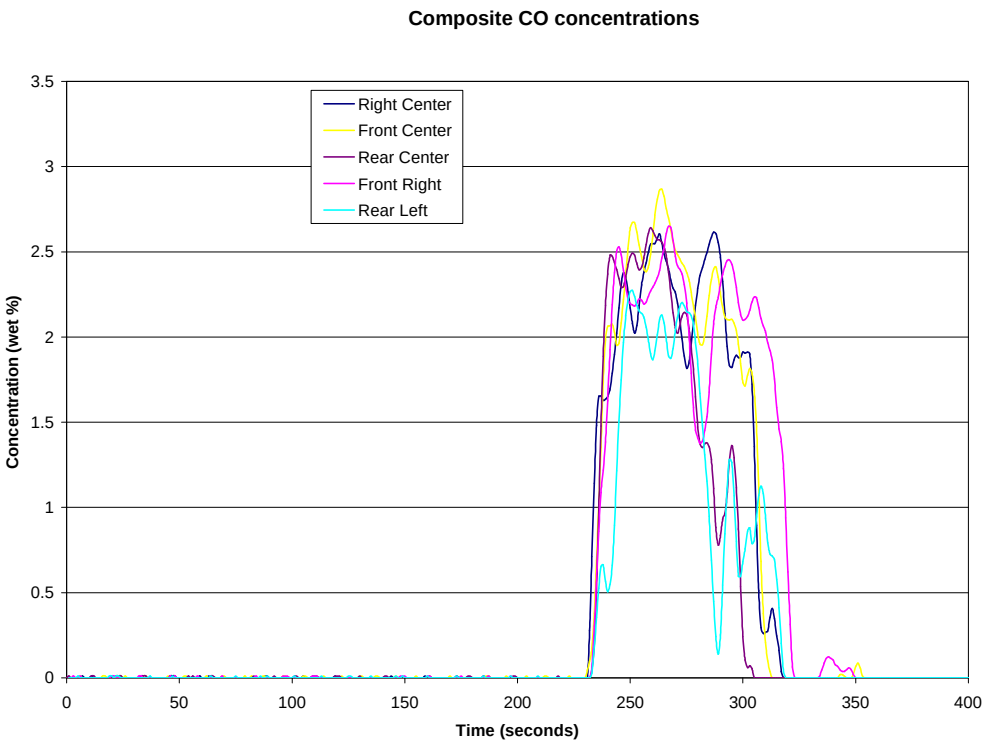

Figure 4.4 Composite of CO mole fractions at five sampling locations (time matched to start of flashover)

4.1.2 Species Yields

Using the above data the species yields were calculated using equations 18-21 and are shown in Figure 4.5 and in Table 4.1. Normalized yields were not calculated for this section as results were not presented for varied equivalence ratios or compared to other data. Both Figure 4.2 and 4.5 show that for this case the upper-layer of the compartment is slightly nonuniform, with an average of 4% higher CO levels in the front of the compartment than in the rear, although this is within experimental error of mole fraction measurement described in Section 3.5.9. This indicated that within the expected error the upper-layer was essentially uniform in CO levels. The composite plot of carbon monoxide mole fractions for five of the tests in Figure 4.4 also supports this uniformity throughout the upper-layer. The work of Gottuk, et al (1992) also showed a uniformly mixed upper-layer. The difference in their compartment configuration, with a separate inlet and outlet, is not the best comparison as the mixing would likely be more uniform

than with a doorway. In Gottuk's compartment the air entered into a plenum below the compartment and was entrained into the fire plume from a n-hexane pool fire in the compartment center. This resulted in a vertical fire plume, which extended into the compartment upper-layer. The upper-layer gases then had time to mix uniformly before exiting through a vent. These results do not agree with the results of Bryner, et al. (1994) who reported up to 50% higher CO mole fractions in the front of their compartment.

Table 4.1 Compartment upper-layer yields and carbon error

Location	**Average CO Yield**	**Average UHC Yield**	**Average CO_2 Yield**	**Average O_2 Yield**	**Carbon Balance Error**
Front Left	0.24	0.14	1.55	2.19	19.6%
Front Center	0.24	0.12	1.64	2.11	20.3%
Front Right	0.23	0.14	1.54	2.17	21.5%
Center Left	0.23	0.15	1.64	2.19	16.8%
Center Right	0.24	0.16	1.72	2.31	13.3%
Rear Left	0.25	0.17	2.02	2.58	24.5%
Rear Center	0.41	0.24	2.66	3.61	69.6%
Rear Right	0.31	0.27	2.42	3.18	43.7%

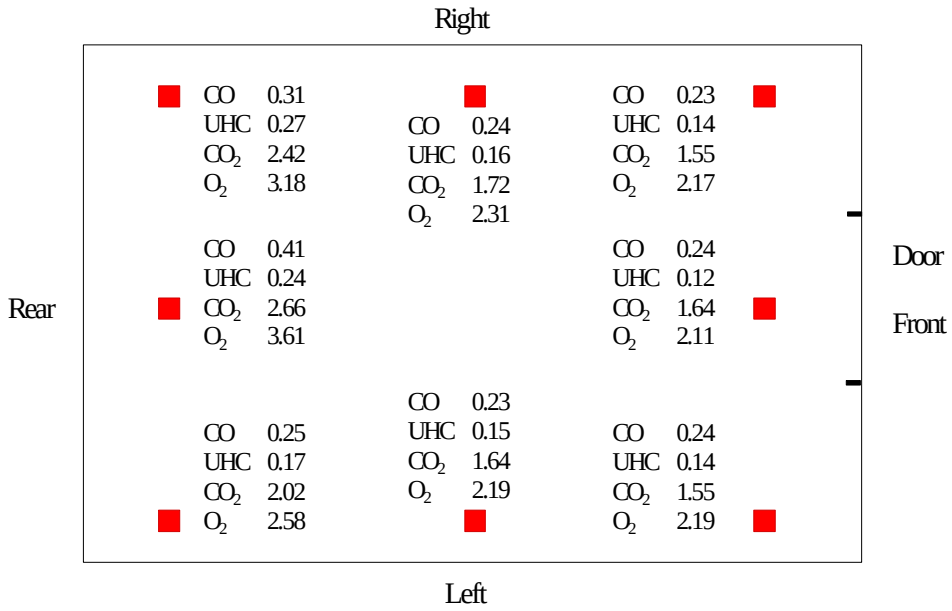

Figure 4.5 Major species yields in upper-layer; ϕ = 1.28, 514 kW fire.

4.1.3 Upper-layer Temperatures

The upper-layer temperature uniformity was also investigated and is plotted in Figure 4.6. This figure shows the temperatures in the upper-layer are not uniform, but exhibit some trends. The front center thermocouple was deemed more representative of the front compartment upper-layer temperatures because it was located directly above the compartment doorway. The back thermocouples showed good relative temperature uniformity across the back of the compartment upper-layer. The temperatures measured on both sides of the compartment were the same and very near the front center thermocouple temperatures. The differences between the front and back of the compartment were not large, only 50 – 70K higher in the front of the compartment, so the trend only indicates small non-uniformity. Although this difference is small, it is greater than the measurement error predicted for the thermocouples with aspiration, thus represents minor upper-layer non-uniformity.

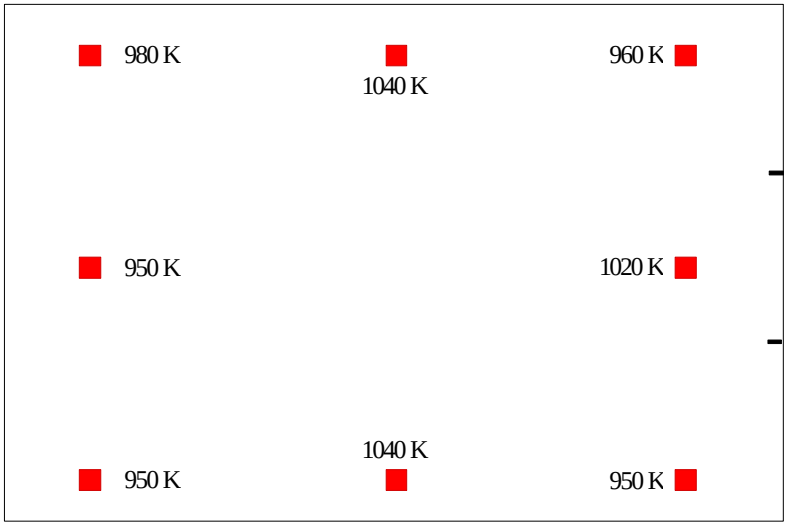

Figure 4.6 Upper-layer temperatures and general compartment flow patterns, ϕ=1.28, 514 kW fire.

4.1.4 Upper-layer Results

The results for carbon error the upper level study are shown in the last column of Table 4.1. These numbers indicate that two of the three rear sampling runs had very high carbon error, which could possibly be due to the fire plume rising in their vicinity. Differences in the species levels and temperatures could also be partially due to experimental variations between tests, which resulted in a standard deviation in fire size of more than 50 kW. Liquid pool fire size cannot be controlled as precisely as a metered gaseous fire which can also have a longer, less transient, steady state time.

Based on these upper-layer measurements a single upper-layer sampling location was chosen for the next phase of testing, a global equivalence ratio study. This location was the center front location, which provided an average of the upper-layer mole fractions in the compartment and was the closest location to the compartment doorway. Only mapping of the doorway outflow could give an accurate description of species exiting the compartment. All data taken at this location is thus only representative of the front of the compartment upper-layer.

4.2 GER Study

All the data gathered during this study of one doorway size, determined by scaling parameters as discussed in Section 3.1, is presented and discussed in this section. The values of the data were determined using the procedures described in the previous chapter and averaged over the quasi-steady state periods of the fires.

4.2.1 Upper-layer Temperatures

The temperatures recorded at the sampling probe location for the various equivalence ratios are shown in Figure 4.7. This figure shows that the sample temperature is almost constant as the equivalence ratio exceeds one. All except one data point falls within the experimental error at about the same temperature. These temperatures are also above 900K, which indicates the upper-layer in the compartment is hot enough to support the oxidation reactions including the conversion of CO to CO_2. This is in contrast to the hood experiments reported by Beyler (1983) where the upper-layer only reached about 550K. The effect of this lower temperature is to "freeze out" oxidation reactions and not consume the available O_2 (Gottuk et al., 1992). This lower temperature has a great influence on the mole fraction of species and yields reported by Beyler and will be discussed in great detail in Sections 4.2.2 and 4.2.3.

The upper-layer extends down from the ceiling a significant distance in the fully developed fires. The top four thermocouples in the compartment thermocouple rake show almost the same temperatures during the quasi-steady state period of the fires. This is further evidenced by visual observations through the compartment door during which the fiery layer interface is clearly seen extending deep into the compartment as shown in Figure 4.24.

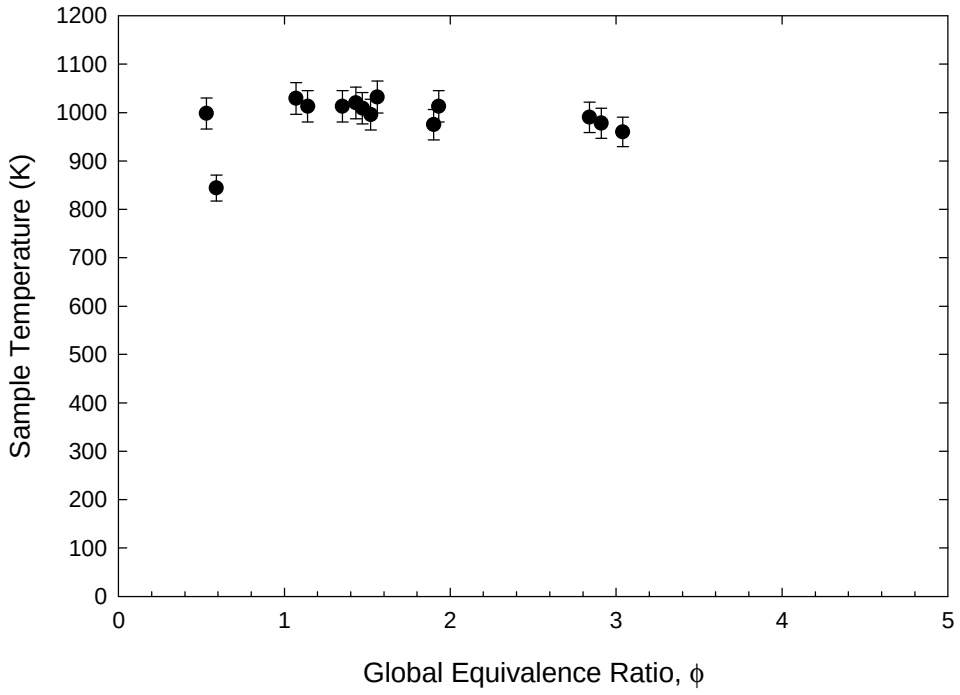

Figure 4.7 Upper-layer temperature as a function of global equivalence ratio

4.2.2 Species Mole Fractions

Each species mole fraction was measured as described in Section 3.4.4. This data was examined for trends by graphing the data from multiple experiments with varying equivalence ratios. These trends are first discussed and then the data is compared to results reported in other fire studies.

4.2.2.1 Carbon Monoxide

The CO wet mole fractions are plotted below in Figure 4.8. This data shows the percentage of CO in the front upper-layer of the compartment for varying global equivalence ratios. This figure shows that the CO mole fraction remains at zero until the

global equivalence ratio reaches approximately 0.5-0.6. At that point it begins to increase rapidly to a level of 3% at about ϕ = 1.4. From that point on the rate of increase appears to slow dramatically. There is also scatter in the data, especially at the higher global equivalence ratios. This scatter is most likely due to the very short quasi-steady state periods and is present in the graphs of all of the data collected for higher global equivalence ratios.

Error is reported for each data point based on the calculated measurement error described in Section 3.5.9. At high equivalence ratios the data shows larger variations than can be explained by measurement error. These variations could be caused by the choice of the quasi-steady state period for those tests because the steady state period was the shortest for the highest equivalence ratio tests as described in Section 3.5.1.

Although no two researchers have used the same compartment size or doorway configuration, a comparison of the present data with the CO mole fraction data previously reported by several researchers is possible. The same trends appear in all the data as shown in Figure 4.9. The data collected from the closest geometrical configuration, Bryner et al. (1994), shows that for the front sampling location, their CO mole fraction data increases very quickly as the equivalence ratio increases. All of the data reported here for Bryner's work has been adjusted by dividing their reported equivalence ratio by $\sqrt{8}$. This is due to an error that they discovered in the data reduction routine used for their tests after their paper was published. This has the effect of shifting all of their data toward lower equivalence ratios. The reason their data rises faster than the other reported data is probably due to a larger door width and resulting airflow into the compartment than other studies. Future studies with a wider door are proposed in Section 6.2 to investigate what effect the door width has on species mole fractions.

Gottuk's data also follows the same trend indicating good agreement from Gottuk's compartment and levels reported in this study (Gottuk et al., 1992). The data from Beyler (1983) shows lower mole fractions of CO above ϕ = 1 then the other reported data. This

is due to the cooler upper-layer temperatures in his hood experiments, which stopped the oxidation of the fuel before all the O_2 was consumed.

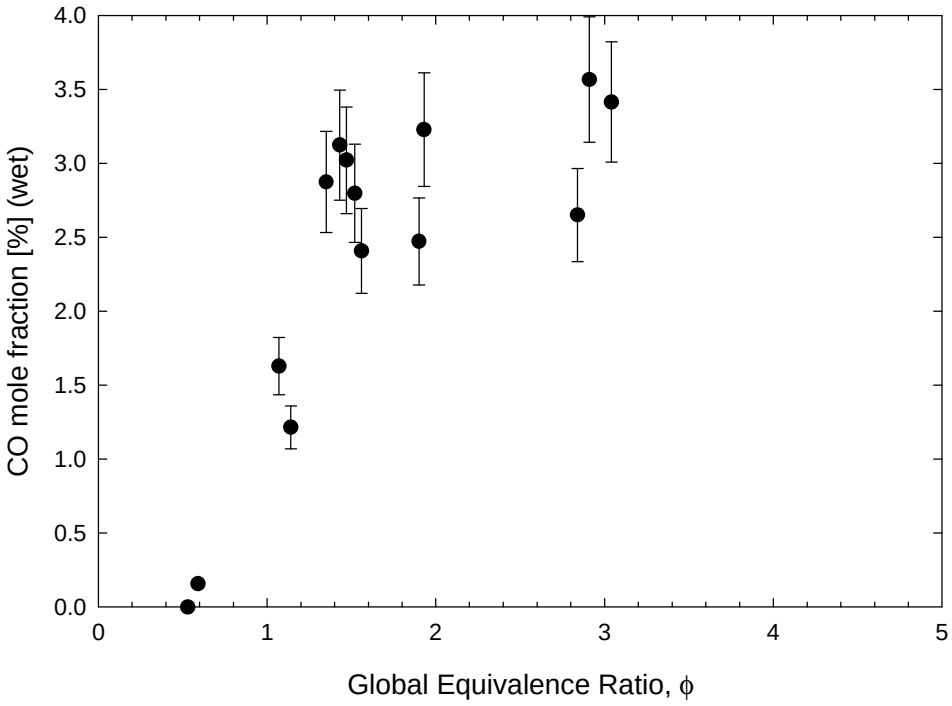

Figure 4.8 CO mole fraction for varied global equivalence ratios

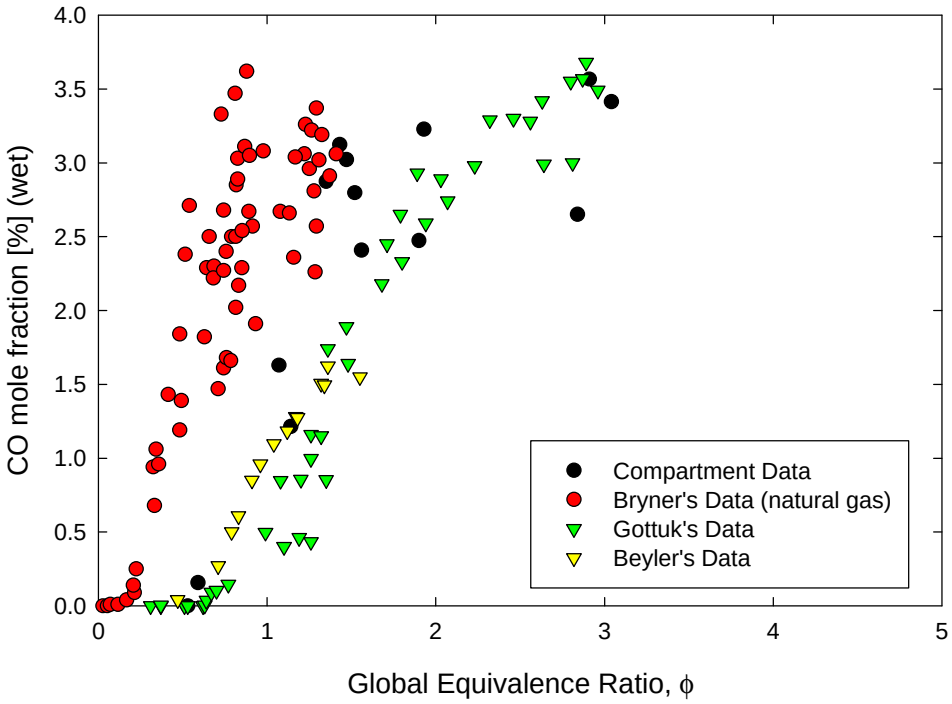

Figure 4.9 CO data including Bryner et al. (1994) for natural gas, Gottuk et al. (1992), and Beyler (1983) for n-hexane studies

4.2.2.2 Carbon Dioxide

The CO_2 data, presented in Figure 4.10, shows the level increases with increasing equivalence ratio until around $\phi = 1.2$. There are two outlying data points at $\phi = 0.5$ and $\phi = 2.9$ that show abnormally high CO_2 mole fractions relative to the data trends. A fixed amount of CO_2 should always be formed at and above $\phi = 1$, for a given amount of available O_2, although past that equivalence ratio the level seems to decrease slightly. This decrease was also noted by Gottuk, et al (1992) and shows up in the data of the other studies shown in Figure 4.11. This probably indicates that the products of incomplete combustion, CO and UHC, are diluting the sample at higher equivalence ratios. Most data points fall within the measurement error of the tests, except as the equivalence ratio

grows large. This is the same problem noted for CO mole fraction, Section 4.2.2.1, and is probably due to the choice of steady state period.

Beyler (1983) shows lower mole fractions of CO_2 at around $\phi = 1$ than the other studies. This is due to the cooler upper-layer temperature described in Section 2, which halt the oxidation reaction before all O_2 can be consumed.

The data from Bryner, et al. (1994) shows that their carbon dioxide levels tend to rise faster, as described in Section 4.2.2.1, and are lower for equivalence ratios greater than one. This is due to their use of natural gas as a fuel, while the other studies used n-hexane pool fires. If yields data was available for these tests the variability due to fuel composition could be removed. The difference in fuels can also be examined by studying the stoichiometric molar flow rate equations for the two fuels for a 100kW fire, equations 30 and 31. The natural gas is mainly composed of methane (95%), so methane was used in its place for these calculations. The heat of combustion of methane is 50 MJ/kg while n-hexane is 44.7 MJ/kg, so a 100 kW fire requires 0.002 kg/s of methane and 0.0022 kg/s of hexane. In terms of molar flow rate (divide mass flow rate by molecular weight), this is 0.000125 kmol/s of methane and 0.0000256 kmol/s of hexane.

n-hexane combustion

$$0.0000256C_6H_{14} + 0.000243O_2 \rightarrow 0.000154CO_2 + 0.000179H_2O \qquad (30)$$

natural gas (methane) combustion

$$0.000125C_6H_{14} + 0.0025O_2 \rightarrow 0.000125CO_2 + 0.00025H_2O \qquad (31)$$

The ratio of the resulting molar flow rates for natural gas fueled fires to n-hexane fueled fires is 0.000125/0.000154 = 0.81. This indicates that the production of CO_2 in natural gas fires would be about 80% of CO2 production in the same size n-hexane fire. Figure 4.11 clearly shows this relationship for equivalence ratios of one and higher.

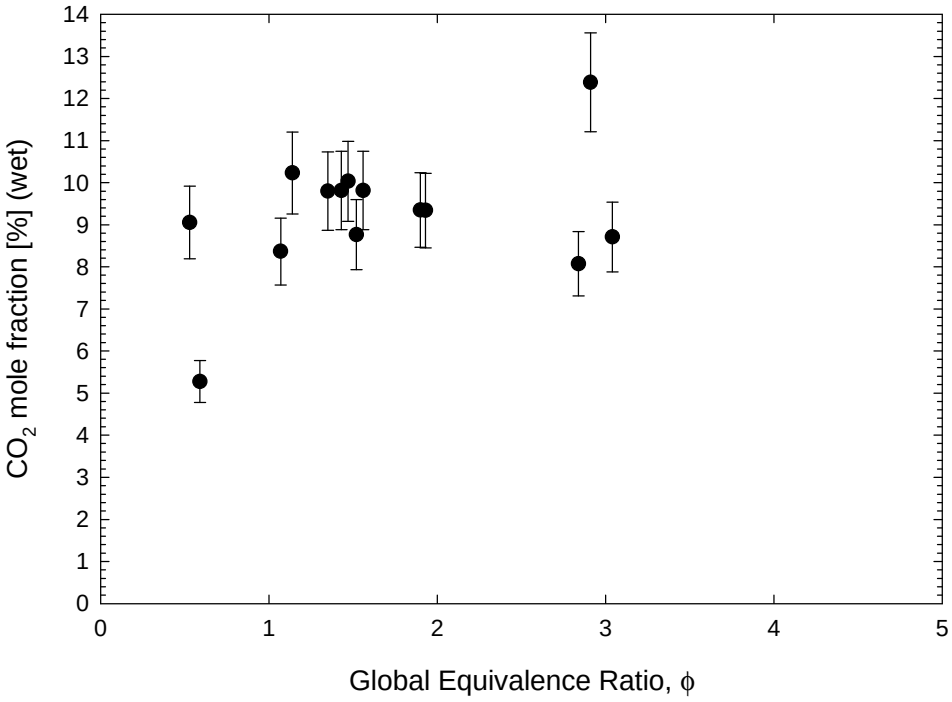

Figure 4.10 CO_2 mole fraction for varied global equivalence ratios

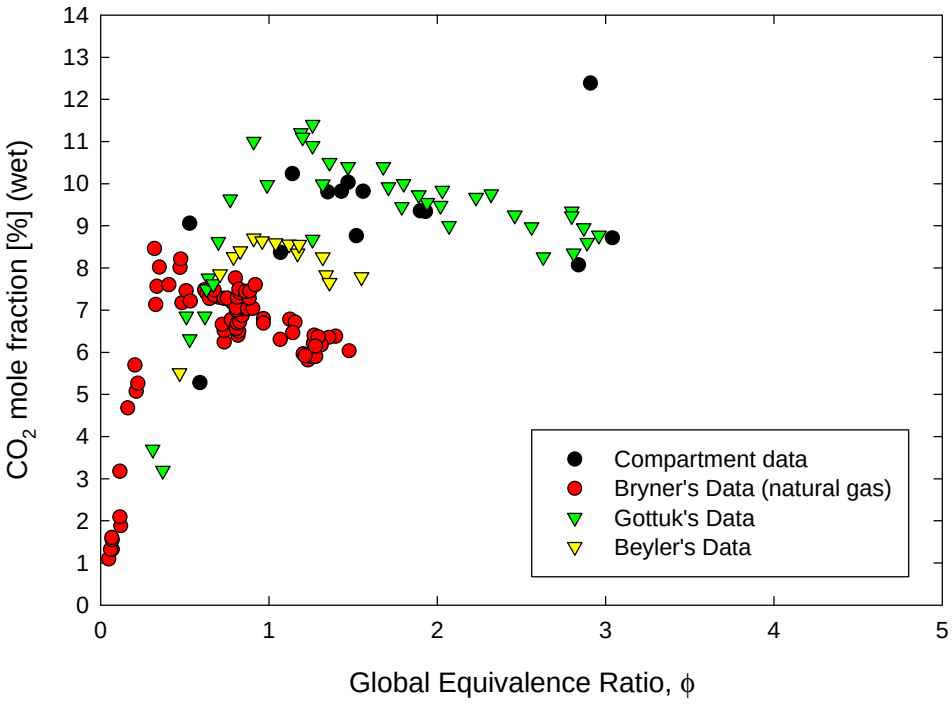

Figure 4.11 CO_2 data including Bryner et al. (1994) for natural gas, Gottuk et al. (1992), and Beyler (1983) for n-hexane studies

4.2.2.3 Oxygen

Data for O_2 presented in Figure 4.12 shows that the oxygen levels decrease rapidly from ambient levels to zero as the equivalence ratio rises to about 1.3 – 1.4. This corresponds to the underventilated fire condition ($\phi > 1$) where no free oxygen is expected to be found. The fact that the oxygen does not decrease to a mole fraction of zero until about $\phi = 1.2$ is probably due to some quantities of oxygen being entrained into the compartment upper-layer due to mixing. As the equivalence ratio increases, oxygen mixing into the upper-layer at the height where the gas probe is located ceases and the oxygen levels drop to zero. The measurement error for the O_2 data appears very small on Figure 4.12 and does not seem to be significant. This in fact is not the case when normalized O_2 species yields are examined in Section 4.2.3.2 and will be discussed further in that section.

Similar results reported by several other researchers, Bryner et al. (1994), Gottuk et al. (1992), as shown in Figure 4.13. Bryner's data tend to fall faster, for the reasons described in Section 4.2.2.1, and reach zero levels at $\phi = 0.6$. The hood fire data from Beyler (1983) shows that his mole fractions only reached a minimum mole fraction of about 3% instead of extending to zero as in other studies. This is due to the temperature of the upper-layer in his hood experiments, which was lower than the compartment studies by about 450K. As described in Section 4.2.1, reactions are "frozen out" in the upper-layer of the hood experiments before all available O_2 is consumed.

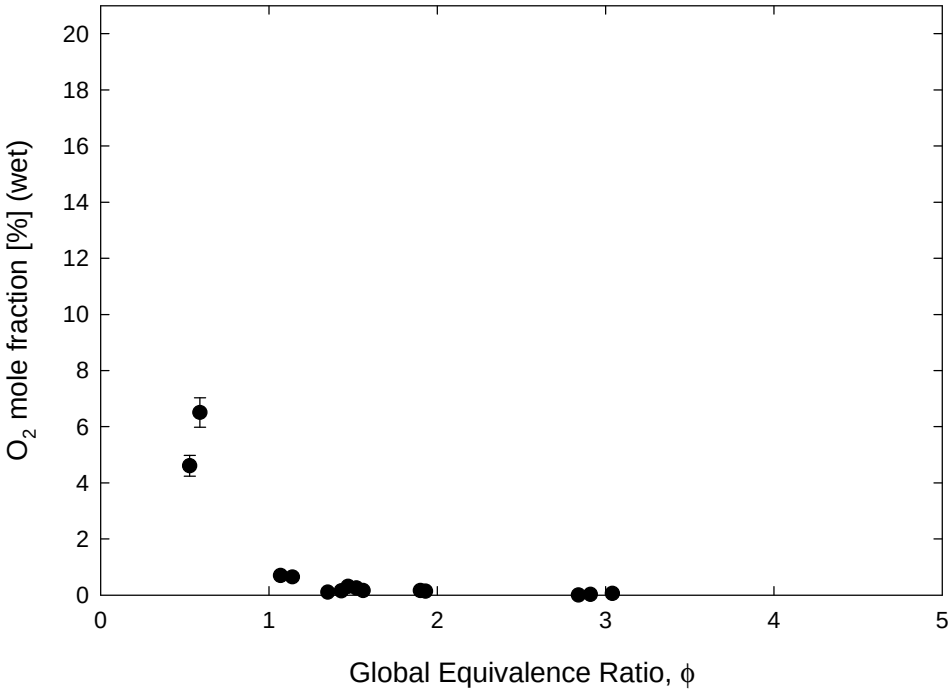

Figure 4.12 Compartment O_2 levels for range of equivalence ratios

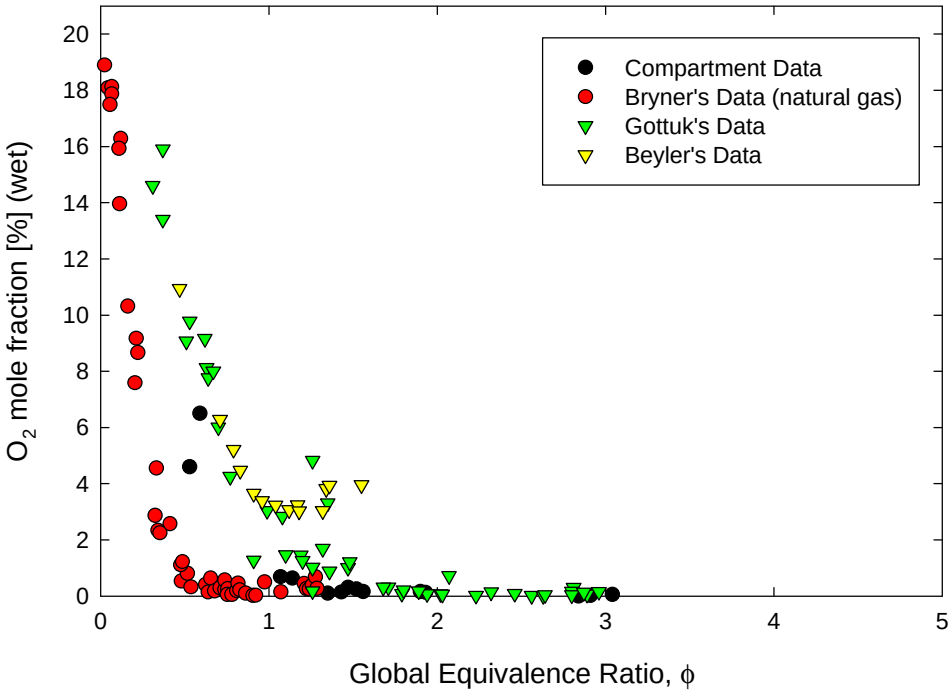

Figure 4.13 O_2 data including Bryner et al. (1994) for natural gas, Gottuk et al. (1992), and Beyler (1983) for n-hexane studies

4.2.2.4 Unburned Hydrocarbons

The data gathered during these experiments for mole fractions of unburned hydrocarbons (UHC), presented in Figure 4.14, shows that the levels of UHC stay at 0% until between an equivalence ratio above 0.6. At that point the combustion in the compartment upper-layer begins to become underventilated and the level of UHC increases. This increase is mirrored in the start of CO production discussed in Section 4.2.2.1 as these both result from the incomplete combustion. The levels then increase in mole fraction as the equivalence ratio increases, but no definite trends can be ascertained past an equivalence ratio of 3.0. The values at large equivalence ratios do not fall within the measurement error. This is probably due in part to the short quasi-steady state times described in

Section 3.5.1. Another factor is probably the span gas used, which was only 4.71%, while mole fractions up to twice that were measured.

This trend is also observed in the data of Gottuk et al. (1992), Figure 4.15, although his data does not show as much scatter at higher equivalence ratios. Beyler's data shows a divergence from the other comparable data as the percentage of unburned hydrocarbons rises faster than the two compartment studies above an equivalence ratio of about 0.8. This is again probably due to the cooler upper-layer temperature present in Beyler's hood experiments, which would not allow the oxygen and fuel to react as well in the upper-layer. This would reduce the oxidation of the fuel, thus increasing the levels of unburned hydrocarbons. For lower equivalence ratios there is no divergence because all of the combustion of the fuel occurs closer to the fuel source where temperatures remain hotter.

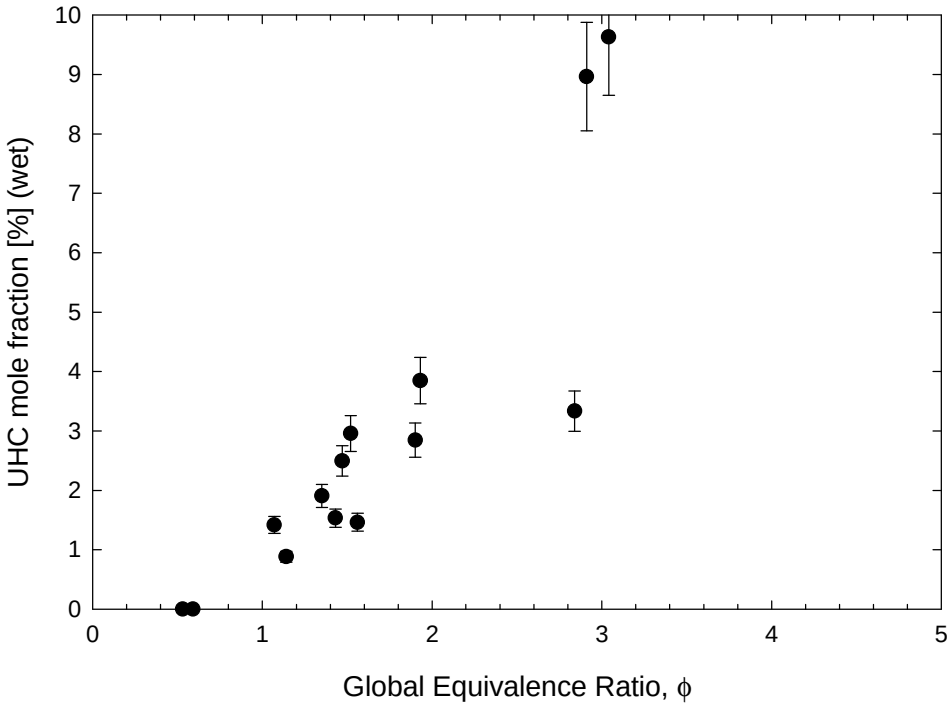

Figure 4.14 Unburned hydrocarbon levels for varied global equivalence ratios

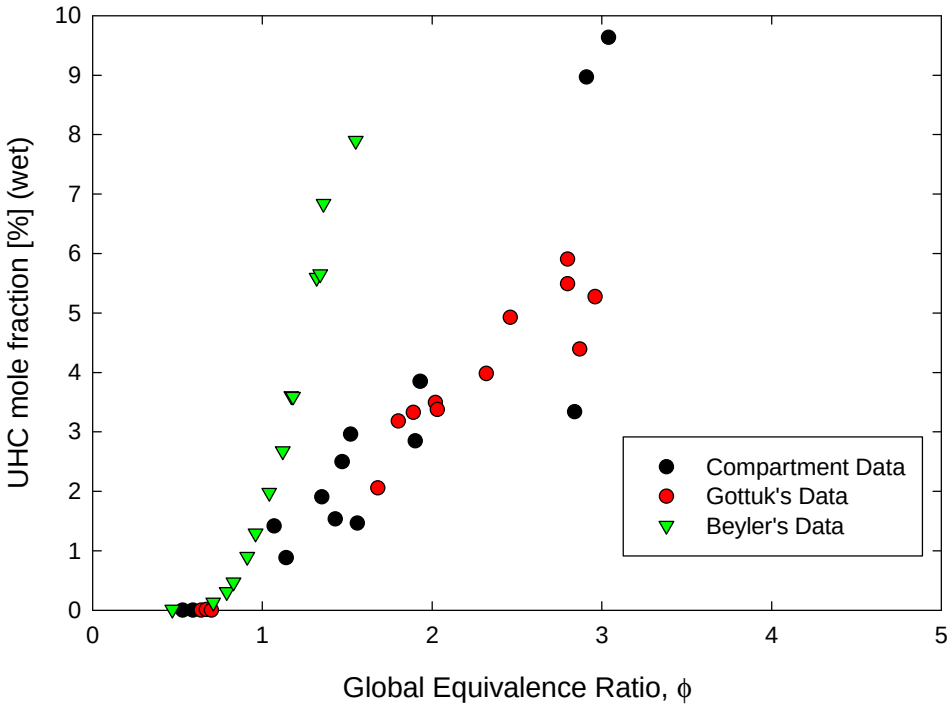

Figure 4.15 UHC data including Gottuk et al. (1992), and Beyler (1983)

4.2.3 Species Yields

The species yields are calculated for each species as shown in Section 3.5.5. These yields describe the production and consumption of species in fires. These species yields represent the individual species production relative to the fuel volatilization rate, except for O_2, which the yield represents the consumption of O_2 relative to the fuel volatilization rate.

4.2.3.1 Carbon Monoxide, Unburned Hydrocarbons, and Carbon Dioxide

The calculated yields are shown in Figures 4.16 and 4.17 and 4.18 for CO, UHC, and CO_2 respectively, with the CO_2 yield shown normalized. The yields for CO and UHC have much scatter in the data and only trends can be noticed. The CO yields increase to a maximum value around $\phi = 1.4$ and then begin to decrease. A similar trend was reported

by Gottuk, et al (1992), although his data peaked at $\phi = 2.0$ and does not show as much of a decrease thereafter. At equivalences ratios above this the dilution of the upper-layer gas with UHC causes CO yields to decrease while UHC yields continue to increase as shown in Figure 4.17. The data from Beyler (1983) seems to level off sooner at around $\phi = 1.0$ at lower yield vales for CO. This again is due to the upper-layer in the hood freezing out oxidation reactions.

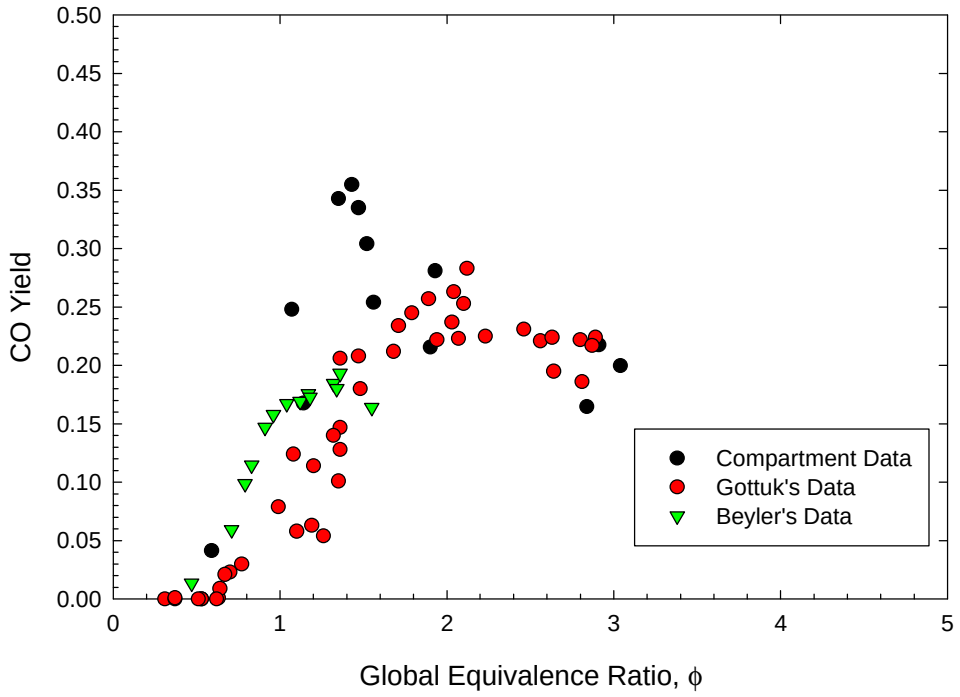

Figure 4.16 CO yields from Compartment Study

The UHC yields continue to trend higher as equivalence ratio increase for all studies as shown in Figure 4.17. The wide scatter in the data from this compartment study matches the scatter reported in the UHC mole fraction data, Section 4.2.2.4. Gottuk's data on the other hand is grouped tighter at the higher equivalence ratios. The data from Beyler rises faster than the other studies, which is due to the cessation of fuel oxidation in his hood's cooler upper-layer.

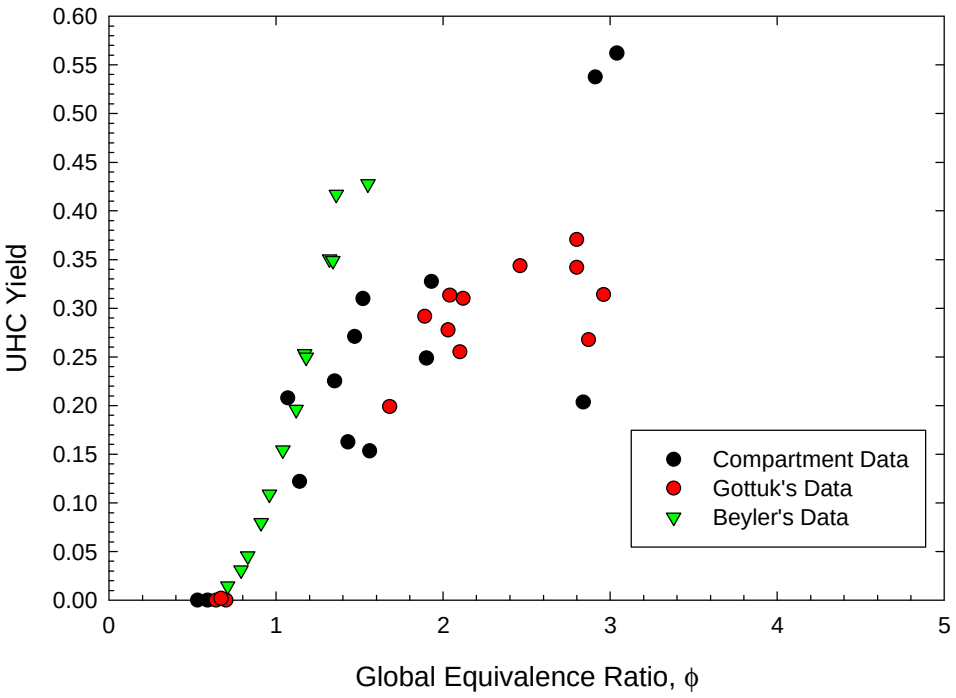

Figure 4.17 UHC yields from Compartment Study

The CO_2 yield data, shown if Figure 4.18, is plotted normalized and additionally the complete combustion model for CO_2 production is shown. Two data points from this study and one from Gottuk et al. (1992) are above the complete combustion model so probably indicate a measurement error. They are also consistent with outlying points in Figure 4.10, showing abnormally high CO_2 mole fractions relative to the data trends. Other wise the data follows a decreasing trend matching the shape of the complete combustion model line. The data from Beyler (1983) is lower than most of the other data after about $\phi = 0.8$. This is probably due to less oxidation of fuel into combustion products such as CO_2 in the upper-layer of his hood experiment.

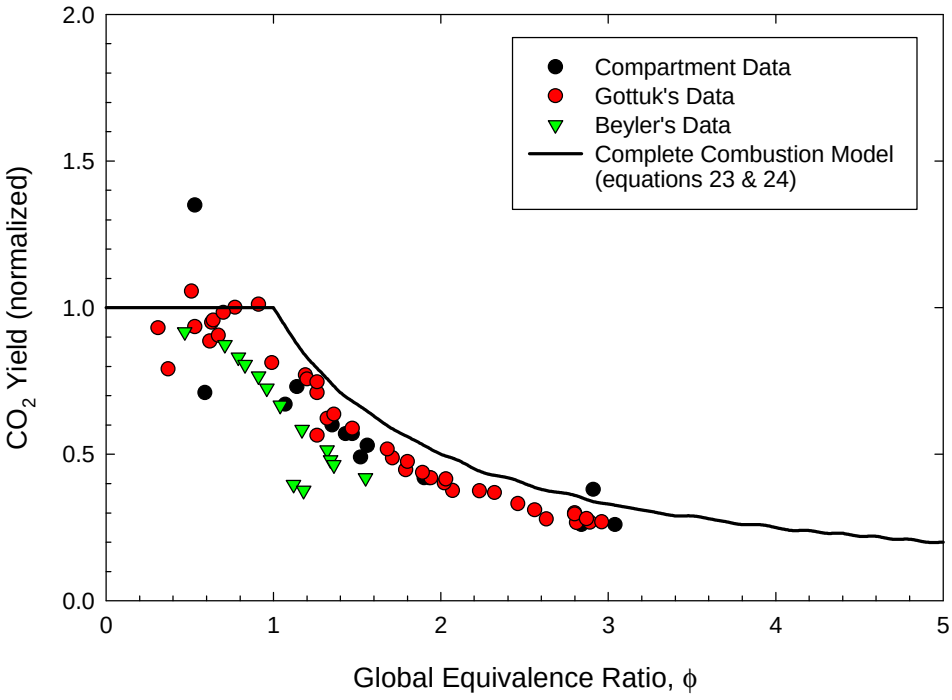

Figure 4.18 Normalized CO_2 yields from Compartment Study

4.2.3.2 Oxygen

The normalized O_2 yields, shown in Figure 4.19, show a decreasing trend as the equivalence ratio increases and follow the trend outlined by the complete combustion model for O_2 consumption. Two data points from this study were way above the complete combustion model O2 consumption for low equivalence ratios indicating that there was probably measurement error in those readings. Again the data from Beyler (1983) is lower than the other reported studies due to the reduced oxidation caused by lower upper-layer temperatures in his hood experiments.

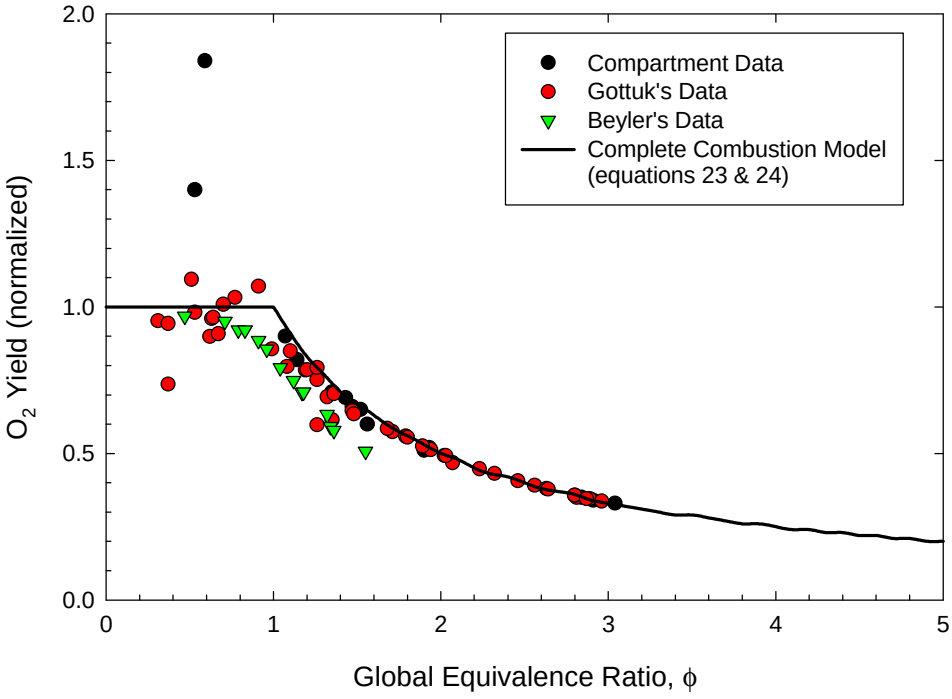

Figure 4.19 Normalized O_2 yields from Compartment Study

4.2.4 Doorway Neutral Plane Height

The doorway neutral plane height during the quasi-steady state period of the fires is the height of the interface between the ambient air entering the compartment and the hot combustion products exiting the compartment at the doorway. The velocity at this point is zero with outflow of combustion gases above the neutral plane and inflow of outside air below it. These calculated values were first normalized by the height of the compartment doorway as z_n/H. The values for the range of global equivalence ratios tested are shown in Figure 4.20. This data shows that the neutral plane height decreases to a fairly steady normalized value, 0.42, as the fire size increases. This constant value begins at approximately the equivalence ratio where the fire begins to become under-ventilated, 1.0-1.2, and is plotted in Figures 4.20 and 4.21 as a dotted horizontal line. These values were determined by calculations using the routine developed by Janssens and Tran (1992) and were verified both visually during fire tests and using photographs. One of these photographs is included as Figure 4.22 showing the fully developed fire (ϕ =

1.28) during one of the early compartment experiments. This result is also consistent with the neutral plane height calculations presented by Drysdale (1998), who reported that the neutral plane height should be 3/10 – 5/10 of the doorway height. For the compartment this works out to a normalized height of 0.30– 0.50, which is consistent with the heights determined in this study.

It is also helpful to look at the vertical distribution of temperature readings on the thermocouples mounted in the compartment doorway during the quasi-steady state burn time in the compartment. Those readings for one under-ventilated case (ϕ = 1.28) are presented in Figure 4.21, and show that below approximately 0.345m (normalized to 0.42) the doorway gas temperatures are only moderately above ambient (up to 435K). This indicates that the gases below that level are cooler air flowing into the compartment. Above that point the gas temperature rises very quickly, indicating that at those doorway heights the temperature is from hot gases exiting the compartment.

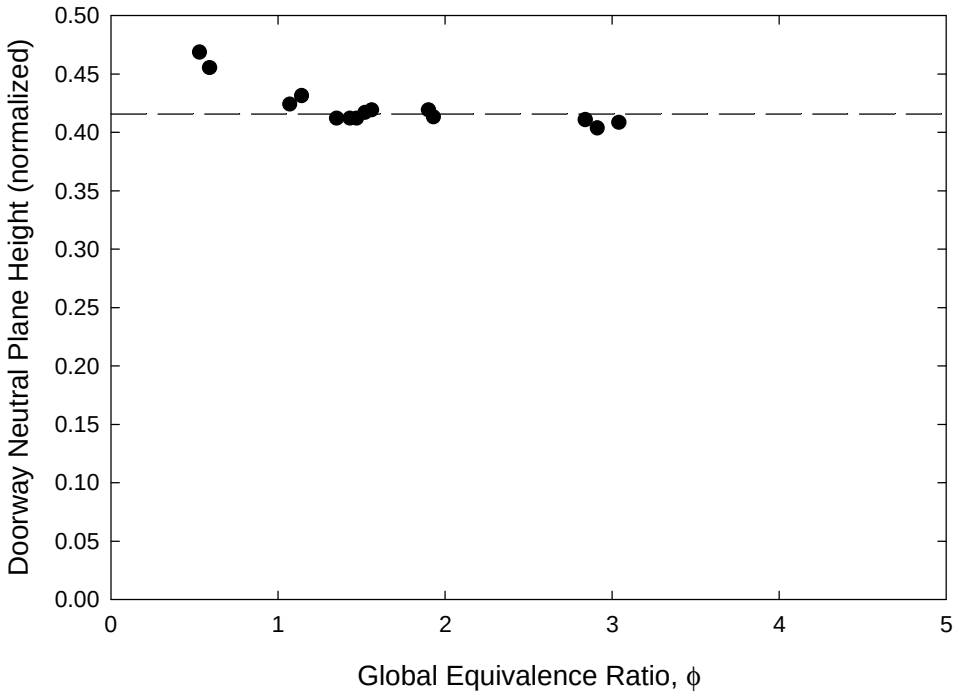

Figure 4.20 Normalized neutral plane height in compartment doorway

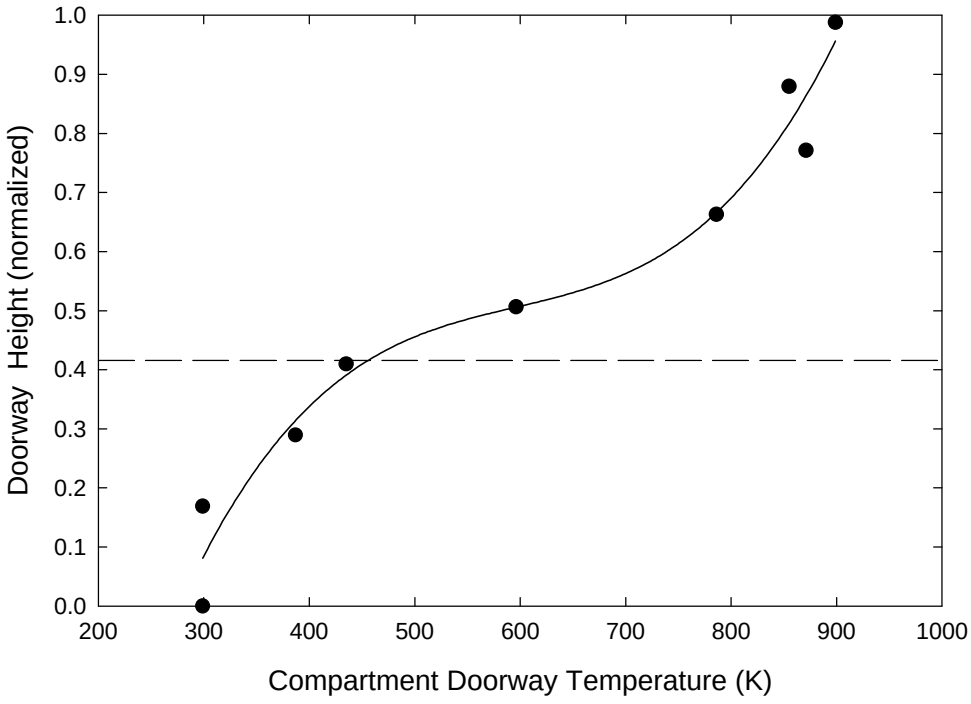

Figure 4.21 Doorway temperature profile during compartment quasi-steady state (case: $\phi = 1.28$), note 300K is ambient temperature

Figure 4.22 Fully developed compartment fire, $\phi = 1.28$, showing doorway neutral plane and upper-layer depth

4.2.5 Door Flow Rates

The airflow into the compartment for the range of compartment equivalence ratios tested in shown in Figure 4.23. The figure shows that the air entrainment rate remains constant as equivalence ratio increases. This indicates that the doorway dimensions limit the rate of air entering the compartment. Since fire size and global equivalence ratios are linearly related (Section 4.2.6), the airflow into the compartment would also remain constant across the tested fire sizes. This was also reported in the work of Nakaya et al (1986), shown in Figure 4.24. They reported similar trends of almost constant mass flow for a given door width and increasing flow through a series of wider doorways. Their range of flow rates is much higher because they used a full size compartment. The maximum airflow (ventilation limit) into the compartment for under-ventilated fires is reported by Drysdale (1998), to be given by equation 32.

$$\dot{m}_{air} \approx 0.52 A_{door} H_{door}^{1/2} \qquad (32)$$

This predicts a ventilation limit of airflow into this study's compartment of 0.13 kg/s, represented with a dashed line in Figure 4.23, to which the calculated airflow approaches. The equation also shows that the ventilation limit is only dependent on the doorway geometry. If the doorway width was held constant and doorway height were doubled to 1.66m (similar to Nakaya et al., 1986) it would suggest that the airflow into the compartment should increase to about 0.37 kg/s. This result is very consistent with interpolating Nakaya's data between doorway widths of 0.29m and 0.44m on Figure 4.24.

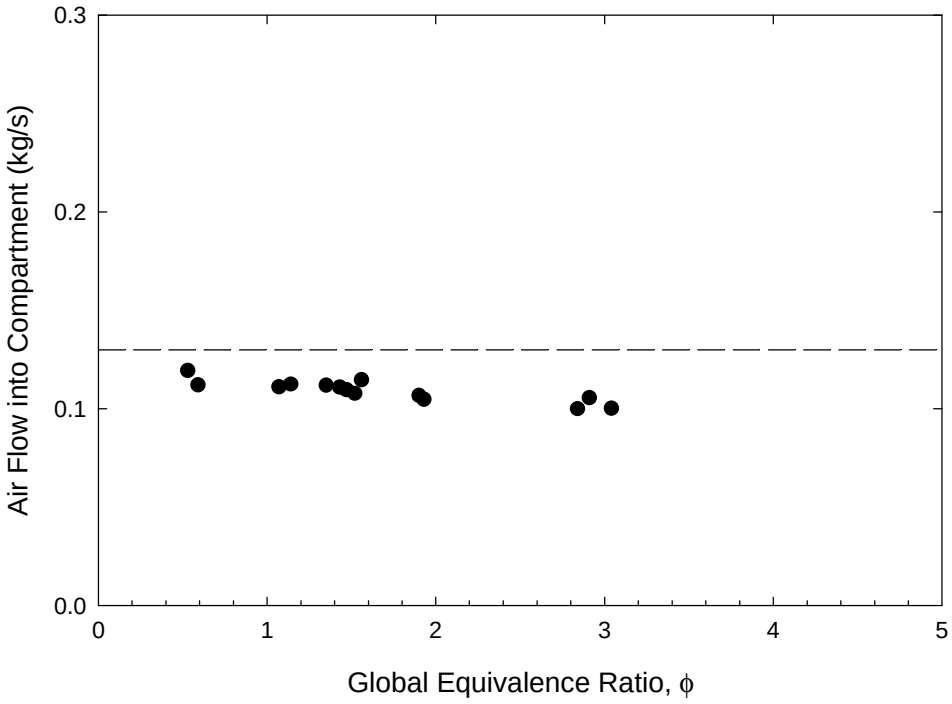

Figure 4.23 Airflow into compartment for varied global equivalence ratios

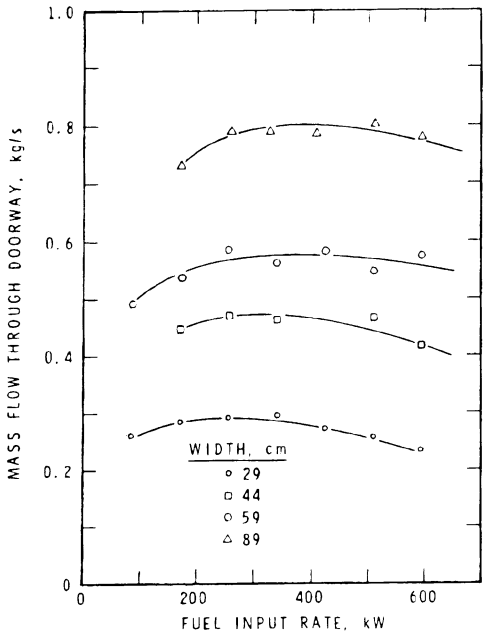

Figure 4.24 Nakaya et al (1986) “Measured opening flow rates versus fire burner intensity”

4.2.6 Fire Size

The fire size (ideal), based on measured fuel evaporation rates, was looked at with the GER. The result was a linear correlation, Figure 4.25, which indicates that the airflow rate into the compartment is relatively constant and an increase in fire size is directly proportional to an increase in equivalence ratio. A larger door would allow a higher airflow into the compartment and increase the slope of the fire size/GER plot. As discussed in Section 4.2.5, the airflow into the compartment is dependent on the geometry of the doorway.

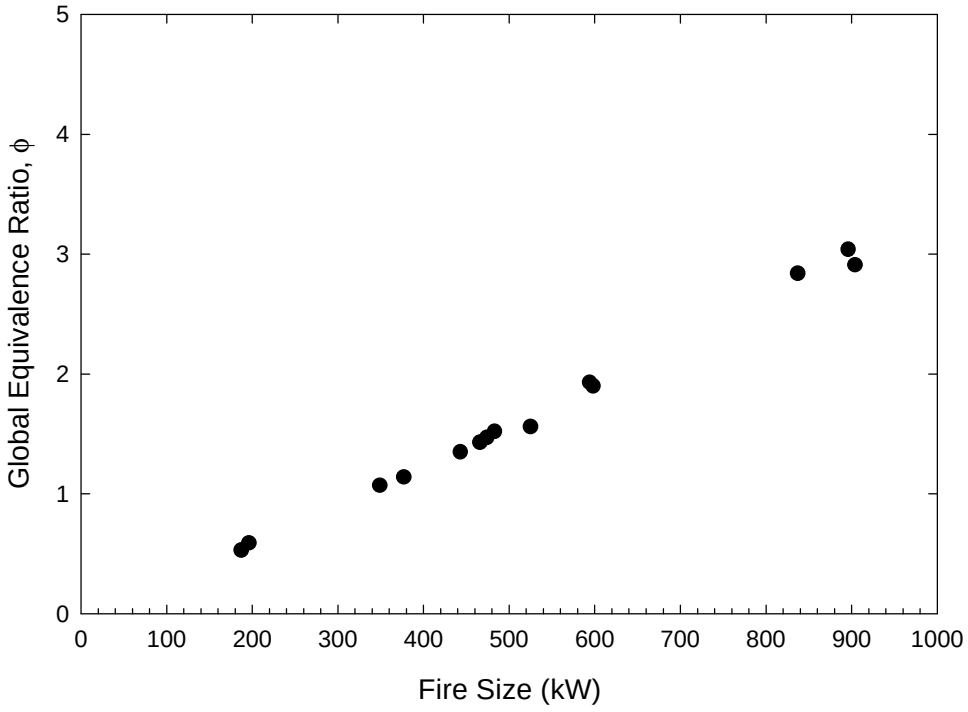

Figure 4.25 Relationship between fire size and global equivalence ratio

4.2.7 Carbon Error

The accuracy of the measurements of species and mass flow rates was examined using the carbon balance method (Equation 29), and the results are plotted in Figure 4.26. This

graph shows generally low carbon error, except as the equivalence ratio approaches zero and at $\phi = 2.85$ (expected range of 0-30%).

The high error at the low equivalence ratios is probably due to the very small fuel vaporization rates, which magnifies any error in species measurement. Equation 29 in Section 3.5.8 shows that the measured species (UHC, CO, CO_2) carbon would dominate the calculated carbon error when the fuel vaporization rate is small. The data point with the worst error for low equivalence ratios corresponds to an outlying data point in Figure 4.18 of CO_2 yield.

The largest outlying point at $\phi = 2.85$ also corresponds to an outlying data points in the plots of UHC mole fractions and yields, Figures 4.14 and 4.17. The trend indicated in Figure 4.14 shows this reading was far lower than it should have been and this could be caused by measurement or calibration error in the FID reading for that test.

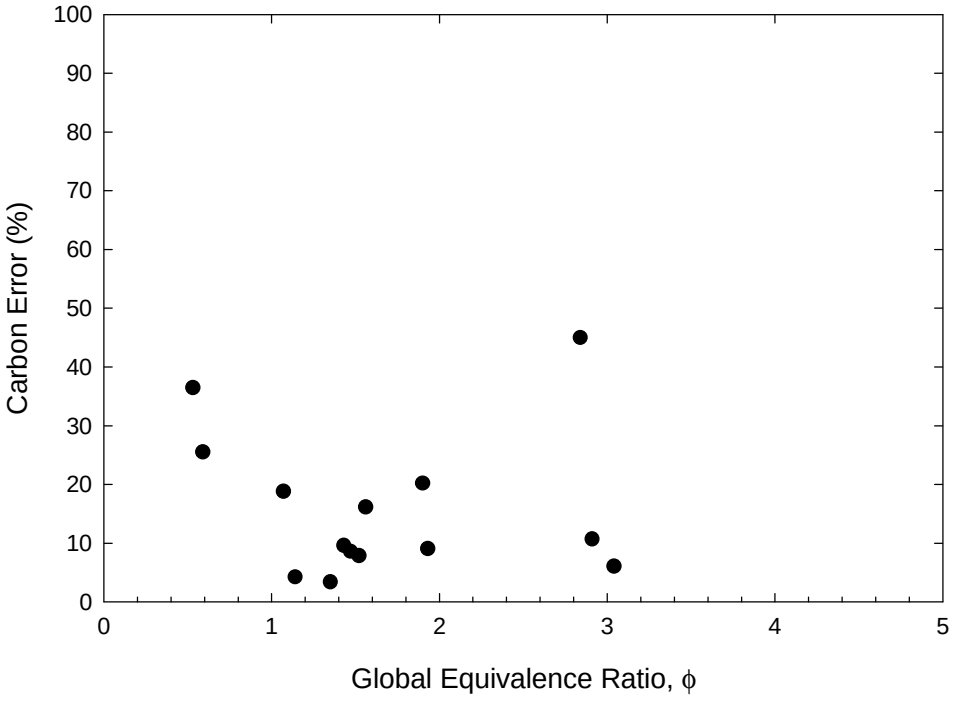

Figure 4.26 Carbon error for varied global equivalence ratios

5 Heat Transfer to an Attached Hallway from a Burning Compartment

The heat transfer study used the same compartment/hallway configuration previously reported in the work of Lattimer (1996) and Lattimer et al (1996 a, b), which consisted of a vented compartment attached to the side of a hallway. Experimental conditions were chosen to mirror the conditions studied by Lattimer so that heat transfer data could be compared to his species mole fraction data. Two cases were examined, first the heat transfer in a hallway with a thin upper-layer and secondly a case with a thick upper-layer. In both cases conditions were used which produced burning external to the compartment in the hallway. The heat transfer was measured and mapped along the ceiling of the hallway, on the sidewall of the hallway opposite the compartment, and along the floor of the hallway. The data is presented as contour maps and compared to mapping performed previously by Lattimer of the species mole fractions for the same conditions.

5.1 Introduction

During the residence of the hot gases in the hallway heat transfer with the walls, ceiling and floor takes place via radiation and convection. There are very few publications in the literature dealing with experimental measurements of heat flux to the surrounding surfaces in the enclosure fires. Mostly, the researchers used detailed heat balance calculations to estimate the level of heat flux. Hinkley et al. (1968 and 1984) studied the heat flux at a few points of the combustible and non-combustible ceiling in a corridor with a gas or wooden crib fire located at the dead end. Water flow calorimeters and copper block calorimeters were used as measurement devices.

Thomas et al. (1965) studied radiative heat flux from pre-flashover compartment fires to the floor trying to relate measured heat transfer levels to the flashover phenomenon. Babrauskas (1982) mapped the distribution of radiative heat flux around items of burning furniture in conjunction with studying fire spread from one fuel “package” to the next. In

a somewhat similar study, Gill et al. (1983) measured heat flux to objects located next to jet fuel pool fire using thermocouple-based calorimeters.

Quite extensive numerical and experimental study of the heat transfer from a buoyant plume in the enclosure fires was performed by Cooper et al. (1982a, 1982b, 1989). Heat transfer from methane flames to the ceiling of different compartment-hallway configurations was studied (1982b) using optical photometers. The major goal was to estimate the development of hazardous conditions in real fire scenarios (not related to toxic species mole fractions).

Comitis et al. (1996) performed an interesting theoretical and experimental study of temperature profiles and heat transfer in a horizontal "fire tunnel", measuring temperature distributions on the walls of the 300x30x7.5 cm tunnel with a moving reacting flow inside.

It was shown by Cooper et al. (1982b), Cooper (1987), and Cooper (1989) that in compartment fires the total heat transfer from the fire plume driven ceiling and wall flows to the enclosing surfaces can be a significant fraction of the fire total energy release. The role of heat transfer in the evolution of the carbon monoxide levels during compartment fires needed, therefore, to be examined.

The focus of this heat transfer study has been the heat flux from the compartment fire exhaust gases to the hallway surfaces. Specifically, it addressed total heat flux from the upper-layer in the hallway to the ceiling, walls and floor.

5.2 Experimental Setup and Techniques

The experiments were conducted with the 1.52 m wide, 1.22 m deep and 1.22 m high compartment connected to the side at the end of the 1.22 m wide, 1.67 m high and 5.18 m long hallway, forming a L-shape, shown in Figure 5.1, which was the same configuration as in the experiments reported in Lattimer (1996) and Lattimer et al. (1996a, b). Air was

naturally drawn into the compartment through a plenum below the compartment, while the combustion gases exited the compartment into the hallway through a vent. The size and location of the vent could be varied by installing soffits, termed the inlet soffit, of different height and shape. For this study, the opening size of 0.12 m^2 (0.5 m wide, 0.24 m high) was chosen, as it corresponded to one of the most representative cases in the earlier CO mole fraction study of Lattimer et al (1996a, b). The soffit at the open end of the hallway, termed the exit soffit, was set at 0.6 m, or was not used at all. The exit soffit height governed the depth of the upper-layer in the hallway.

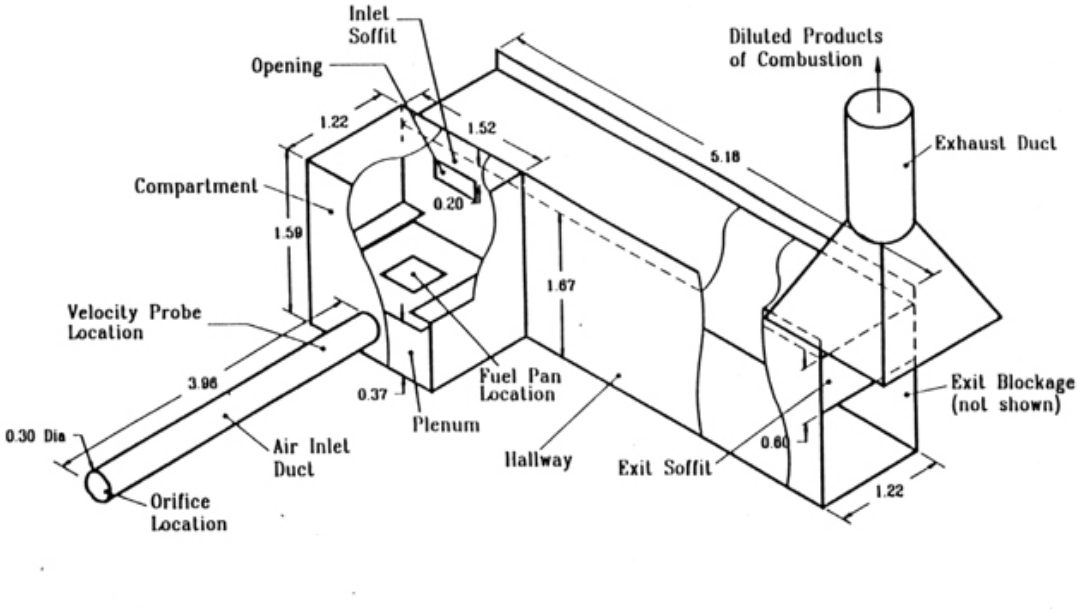

Figure 5.1 Experimental facility used in heat transfer study

Two types of heat flux gages were used in this study. Heat flux to the floor was measured using water cooled Gardon type gages, manufactured by Medtherm Corporation, while heat flux to the ceiling and the walls of the hallway was measured using the heat flux microsensors, manufactured by Vatell Corporation.

The Gardon gages, Figure 5.2, absorb heat into a thin metallic foil and transfer it radially to the heat sink attached to the periphery of the foil. The transducer provides a self-generated output which is directly proportional to the heat flux level. These gauges were painted black with a special flat black paint that came with them. The black paint ensured that total heat flux was measured by eliminating reflection of heat flux from the

gauge back to the surroundings. The response time for this type of gage is less than 300msec. Gordon gages require water cooling if the temperature of the surface reaches over 200 C, which was a definite possibility in the tests that were run. That requirement led to the construction of a water cooling system with flexible pipe lines to the gages.

Three Gardon gages were used in this study. One of them was placed 10 cm above the floor directly beneath the center of the compartment vent and was used for reference purposes. This was to ensure similarity between the runs required to complete the hallway mapping study. The other two were mounted on the traversing mechanism of a sampling cart 30.5 cm apart from each other and 15 cm above the floor, which allowed for movement around the hallway. Sampling of the heat flux to the hallway floor was taken at twenty one location in the hallway, including the one directly under the compartment vent. The sampling cart was constructed of thick steel with wheels and allowed the mounting of various sensors, including the heat flux gauges. In previous work by Lattimer (1996) the cart was used for mapping of the vertical temperature profiles and species mole fractions in the hallway.

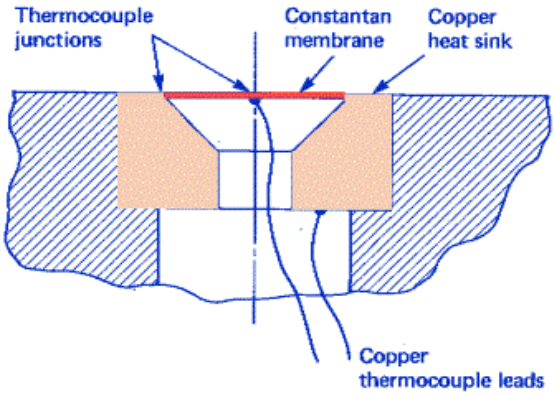

Figure 5.2 Diagram of the Gardon type gage

A special attempt was made to account for the radiation reflected from the floor back into the hallway. For this purpose one of the cart-mounted gages was turned facing the floor. It was quickly found that the reflected radiation level was within the noise level of the

measurement technique; therefore these measurements were discontinued, as the level of reflected heat flux was deemed negligible. The gage was returned to the upward facing position and used in the hallway mapping.

Levels of heat flux to the walls were measured with four heat flux microsensors (Figure 5.3), model HFM-6C/L., which uses two thermopiles. The thermopiles are arrays of thermocouples and are separated by an insulator. When heat flows into or out of the sensor small temperature differences are measured across the insulator and each thermocouple pair produces a small voltage proportional to the heat flux. These voltages are summed across the thermopile and indicate the magnitude and direction of the heat flux.

These gages were designed and manufactured by Vatell Corp. The sensor had a rapid response time of 6 μsec and sensitivity of 30 $\mu V/W/m^2$. The gages also incorporated an RTS (resistance temperature sensor), which is a platinum resistor surrounding the heat flux sensor and measuring the surface temperature of the gauges. This surface temperature was used to correct the output signal of the heat flux sensor for variation in conductivity of the insulator as a function of temperature.

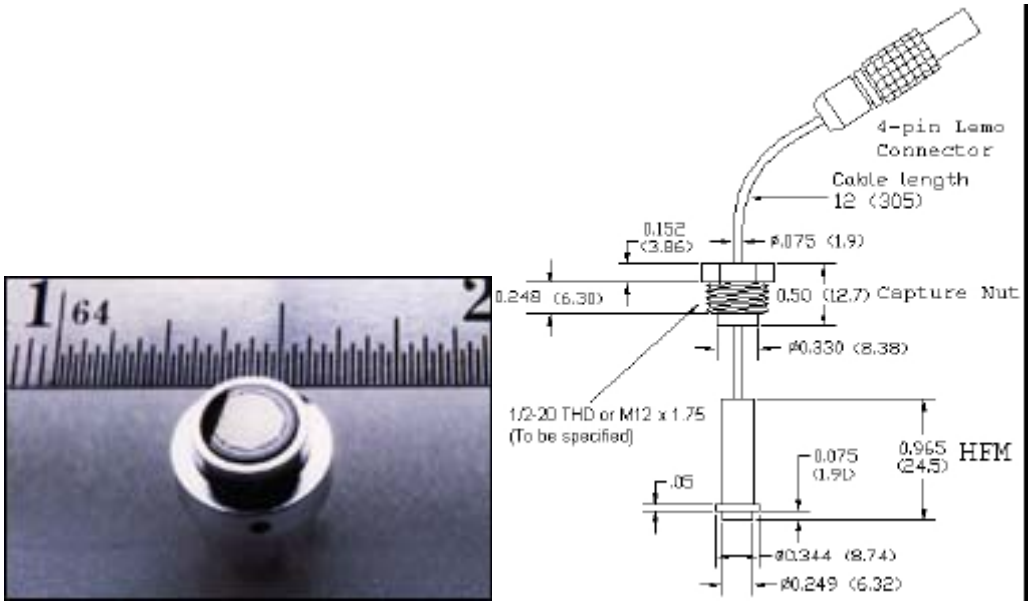

Figure 5.3 Picture and diagram of the HFM-6 microsensor by Vatell

Four gages of this type were sequentially placed in a grid of thirty two different locations on the ceiling of the hallway, mounted flush with the ceiling. Heat flux was also measured at sixteen locations on the wall opposite the compartment, using the same mounting technique. These locations are shown in Figure 5.4 along with the floor sampling locations. These heat flux gauges were also thinly coated with flat black paint so that the total heat flux could be measured. Nitrogen purging across the face of the sensors was implemented to ensure that the gages were not affected by soot in the hallway.

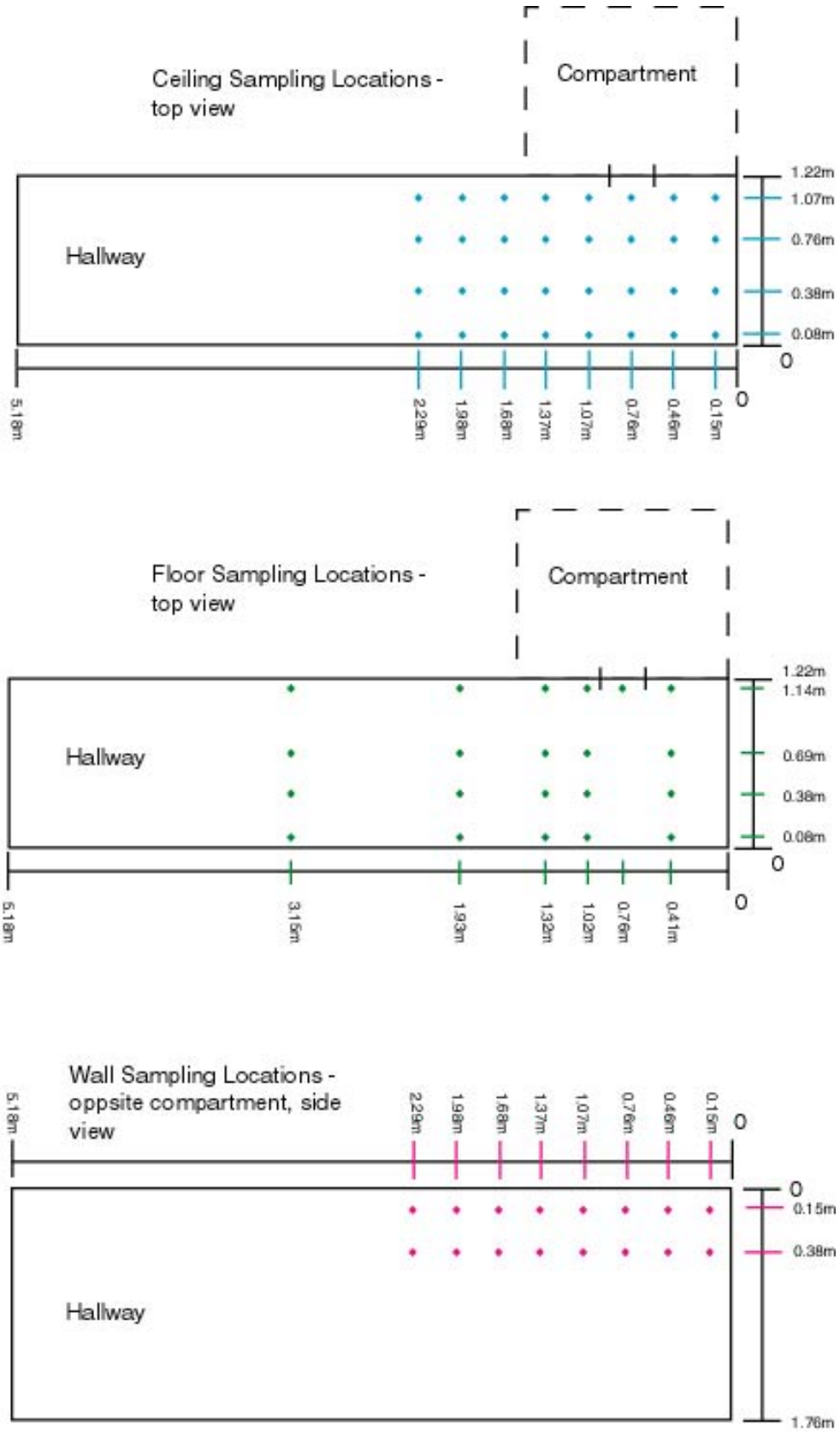

Figure 5.4 Heat flux sampling locations in hallway ceiling, floor, and wall

5.3 Experimental Parameters, Conditions and Procedures

A 0.12 m^2 opening and a 0.2 m inlet soffit were used in all experiments described in this chapter. Since it was desirable to have external burning in all tests, 2 sets of conditions were selected from the previous CO transport study of Lattimer, et al. (1996a, b). These conditions provided an equivalence ratio of about 3.0 +/- 0.5, resulting in high levels of unburned hydrocarbons (UHC) and CO entering the hallway. In order to study the influence of the upper-layer depth on the heat transfer in the hallway, the soffit height at the exit of the hallway was varied. Specifically, the mapping of the hallway was carried out without the exit soffit and with an exit soffit 0.60 m high.

The heat flux measurements were taken at the same (or as close as possible) locations, used for the CO mole fractions mappings in the earlier study of Lattimer et al. (1996a, b) in an attempt to relate the measured heat fluxes to previously measured CO mole fractions. Lattimer took his entire hallway upper-layer mapping measurements at elevations of 5 cm below the hallway ceiling, although in some of his other studies he examined the vertical variations in gas mole fraction for selected sections of the hallway. The data being used in this comparison only represents the measurements of species present in the hallway upper-layer mapping location 5cm below the hallway ceiling.

The experiments showed that when sustained external burning occurred, the heat flux levels would reach steady state approximately 30 seconds after flashover in the compartment. The steady state duration was about 60-80 seconds, during which the data reported below were acquired. This time period was compared to the steady state periods reported by Lattimer, et al. (1996a, b) using his definition of “steady state” as described in Section 2.5.1. The exact facility and conditions were used to ensure repeatability of conditions between Lattimer and this study. The equivalence ratio was also verified to correspond to Lattimer’s work and checked throughout the study to ensure consistency between the fires in the study.

5.4 Heat Flux Measurements

Results are presented for two upper-layers characterized by the non-dimensional upper-layer depth, $\gamma=\delta/z$, where δ is the upper-layer depth and z is the distance from the ceiling to the vent bottom or door neutral plane, see Figure 5.5.

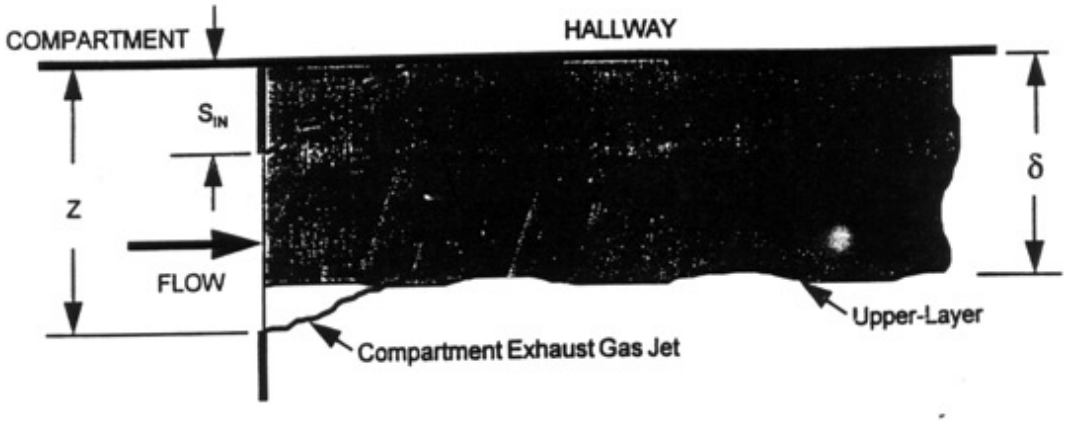

Figure 5.5 Definition of nondimensional upper-layer depth

Case 1: No exit soffit case (g=0.45)

The contour maps of the measured heat fluxes to the ceiling, floor and opposite wall of the hallway with no hallway exit soffit height are shown in Figures 5.6, 5.7, 5.8 for the ceiling, floor and side wall respectively. The gases exiting the compartment for this case have significant burning in the hallway upper-layer. The center of the compartment opening is located at 0.6m on the horizontal of all the plots of the hallway.

The heat flux contours shown in the ceiling and floor mapping clearly indicate the large amount of heat flux was produced by the burning jet exiting the compartment. The high heat flux (about 30-40 kW/m^2) is measured in the area across the hallway of the compartment exit and spreads down the opposite wall. This is consistent with visual observations of the fire and with the movement of the exiting jet as documented by Lattimer (1996). Lattimer noted for this configuration that flames extended out of the compartment vent, 1.22m across the hallway, impinged on the opposite wall, then extended an additional 1.22m down the hallway. Another flaming region was located in the closed end of the hallway where upper-layer gases recirculate. Lattimer also determined that the bulk of the combustion gases exiting the compartment impinge on the wall opposite the compartment and form a rotating vortex. The vortex motion transports the hot combustion gases down the hallway wall opposite the compartment. Figure 5.10, from Lattimer's work, illustrates this combustion gas movement in the hallway. The gases not transported toward the open end of the hallway are transported to the closed end and recirculate in that area.

A region of high heat flux (>$10kW/m^2$) can be seen extending along the wall opposite the compartment in Figure 5.6. This extends for just over a meter, the same distance the flame length extended down the hallway. This high heat flux is also seen in the closed end of the hallway where significant flames were observed.

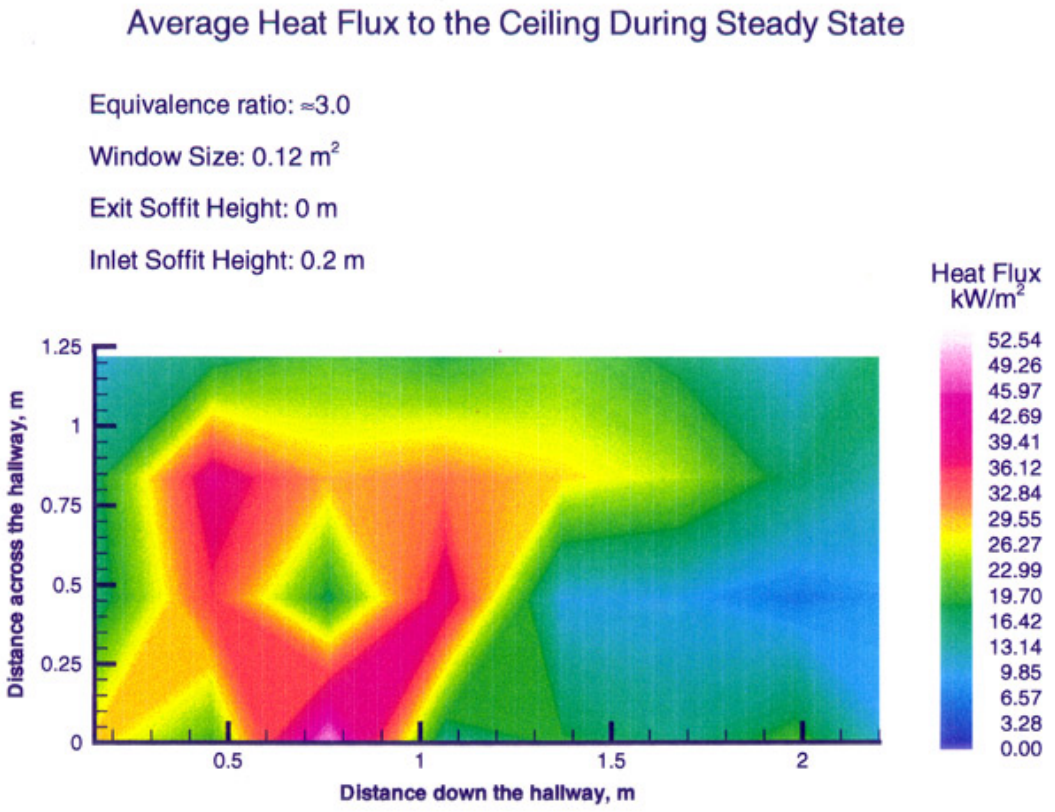

Figure 5.6 Average heat flux to the ceiling, case with no soffit

The heat flux to the ceiling, Figure 5.6, is significantly higher compared to the floor, Figure 5.7, due to the proximity of the flame sheet to the ceiling, while being over a meter away from the floor.

Another factor is the contribution of convective and conductive heat transfer from the hot gases near the ceiling to the heat flux gauges, while the floor mounted gages are located in cooler air add record mainly radiative heat flux.

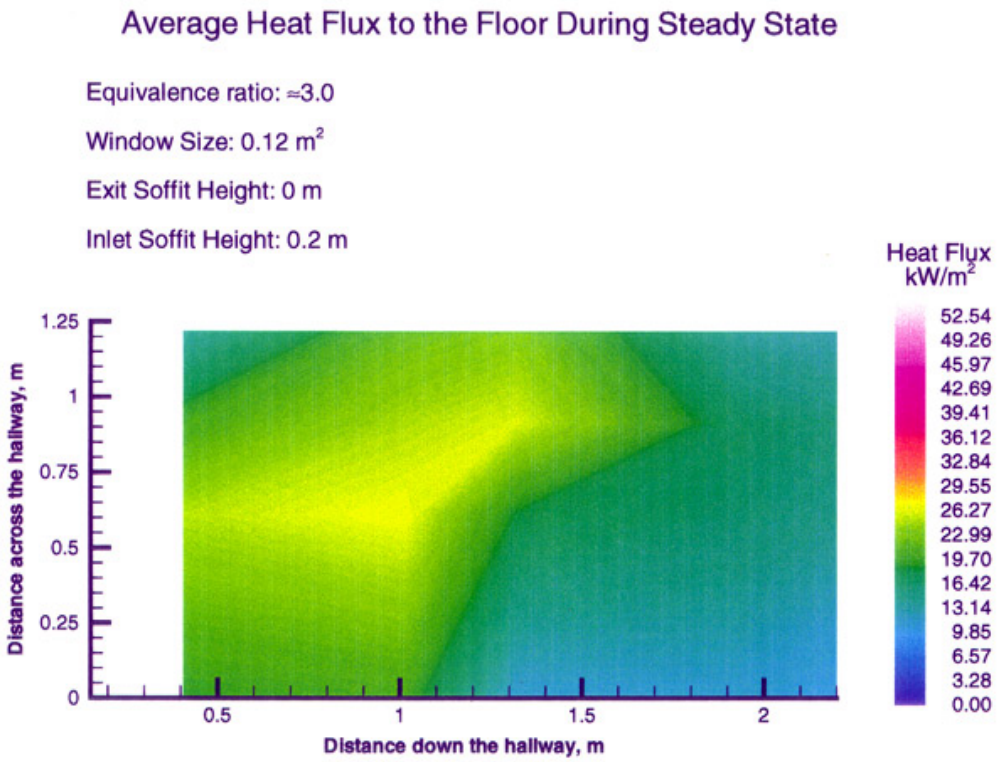

Figure 5.7 Average heat flux to the floor, case with no soffit

The mapping of the wall opposite the compartment, Figure 5.8, was performed from the ceiling height (1.67 m high) down to a depth of 0.66m. This shows that the area directly across from the compartment, at 0.7m down the hallway, receives the highest heat flux of 40 kW/m^2. This is the area where the jet exiting the compartment impinges on the opposite wall and forms a vortex. This wall also shows tha the flames continued down the hallway, documented by heat fluxes greater than 10kW/m^2.

A map of CO mole fractions 5 cm below the ceiling in the hallway for the same set of experimental parameters and at the same locations as the heat flux measurements were recorded by Lattimer, and are shown in Figure 5.9. This figure clearly shows increased CO in the hallway upper-layer exiting the compartment and traveling across and then down the hallway. The levels are reduced as the gases move across the hallway from the compartment indicating that the CO is being oxidized to CO_2 through O_2 entrainment into

the plume ceiling jet. This oxidation is an exothermic reaction, which releases significant heat, explaining this increased heat flux. Outside the flaming, temperatures are not sufficient to support oxidation reactions and the areas without flames show a reduced heat flux.

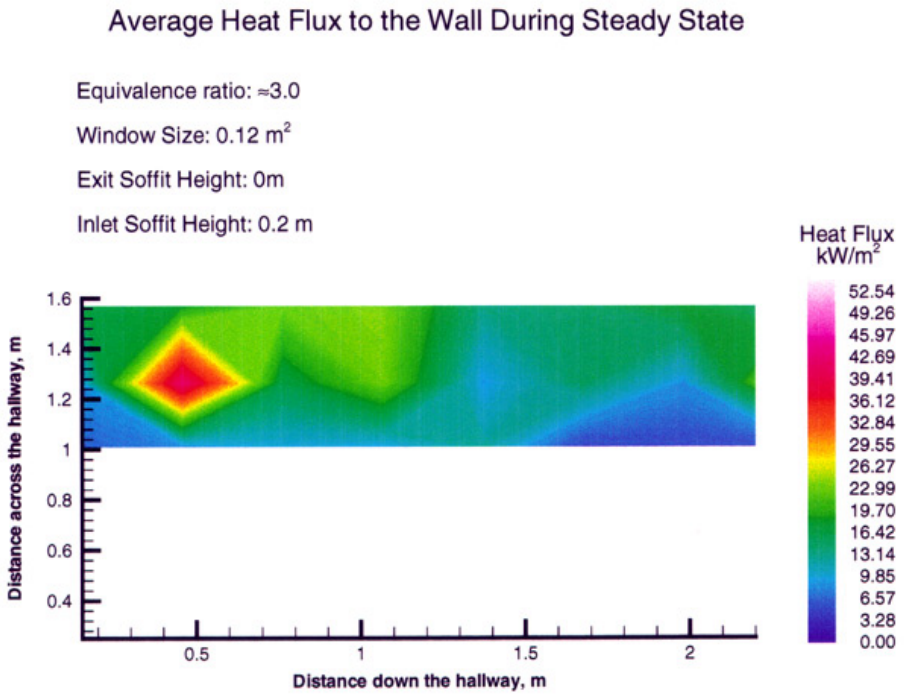

Figure 5.8 Average heat flux to the wall, case with no soffit

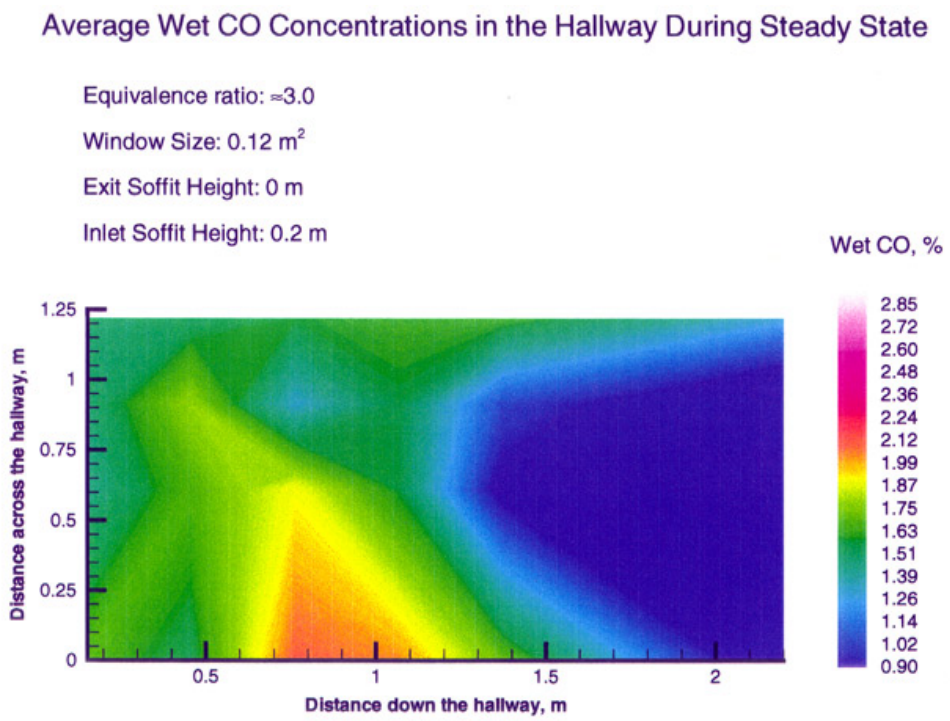

Figure 5.9 Average wet CO mole fractions, case with no soffit

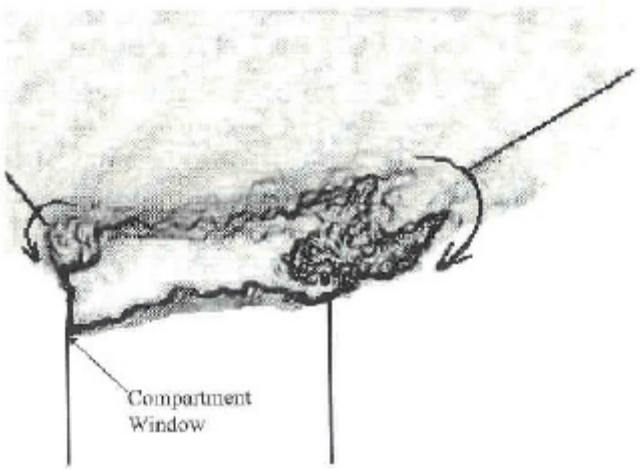

Figure 5.10 Image of external burning in the hallway from viewpoint at hallway end

Case 2: 0.61 m exit soffit case (g=1.4)

The heat flux maps for the ceiling and floor of the hallway and wall opposite the compartment for the second case of a 0.6m exit soffit as shown in Figures 5.11, 5.12, 5.13 respectively. For this case there is burning of the hallway upper-layer gases, but it does not occur throughout the upper-layer of the hallway. The burning was attached to the compartment, extended across the hallway, and 2m down the hall (Lattimer, 1996).

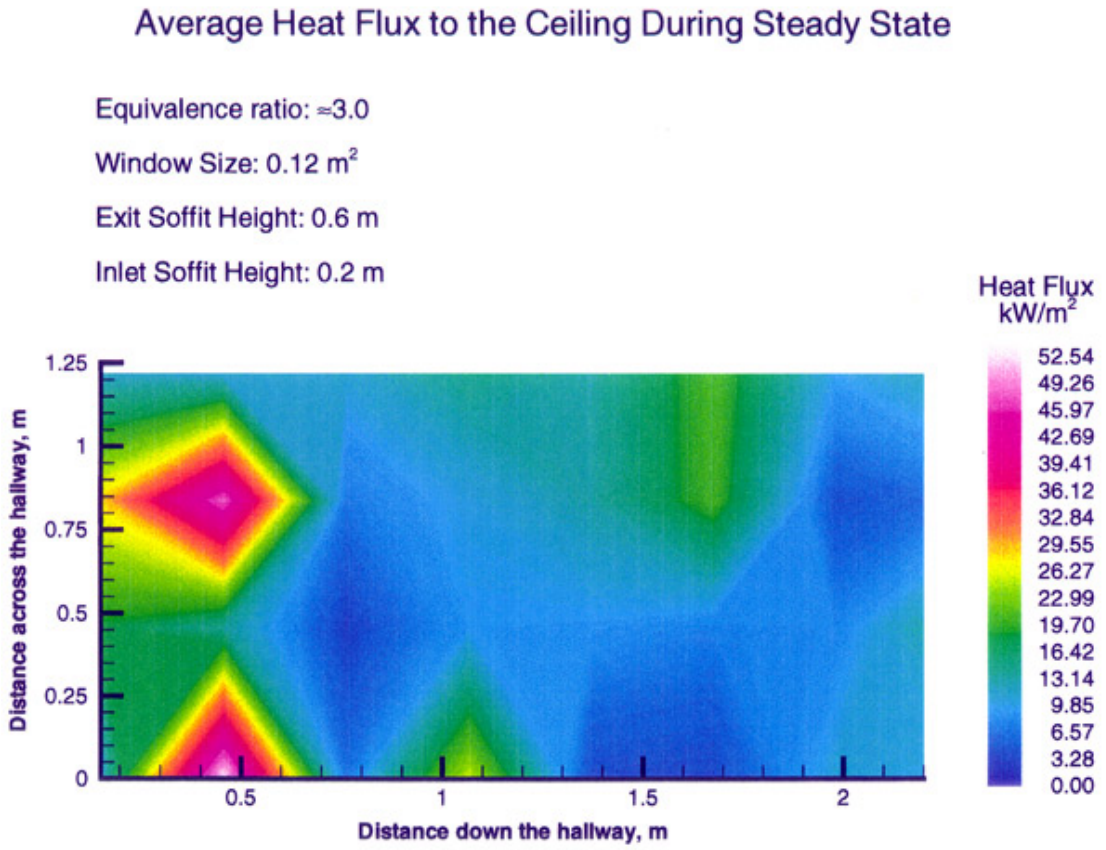

Figure 5.11 Average heat flux to the ceiling, exit soffit height 0.6 m

As can be seen in the ceiling and floor maps, Figures 5.11 and 5.12, the principle areas of heat release are found in the closed end of the hallway and along the wall opposite the compartment. In this experimental setup the bottom of the compartment exit is located within the thick upper-layer of combustion products. This results in the buoyant jet of compartment exhaust gases entraining combustion products in the upper-layer with low

oxygen mole fractions as it enters the hallway. The exhaust jet impinges on the opposite wall and forms a vortex structure, which entrains oxygen into the flow, resulting in oxidation of UHC and some CO, and the heat flux shown along the opposite wall, Figure 5.13. This effect could also be occurring in the closed end of the hallway where the swirling gases entrain oxygen from the lower layer resulting in increased measured heat flux.

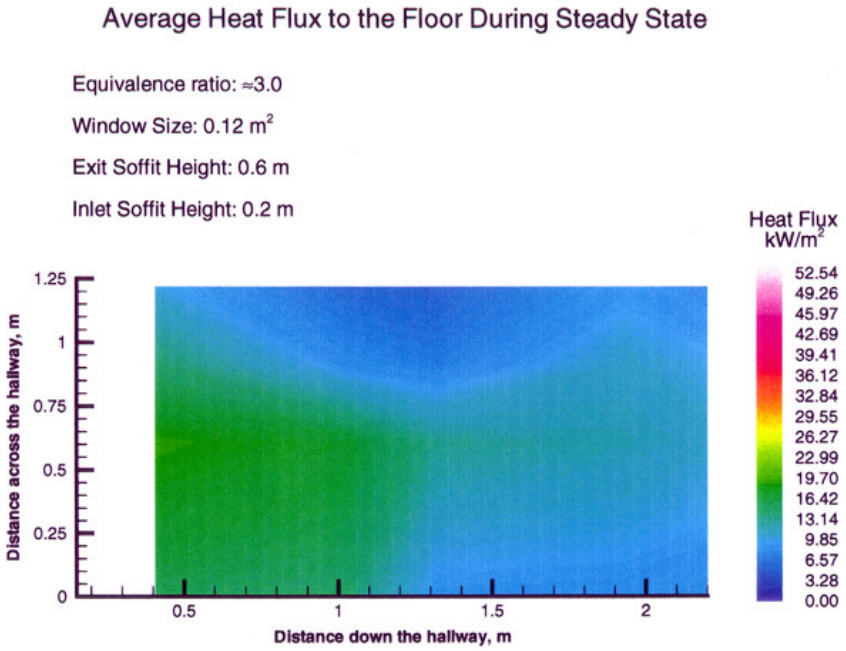

Figure 5.12 Average heat flux to the floor, exit soffit height 0.6 m

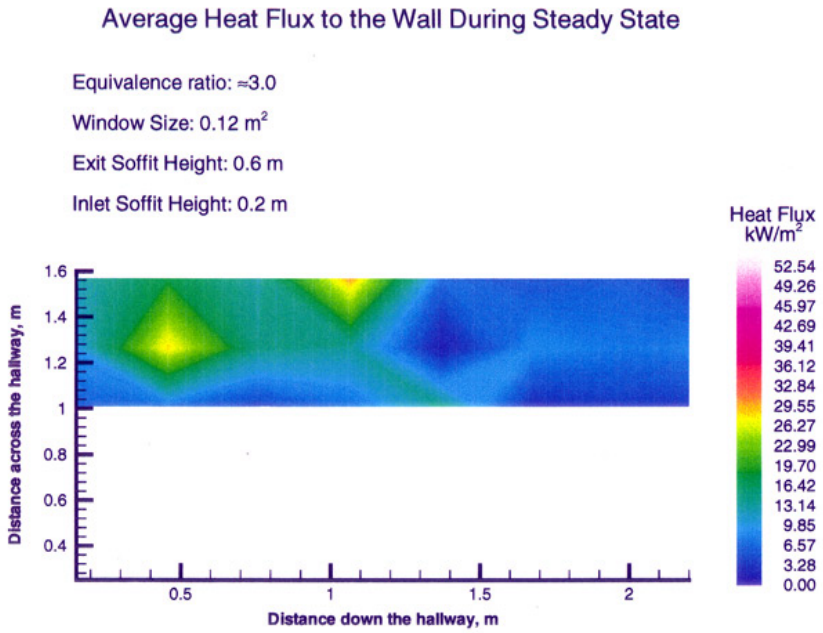

Figure 5.13 Average heat flux to the wall, exit soffit height 0.6 m

When mapping of CO mole fractions for the same conditions in Figure 5.14 are examined (Lattimer et al., 1996a, b), the CO mole fractions are relativity high throughout the entire hallway. Lattimer (1996) explained the external burning in this case primarily reduced the UHC levels, but that CO levels remained relatively unaltered. In this case the measure of high heat flux can again only denote those areas were some burning is occurring, but is not directly related to the levels of CO present or oxidized in the hallway.

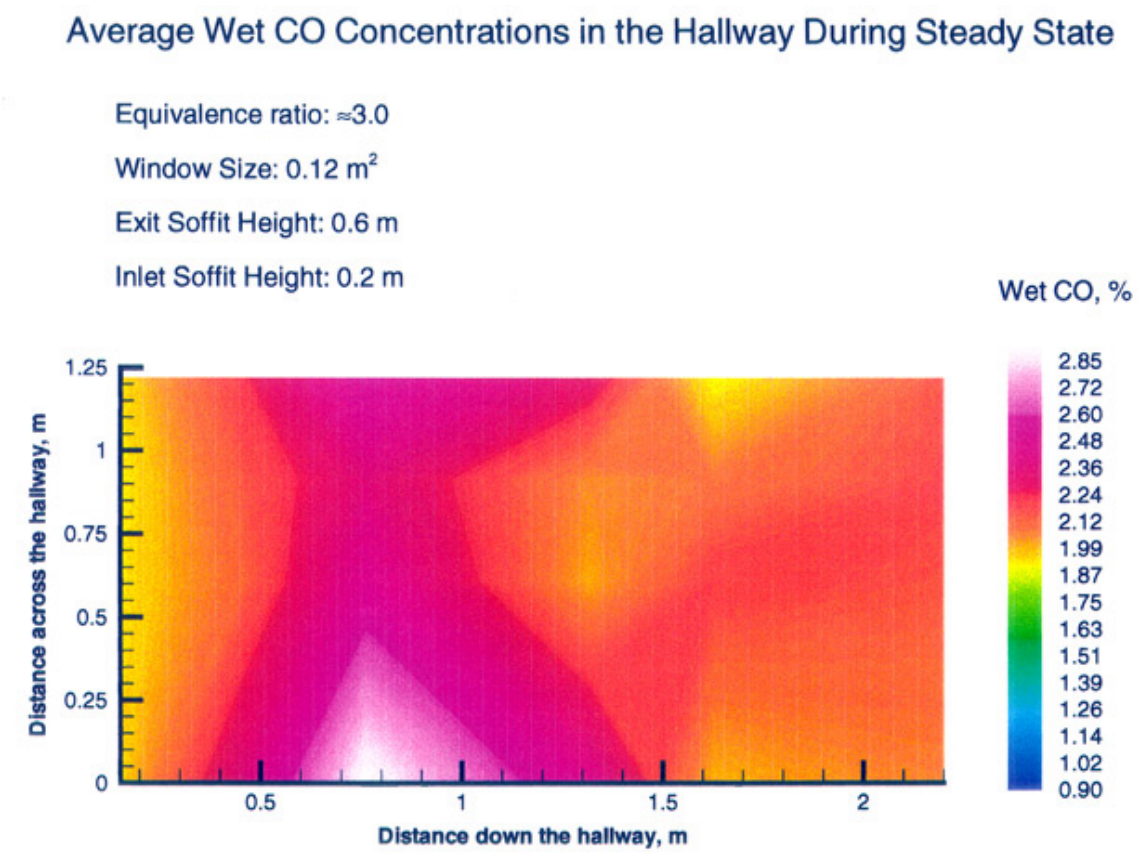

Figure 5.14 Average wet CO mole fractions, exit soffit height 0.6 m

5.5 Discussion

The results for the two cases of γ = 0.45 and 1.4 exhibited a direct relationship between flames in the upper-layer and total heat flux measured. The heat flux measured on the ceiling and sidewall opposite the exhaust vent correlated directly with the combustion intensity. Oxidation was shown by Lattimer et al. (1996a, b) to be strongly dependent on the levels of O_2 entrained into the upper-layer. It can be clearly seen that for the deeper non-dimensional upper-layer depth, reduced oxygen entrainment contributes to less flames in the hallway, and corresponding lower heat flux values. In the thinner upper-layer depth, where plenty of oxygen is available for combustion, high heat flux measurements correspond to the extent of flaming in the hallway.

6 Conclusions and Recommendations

6.1 Summary and Conclusions

Carbon monoxide formation in compartment fires was investigated using a series of n-hexane pool fires in a reduced (½ISO 9705) scale compartment. A series of eight experiments at a global equivalence ratio of 1.28 were performed to determine upper-layer uniformity. Upper-layer sampling at various points throughout the compartment, has shown that the compartment upper-layer is relatively uniform in species mole fractions, yields, and temperature. The small differences reported for species fall within the experimental measurement error and the temperature differences are just outside the experimental error. Additional mapping at various heights within the upper-layer and at a range of equivalence ratios would be required to confirm uniformity of the upper-layer completely. A sampling location, representative of the front upper-layer of the compartment, was used for gas samples in a series of experiments where the equivalence ratio was varied.

Another series of fires, which ranged in global equivalence ratio from 0.5 to 3.1, were performed to look at the variation of species, temperatures, and flows within the compartment. Sampling was only performed in the front upper-layer of the compartment. Trends similar to those reported by previous researchers were found for species mole fraction measurements. Products of incomplete combustion, carbon monoxide and unburned hydrocarbons, started to be formed at global equivalence ratios of 0.6 and rose as the fires became more underventilated at higher equivalence ratios. Oxygen was no longer present in upper-layer samples for equivalence ratios higher than 1.2, while carbon dioxide levels began to level out and drop slightly at those equivalence ratios. Lack of available oxygen in the compartment upper-layer as the fires became underventilated drove species production from products of complete combustion, CO_2 and H_2O toward those products indicated incomplete combustion, CO and UHC. Temperatures in the upper-layer remained consistent across the range of global equivalence ratios at about 1000K, which ensured all oxidation reactions would proceed

as long as oxygen was available in the upper-layer. These temperatures also extended through the entire depth of the compartment upper-layer as reported by compartment thermocouple rakes. All fires were ventilation limited as evidenced by a constant doorway inflow, which approached the calculated theoretical ventilation limit for doorway flows. The calculated doorway neutral plane height showed good agreement with both temperature profiles taken in the doorway and visual observations of the fires. Neutral plane values from previous work also agreed well with the reported values.

Heat flux from combustion products exiting a compartment vent into a hallway was also investigated to compare to previous carbon monoxide mapping the hallway upper-layer. Total heat flux from the gases was measured at thirty two locations on the hallway ceiling, sixteen locations on the wall of the hallway opposite the burning compartment, and twenty one locations on the hallway floor. Carbon monoxide data from two previous hallway mapping studies, a deep and shallow hallway upper-layer, was compared to the heat flux mapping of the same experimental conditions.

The results for the two cases of a deep and shallow hallway upper-layer exhibited a direct relationship between flames in the upper-layer and total heat flux measured. The heat flux measured on the ceiling and sidewall opposite the exhaust vent correlated directly with the combustion intensity. Oxidation was shown by Lattimer et al. (1996a, b) to be strongly dependent on the levels of O_2 entrained into the upper-layer. It can be clearly seen that for the deeper non-dimensional upper-layer depth, reduced oxygen entrainment contributes to less flames in the hallway, and corresponding lower heat flux values. In the thinner upper-layer depth, where plenty of oxygen is available for combustion, high heat flux measurements correspond to the extent of flame spread in the hallway. High heat flux can only denote those areas were flames are present, but is not directly related to the levels of CO present or oxidized in the hallway.

6.2 Recommendations for Future Work – as of December 1998

Future work should include studies that would allow for an increase in the available steady state time of the fires to collect more consistent data. Use of a gaseous fuel, such as used in the work of Bryner, et al. would allow for a better controlled and a longer steady state period. Special attention should also be paid to the horizontal and vertical differences in the doorway measurements. A complete species mapping of the gases exiting the compartment doorway would allow for more precise measurements of species production versus the single point measurements taken in the study.

A detailed study comparing the compartment scaling with the ISO 9705 compartment should be performed. Also this study should examine scaling up results from reduced scale compartments to different geometric configurations. This would allow a determination of where the scaling laws used are valid. The first step before experimentation should be a thorough literature search to examine other scaling work and data available for comparison.

Future studies should also address the effect of varied door widths on species mole fraction production. These studies might address the differences seen in Bryner et al. (1994) compared to other compartment data.

Another phase of work should include a scaled hallway attached to the scaled compartment to measure species movement within a realistic building design. In general the hallway should be half size. Exact scaling should follow the similarity of:

Residence Time – flow rates and upper-layer structure

Thermal Environment – heat transfer

Hallway Ventilation Pattern – flow rates

Both the width and height of the hallway should be variable, enabling different modes of evolution of the fire plume exiting the compartment. The height of the inlet soffit strongly affects the entrainment of hallway fluid into the fire products jet, since the vertical jet entrains much more ambient air than a ceiling jet. The width of the hallway is

important to the fire products evolution especially in the side-on configuration, determining the distribution of the various products, i.e., along the far wall, center and near wall as shown by Lattimer (1996). Species levels should be evaluated within adjacent hallway. Multiple “target” rooms should be attached to this hallway –connected to the hallway and located downstream of the fire source to allow for quantification of species movement in a realistic building environment.

7 References

Babrauskas, V. 1982, "Will The Second Item Ignite?," *Fire Safety Journal*, **4**, pp.281-292

Beyler, C.L., 1983, "Development and Burning of a Layer of Products of Incomplete Combustion Generated by a buoyant Diffusion Flame," Ph.D. Thesis, Harvard University.

Beyler, C.L., 1986, "Major Species Production by Solid Fuels in a Two Layer Compartment Fire Environment," *First International Symposium on Fire Safety Science*, p. 431.

Blevins, L.G., 1999, "Behavior of Bare and Aspirated Thermocouples in Compartment Fires", Proceedings of the 33rd National Heat Transfer Conference, Albuquerque, New Mexico, August 15-17, 1999.

Bryner, N., Johnsson, E.L., Pitts, W.M., 1994, "Carbon Monoxide Production in Compartment Fires – Reduced-Scale Enclosure Test Facility," NISTIR 5568.

Chow, W.K., Ng, Y.S., 1994-95, "Experimental Studies of Compartment Fire," *Journal of Applied Fire Science*, Vol. 4(1), pp.17-30.

Comitis, S.C., Glasser, D., Young, B.D., 1996, "An Experimental and Modeling Study of Fires in Ventilated Ducts. Part II: PMMA and Stratification", *Combustion and Flame*, v. 104.

Cooper, L.Y., 1982a, "Heat Transfer From a Buoyant Plume to an Unconfined Ceiling", *ASME Journal of Heat Transfer*, Vol. 104.

Cooper, L.Y., Harkleroad, M., Quintiere, J., and Rinkinen, W., 1982b, "An Experimental Study of Upper Hot Layer Stratification in Full-Scale Fire Scenarios", *ASME Journal Of Heat Transfer*, Vol. 104

Cooper, L.Y., 1987, "Thermal Response of Unconfined Ceilings Along Growing Fires and the Importance of Convective Heat Transfer", *ASME Journal of Heat Transfer, Vol. 109*

Cooper, L.Y., 1989, "Heat Transfer in Compartment Fires Near Regions of Ceiling-Jet Impingement on a Wall", *ASME Journal of Heat Transfer*, Vol. 111

Dembsey, N.A., Pagni, P.J., Williamson, R.B., 1995, "Compartment Fire Near-field Entrainment Measurements", *Fire Safety Journal*, **24**, pp. 383-419.

Drysdale, D., An Introduction to Fire Dynamics, 2nd Edition, John Wiley & Sons, New York, 1998

Ewens, D.S., "The Transport and Remote Oxidation of Compartment Fire Exhaust Gases", Master of Science Thesis, Department of Mechanical Engineering, Virginia Polytechnic Institute and State University, 1994.

Gill, W., Blackwell, B.F., Neff, J.J., 1983, "Experimental Measurement of Heat Flux to Large and Small Calorimeters in an Engulfing Pool Fire", *Fire Dynamics and Heat Transfer*, Vol. 25.

Gottuk, D.T., Roby, R.J., Peatross, M.J., Beyler, C.L., 1992, "Carbon Monoxide Production in Compartment Fires", *Journal of Fire Protection Engineering*, pp 133-150.

Hall, J.R. and Harwood, B., 1995, "Smoke or Burns – Which is Deadlier?," *NFPA Journal*, January/February, pp.38-43.

Hinkley, P.L., Wraight, H.G.H. and Theobald, C.R., 1968, "The Contribution of Flames Under Ceilings to Fire Spread in Compartments. Part 1. Incombustible Ceilings", *Fire Research Note 712.*

Hinkley, P.L., Wraight, H.G.H. and Theobald, C.R., 1984, "The Contribution of Flames Under Ceilings to Fire Spread in Compartments", *Fire Safety Journal*, Vol. 7.

International Organization for Standardization, 1993, "ISO 9705: 1993 (E)", prepared by Technical Committee ISO/TC 92, *Fire tests on building materials, components, and structures*, Subcommittee SC1, *Reaction to fire*.

Janssens, M., Hao C. Tran, 1992, "Data Reduction of Room Tests for Zone Model Validation," *Journal of Fire Sciences*, **10**, 528-555.

Kuhn, R.L., Potts, W.J., Waterman, T.E., 1978, "A Study of the Inhalation Toxicity of Smoke Produced Upon Pyrolysis and Combustion of Polyethylene Foams. Part II. Full Scale Studies," *Journal of Combustion Toxicology*, Vol. 5, p.434-464.

Lattimer, B.Y., 1996, "The Transport of High Concentrations of Carbon Monoxide to Locations Remote from the Burning Compartment", Dissertation for PhD in Mechanical Engineering, Virginia Polytechnic Institute and State University.

Lattimer, B.Y., Personal Communication, June 1998.

Lattimer, B.Y., Vandsburger, U. and Roby, R.J., 1996a "The Transport of Carbon Monoxide from a Burning Compartment Located on the Side of a Hallway", 26th International Symposium on Combustion, Napoli, Italy, July - August 1996

Lattimer, B.Y., Vandsburger, U. and Roby, R. J., 1996b "The Transport of High Concentrations of Carbon Monoxide to Locations Remote from the Burning Compartment", NIST/BFRL, Annual Report, Grant No. 60NANB4D1651.

Lattimer, B.Y., Vandsburger, U. and Roby, R.J., 1997, "The Transport of High Concentrations of Carbon Monoxide to Locations Remote from the Burning Compartment," NIST-GCR-97-713.

Morehart, J.H., Zukoski, E.E., Kubota, T., 1990, "Species Produced in Fires Burning in Two Layered and Homogeneous Vitiated Environments," National Institute of Standards and Technology, Center for Fire Research, Report NBS-GCR-90-585.
Morikawa, T., Yanai, E., Nishina, T., "Evolution of Toxic Gases from Experimental Fires in an Existing Building," pp.443-453.

Nakaya, I., T. Tanaka, M. Yoshida, and Steckler K., 1986, "Doorway Flow Induced by a Propane Fire," *Fire Safety Journal*, **10**, 185-195.

Nelson, H.E., 1988, "Engineering Analysis of Fire Development in the Hospice of Southern Michigan," *Fire Safety Science Proceedings from the Second International Symposium*, pp.927-938

Nelson, H.E., and Tu, K.M., 1991, "Engineering analysis of Fire Development in the Hillhaven Nursing Home Fire, October 5, 1989," NISTIR 4664, 51 p.

Peacock, R.D., Reneke, P.A., Bukowski, R.W., Babrauskas, V., 1999, "Defining flashover for fire hazard calculations," *Fire Safety Journal*, **32**, pp.331-345.

Pitts, W.M., Braun, E., Peacock, R.D., Mitler, H.E., Johnsson, E.L., Reneke, P.A., Blevins, L.G., "Temperature Uncertainties for Bare-bead and Aspirated Thermocouple Measurements in Fire Environments", 14th Meeting of the United States/Japan Conference on Development of Natural Resources, Japan, May 1998.

Thomas, P.H., Simms, D.L., Wraight, H., 1965, "Fire Spread in Wooden Cribs. Part 2: Heat Transfer Experiments in Still Air", *Fire Research Note 799*.

Toner, S.J., Zukoski, E.E., and Kubota, T., 1987, “Entrainment, Chemistry and Structure of Fire Plumes,” National Institute of Standards and Technology, Center for Fire Research, Report NBS-GCR-87-528.

Vandsburger, U., 2001, “Evolution of Compartment Exhaust Gases Providing Evaluation Criteria and Design Tools,” Final Report, NIST BFRL Contract #60NAND7D0066, p. 8.

Westbrook, C.K. and Dryer, F.L., 1984, “Chemical Kinetic Modeling of Hydrocarbon Combustion”, *Progress in Energy and Combustion Science*, **10**, pp.1-57.

Zukoski, E.E., Kubota, T., Lim, C., 1985, “Experimental Study of Environment and Heat Transfer in a Room Fire. Mixing in Doorway Flows and Entrainment in Fire Plumes,” NBS Report, CGR-85-493.

Zukoski, E.E., Morehart, J.H., Kubota, T., and Toner, S.J., 1991, *Combustion and Flame*, **83**, pp. 324-332.

Appendix A – FORTRAN data reduction code

```
c  THIS PROGRAM DETERMINES THE MASS FLOW RATES IN AND OUT
c  OF A ROOM OR HALLWAY USING A TEMPERATURE PROFILE(S).  THE
c  PROGRAM DETERMINES THE NEUTRAL PLANE, WHICH IS THEN USED TO
c  DETERMINE THE MASS FLOW RATES.
      DOUBLE PRECISION T(100),Z(100),ZD(100),TD(100)
      DOUBLE PRECISION MASS(5000),DMDT(5000)
      DOUBLE PRECISION TAMB,PAMB,HO,WO,RHOAMB,MRES,CD,GRAV
      DOUBLE PRECISION XHALL1,XHALL2,XERROR,RTSEC,HN,MEXIT,MENT
      DOUBLE PRECISION X,Y,ZNLIM
      DOUBLE PRECISION WR,LR,HR,FR,RHONEW,TIME,TIMOLD
      DOUBLE PRECISION FAST,PHI,MFUEL,RATES
      INTEGER I,TEST,NUMTC,NUMTCD,II,JJ,KK,ISTEP
      EXTERNAL FDEN

      COMMON/CONDITIONS/TAMB,PAMB,HO,WO,MFUEL,RHOAMB,CD,GRAV
      COMMON/COND2/DMDT,NUMTC,NUMTCD,ISTEP
      COMMON/TEMPS/T,Z,TD,ZD
      COMMON/XY/X,Y
      COMMON/PLANE/ZNLIM

      OPEN(1,FILE='INFO.DAT')
      OPEN(2,FILE='CTEMP.DAT')
      OPEN(3,FILE='FUEL.DAT')
      OPEN(4,FILE='RESULT.OUT')
      OPEN(5,FILE='CHECK.OUT')
c Stecklers number of TC's is 19 and 16
      NUMTC = 8
      NUMTCD = 8

C*****************************************************************
C     NOTE: TC's SHOULD BE IN FILE STARTING WITH TC CLOSEST TO THE
```

```
C          CEILING AND ENDING WITH THE TC CLOSEST TO THE FLOOR,

C          THE LIST OF LOCATIONS, Z AND ZD, SHOULD START AT THE CEILING

C          (OR THE TOP OF THE DOOR FOR ZD) AND GO TO "0"

C          (FOR THE TEMPERATURE AT THE FLOOR)
C*****************************************************************


      READ(1,*) TEST,TAMB,PAMB,HO,WO,HR,WR,LR,CD

     +,(Z(I), I=1,NUMTC+2),(ZD(I),I=1,NUMTCD+2)


c     print *,ZD(NUMTCD),ZD(NUMTCD+1),ZD(NUMTCD+2)
c     pause


      PAMB=PAMB*101.325D0/760.D0

c    This was the originial line written by Brian to calculate the
ambient density
c      RHOAMB=PAMB/TAMB/0.286D0
c    This is the line that CJW inserted instead of original line above
based on pressure

      RHOAMB = 352.8/TAMB

      GRAV=9.81D0
c     Methane
c     FAST = 0.0583
c     Hexane
      FAST = 0.0658
c     FAST = 0.0641

      FR=0

      RHOOLD=RHOAMB

      TIMOLD=0.0D0

      DELTAT=1.0D0

      II=0

      ISTEP = 0



***CALCULATE MASS ACCUMULATED IN COMPARTMENT

 30   READ(2,*,END=31) TIME, (T(I),I=2,NUMTC+1)

     +,(TD(I),I=2,NUMTCD+1)
```

```
      T(1)=T(2)
      TD(1)=TD(2)
      T(NUMTC+2)=T(NUMTC+1)
      TD(NUMTCD+2)=TD(NUMTCD+1)
      II=II+1

C**Calculate mass accumulated in compartment
      CALL QGAUSX(FDEN,FR,HR,RHONEW)
      MASS(II) = RHOAMB*TAMB*WR*LR*RHONEW
      GOTO 30
 31   CLOSE (2)
      OPEN(2,FILE='CTEMP.DAT')
      DO 37 JJ=1,II
       IF (JJ.EQ.1) THEN
         DMDT(JJ) = -(25.D0*MASS(JJ)-48.D0*MASS(JJ+1)+36.D0*MASS(JJ+2)
     +     -16.D0*MASS(JJ+3)+3.D0*MASS(JJ+4))/(12.D0*DELTAT)
       ELSE IF (JJ.EQ.2) THEN
         DMDT(JJ) = -(3.D0*MASS(JJ-1)+10.D0*MASS(JJ)-18.D0*MASS(JJ+1)
     +     +6.D0*MASS(JJ+2)-MASS(JJ+3))/(12.D0*DELTAT)
       ELSE IF (JJ.EQ.(II-1)) THEN
         DMDT(JJ) = -(-3.D0*MASS(JJ+1)-10.D0*MASS(JJ)+18.D0*MASS(JJ-1)
     +     -6.D0*MASS(JJ-2)+MASS(JJ-3))/(12.D0*DELTAT)
       ELSE IF (JJ.EQ.II) THEN
         DMDT(JJ) = -(-25.D0*MASS(JJ)+48.D0*MASS(JJ-1)-36.D0*MASS(JJ-2)
     +     +16.D0*MASS(JJ-3)-3.D0*MASS(JJ-4))/(12.D0*DELTAT)
       ELSE
         DMDT(JJ) = -(-MASS(JJ-2)+8.D0*MASS(JJ-1)-8.D0*MASS(JJ+1)
     +     +MASS(JJ+2))/(12.D0*DELTAT)
       END IF
```

```
 37   CONTINUE


      ISM=10
      NSUM=ISM*2
      DO 38 JJ=1,II
      SUM = 0.0D0
       IF (JJ.LT.JJ+ISM) THEN
         DO 41 KK=JJ,NSUM+JJ
           SUM = SUM+DMDT(KK)
 41      CONTINUE
         GOTO 46
       ELSE IF (JJ.GT.II-ISM) THEN
         DO 42 KK = JJ-NSUM,JJ
           SUM = SUM+DMDT(KK)
 42      CONTINUE
         GOTO 46
       ELSE
         DO 43 KK=JJ-ISM,JJ+ISM
           SUM = SUM+DMDT(KK)
 43      CONTINUE
       END IF
 46    DMDT(JJ) = SUM/DBLE(FLOAT(NSUM+1))
 38    CONTINUE


C***READING IN TEMPERATURES FOR MASS FLOW RATE CALCULATIONS
 50   READ(2,*,END=60) TIME, (T(I),I=2,NUMTC+1)
     +,(TD(I),I=2,NUMTCD+1)

      READ(3,*) MFUEL
```

```
C***TEMPERATURE VALUES AT CEILING OR TOP OF DOOR
      T(1)=T(2)
      TD(1)=TD(2)
C***TEMPERATURE VALUES AT FLOOR
      T(NUMTC+2)=T(NUMTC+1)
      TD(NUMTCD+2)=TD(NUMTCD+1)

      DO 10 I=1,NUMTC+2
        WRITE(5,*) Z(I),T(I)
 10   CONTINUE

      DO 20 I=1,NUMTC+2
        WRITE(5,*) ZD(I),TD(I)
 20   CONTINUE

      ISTEP = ISTEP+1
c**initial guess for neutral plane height
      XHALL1=0.95D0*HO
      XHALL2=0.2D0*HO
      XERROR = 1.D-4

C**Determine nuetral plane by conservation of mass
      HN=RTSEC(XHALL1,XHALL2,XERROR)
      IF ((HN.GT.HO).OR.(HN.LT.0.0D0)) THEN
        HN=HO
      END IF

C**Determine the mass flows in and out of compartment and
C**Calculate compartment equivalence ratio
```

```
      RATES = MRES(HN,MEXIT,MENT)

      IF (HN.EQ.HO) THEN

c        MEXIT=MENT-DMDT(ISTEP)

c***Originial line in code, taken out by CJW and replaced by one not
using DMDT
c         MEXIT=MENT+MFUEL-DMDT(ISTEP)
          MEXIT=MENT+MFUEL

      ENDIF


      if (MENT.EQ.0) then

      PHI=0

      else

      PHI=(MFUEL/MENT)/FAST

      endif

C**Print results to output file

      WRITE(4,24) TIME,DMDT(ISTEP),HN,MEXIT,MENT,MFUEL,PHI

C      WRITE(4,25) TIME,DMDT(ISTEP),HN,MEXIT,MENT

 24   FORMAT(F5.1,2X,6(E10.4,1X))


 25   FORMAT(F5.1,2X,E10.4,2X,E10.4,2X,F10.4,2X,F10.4)

      RHOOLD=RHONEW

      TIMOLD=TIME

      GOTO 50


60    CLOSE(1)

      CLOSE(2)

      CLOSE(3)

      CLOSE(4)

      CLOSE(5)
```

```
      STOP
      END

C*************************************************************
C  FUNCTION USES LINEAR INTERPOLATION TO DETERMINE COMPARTMENT
C  TEMPERATURES BETWEEN TWO DATA POINTS
C*************************************************************
      FUNCTION TMP(XL1)

      DOUBLE PRECISION T(100),Z(100),ZD(100),TD(100)
      DOUBLE PRECISION DMDT(5000)
      DOUBLE PRECISION TAMB,PAMB,HO,WO,MFUEL,RHOAMB,CD,GRAV
      INTEGER J1,DUMI,NUMTC,NUMTCD,ISTEP
      DOUBLE PRECISION TMP,XL1

      COMMON/CONDITIONS/TAMB,PAMB,HO,WO,MFUEL,RHOAMB,CD,GRAV
      COMMON/COND2/DMDT,NUMTC,NUMTCD,ISTEP
      COMMON/TEMPS/T,Z,TD,ZD

      DUMI=0

      DO 80 J1=1,NUMTC+2
        IF ((Z(J1).LE.XL1).AND.(DUMI.EQ.0)) THEN
          IF (J1.EQ.1) THEN
           TMP=T(J1)
           DUMI=1
          ELSE
           TMP=T(J1)+(T(J1-1)-T(J1))*(XL1-Z(J1))/(Z(J1-1)-Z(J1))
           DUMI=1
```

```
          END IF
        END IF
 80   CONTINUE
      RETURN
      END

C*************************************************************
C  FUNCTION USES LINEAR INTERPOLATION TO DETERMINE DOOR TEMPERATURES
C  BETWEEN TWO DATA POINTS
C*************************************************************
      FUNCTION TMPD(XL2)

      DOUBLE PRECISION T(100),Z(100),ZD(100),TD(100)
      DOUBLE PRECISION DMDT(5000)
      DOUBLE PRECISION TAMB,PAMB,HO,WO,MFUEL,RHOAMB,CD,GRAV
      INTEGER J1,DUMI,NUMTC,NUMTCD,ISTEP
      DOUBLE PRECISION TMPD,XL2

      COMMON/CONDITIONS/TAMB,PAMB,HO,WO,MFUEL,RHOAMB,CD,GRAV
      COMMON/COND2/DMDT,NUMTC,NUMTCD,ISTEP
      COMMON/TEMPS/T,Z,TD,ZD

      DUMI=0

      DO 90 J1=1,NUMTCD+2
        IF ((ZD(J1).LE.XL2).AND.(DUMI.EQ.0)) THEN
           IF (J1.EQ.1) THEN
            TMPD=TD(J1)
            DUMI=1
           ELSE
            TMPD=TD(J1)+(TD(J1-1)-TD(J1))*(XL2-ZD(J1))/
```

```
     +      (ZD(J1-1)-ZD(J1))
            DUMI=1
           END IF
         END IF
 90   CONTINUE
      RETURN
      END

C*************************************************************
C  Y1(X) BOUNDARY DETERMINATION, LOWER LIMIT OF INTEGRATION
C*************************************************************
      FUNCTION Y1(X6)

      DOUBLE PRECISION X,Y,Y1,X6,ZNLIM
      DOUBLE PRECISION TAMB,PAMB,HO,WO,MFUEL,RHOAMB,CD,GRAV

      COMMON/CONDITIONS/TAMB,PAMB,HO,WO,MFUEL,RHOAMB,CD,GRAV
      COMMON/XY/X,Y
      COMMON/PLANE/ZNLIM

       Y1=ZNLIM

      RETURN
      END
C*************************************************************
C  Y2(X) BOUNDARY DETERMINATION, UPPER LIMIT OF INTEGRATION
C*************************************************************
      FUNCTION Y2(X5)
      DOUBLE PRECISION X,Y,Y2,X5
      DOUBLE PRECISION TAMB,PAMB,HO,WO,MFUEL,RHOAMB,CD,GRAV
```

```
      COMMON/CONDITIONS/TAMB,PAMB,HO,WO,MFUEL,RHOAMB,CD,GRAV
      COMMON/XY/X,Y
      Y2=X5
      RETURN
      END
C*************************************************************
C  FUNC(X,Y) DETERMINATION
C*************************************************************
      FUNCTION FUNC(X4,Y4)
      DOUBLE PRECISION X,Y,FUNC,X4,Y4,TMP,TMPD
      DOUBLE PRECISION TAMB,PAMB,HO,WO,MFUEL,RHOAMB,CD,GRAV

      COMMON/CONDITIONS/TAMB,PAMB,HO,WO,MFUEL,RHOAMB,CD,GRAV
      COMMON/XY/X,Y
      FUNC=1.D0/TMPD(X4)*(1.D0/TAMB-1.D0/TMP(Y4))
      RETURN
      END

C*************************************************************
C  FDEN(X,Y) DETERMINATION
C*************************************************************
      FUNCTION FDEN(X5)
      DOUBLE PRECISION X,Y,FDEN,X5,TMP
      DOUBLE PRECISION TAMB,PAMB,HO,WO,MFUEL,RHOAMB,CD,GRAV

      COMMON/CONDITIONS/TAMB,PAMB,HO,WO,MFUEL,RHOAMB,CD,GRAV
      COMMON/XY/X,Y

      FDEN=1.D0/TMP(X5)
```

```
      RETURN
      END
C*************************************************************
C  SUBROUTINE FOR INTEGRATION OF OUTER INTEGRAL
C  SUBROUTINE USES GUASSIAN QUADRATURE FORMULAS TO INTEGRATE
C  TEMPERATURE PROFILES FOR DETERMINATION OF MASS FLOW RATES
C*************************************************************
      SUBROUTINE QGAUSX (FUNCX,AX,BX,SX)
      DOUBLE PRECISION AX,BX,SX,FUNCX
      EXTERNAL FUNCX
      INTEGER J
      DOUBLE PRECISION DXX,XMX,XRX,WX(5),XG(5)
      SAVE WX,XG
      DATA WX/0.2955242247D0,0.2692667193D0,0.2190863625D0,
     +0.1494513491D0,0.0666713443D0/
      DATA XG/0.1488743389D0,0.4333953941D0,0.6794095682D0,
     +0.8650633666D0,0.9739065285D0/
      XMX=0.5D0*(BX+AX)
      XRX=0.5D0*(BX-AX)
      SX=0.0D0
      DO 515 J=1,5
        DXX=XRX*XG(J)
        SX=SX+WX(J)*(FUNCX(XMX+DXX)+FUNCX(XMX-DXX))
 515  CONTINUE
      SX=XRX*SX
      RETURN
      END
```

```
C************************************************************
C  SUBROUTINE FOR INTEGRATION OF INNER INTEGRAL
C  SUBROUTINE USES GUASSIAN QUADRATURE FORMALAS TO INTEGRATE
C  TEMPERATURE PROFILES FOR DETERMINATION OF MASS FLOW RATES
C************************************************************
      SUBROUTINE QGAUSY (FUNCY,AY,BY,SY)
      DOUBLE PRECISION AY,BY,SY,FUNCY
      EXTERNAL FUNCY
      INTEGER J
      DOUBLE PRECISION DXY,XMY,XRY,WY(5),YG(5)
      SAVE WY,YG
      DATA WY/0.2955242247D0,0.2692667193D0,0.2190863625D0,
     +0.1494513491D0,0.0666713443D0/
      DATA YG/0.1488743389D0,0.4333953941D0,0.6794095682D0,
     +0.8650633666D0,0.9739065285D0/
      XMY=0.5D0*(BY+AY)
      XRY=0.5D0*(BY-AY)
      SY=0.0D0
      DO 515 J=1,5
        DXY=XRY*YG(J)
        SY=SY+WY(J)*(FUNCY(XMY+DXY)+FUNCY(XMY-DXY))
 515  CONTINUE
      SY=XRY*SY
      RETURN
      END
C************************************************************
C  USED TO PERFORM DOUBLE INTEGRATION OF FUNCTION
C************************************************************
```

```
      SUBROUTINE QUAD2D(X1,X2,SS)
      DOUBLE PRECISION SS,X1,X2,H
      EXTERNAL H
        CALL QGAUSX(H,X1,X2,SS)
C        WRITE(*,*) SS
      RETURN
      END



      FUNCTION G(YY)
      DOUBLE PRECISION G,YY,FUNC,X,Y
      COMMON/XY/X,Y
        Y=YY
        G=FUNC(X,Y)
      RETURN
      END



      FUNCTION H(XX)
      DOUBLE PRECISION H,XX,G,Y1,Y2,X,Y
      EXTERNAL G,Y1,Y2
      COMMON/XY/X,Y
      DOUBLE PRECISION SS,XH1,XH2
        X=XX
        XH1=Y1(X)
        XH2=Y2(X)
        IF (XH1.EQ.XH2) THEN
         SS=0.D0
         GOTO 450
```

```
        END IF

        CALL QGAUSY(G,Y1(X),Y2(X),SS)
        IF (SS.LT.0.0D0) THEN
         SS = 0.0D0
        ELSE
         SS=DSQRT(SS)
        END IF
450     H=SS
      RETURN
      END


C*************************************************************
C  FUNCTION "MRES" USES TEMPERATURE DATA TO DETERMINE INFLOW AND
C  OUTFLOW BASED ON A GIVEN NEUTRAL PLANE (ZN) VALUE.  THE VALUE
C  MRES IS DETERMINED FROM CONSERVATION OF MASS
C*************************************************************
      FUNCTION MRES(ZN,ME,MI)

      DOUBLE PRECISION T(100),Z(100),ZD(100),TD(100)
      DOUBLE PRECISION DMDT(5000)
      DOUBLE PRECISION TAMB,PAMB,HO,WO,MFUEL,RHOAMB,CD,GRAV
      DOUBLE PRECISION ME,MI,ZN,COEFF,MRES,B1,B2,B3,ZNLIM
      INTEGER NUMTC,NUMTCD,ISTEP

      COMMON/CONDITIONS/TAMB,PAMB,HO,WO,MFUEL,RHOAMB,CD,GRAV
      COMMON/COND2/DMDT,NUMTC,NUMTCD,ISTEP
      COMMON/TEMPS/T,Z,TD,ZD
```

```
      COMMON/PLANE/ZNLIM

      B1=0.

      B2=ZN

      B3=HO

      ZNLIM=0.0D0

      CALL QUAD2D(B1,B2,MI)

      ZNLIM=ZN

      CALL QUAD2D(B2,B3,ME)

c original line with fixed CD

C      COEFF=CD*WO*RHOAMB*TAMB*DSQRT(2.D0*GRAV)

      COEFF=WO*RHOAMB*TAMB*DSQRT(2.D0*GRAV)

      ME=0.73D0*COEFF*ME

      MI=0.68D0*COEFF*MI

C  CONSERVATION OF MASS

C      original line commented out by Brian and Chris on January 24
C      MRES=MI+MFUEL-ME-DMDT(ISTEP)

C       MRES=MI-ME-DMDT(ISTEP)
C       MRES=MI-ME

      MRES = MI-ME+MFUEL

C      WRITE(3,*) ZN,MRES,ME,MI

      RETURN
      END


C*************************************************************

C  FUNCTION "RTSEC" USES SECANT METHOD TO DETERMINE THE NEUTRAL

C  PLANE BY DETERMINING WHEN MRES=0 (CONSERVATION OF MASS)

C*************************************************************

      FUNCTION RTSEC(X1,X2,XACC)

       INTEGER MAXIT
```

```
      DOUBLE PRECISION RTSEC,X1,X2,XACC
      EXTERNAL MRES
      PARAMETER (MAXIT=30)
      INTEGER J
      DOUBLE PRECISION DX,F,FL,SWAP,XL,MEX,MAIR
      DOUBLE PRECISION TAMB,PAMB,HO,WO,MFUEL,RHOAMB,MRES,CD,GRAV

      COMMON/CONDITIONS/TAMB,PAMB,HO,WO,MFUEL,RHOAMB,CD,GRAV

      MEX=0.D0
      MAIR=0.D0

      FL = MRES(X1,MEX,MAIR)
      F = MRES(X2,MEX,MAIR)

      IF (ABS(FL).LT.ABS(F)) THEN
        RTSEC = X1
        XL = X2
        SWAP = FL
        FL = F
        F = SWAP
      ELSE
        XL = X1
        RTSEC = X2
      ENDIF
C      WRITE (*,*) F,FL
C      STOP

      DO 200 J=1,MAXIT
        IF (F.EQ.0.0D0.OR.F.EQ.FL) THEN
         DX = 0.0D0
```

```
          ELSE
           DX=(XL-RTSEC)*F/(F-FL)
          END IF
          XL=RTSEC
          FL=F
          RTSEC=RTSEC+DX
          F=MRES(RTSEC,MEX,MAIR)
          IF (DABS(DX).LT.XACC.OR.F.EQ.0.D0) THEN
            FOLD = F
            RETURN
          ENDIF
 200   CONTINUE

      WRITE(*,*) 'RTSEC EXCEED MAXIMUM ITERATIONS'
      F=FOLD
      RETURN
c      STOP
      END
```

Appendix B – Summary of flow estimation routine

Janssens, et al., 1992

The methods documented by Janssens et al. (1992) were reported as a way to examine full-scale fire data in a format compatible with the output of a two layer room fire zone model. The authors detail a novel technique which uses measured temperature profiles to determine the doorway flows, neutral plane and interface height, and uniform upper and lower layer temperatures from compartment fire studies. These computed quantities are useful to provide validation of fire models. Also, as in the case of the study documented in this paper, these calculations can document fire characteristics in experimental studies.

This technique uses two thermocouple rakes positioned as shown below. One rake is located in the quiescent corner of the compartment, in this case the right front corner, where there is very little flow. The other is located in the doorway of the compartment.

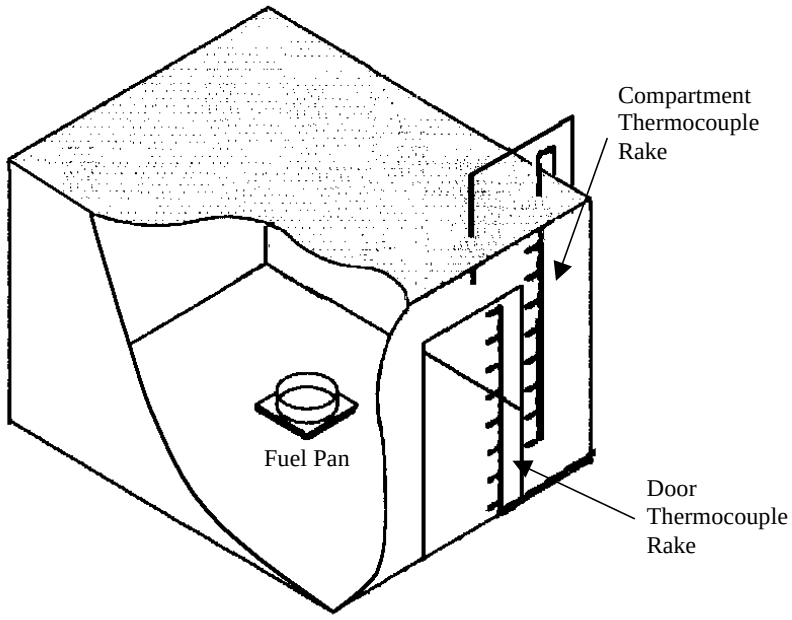

The technique is based on conservation of mass to obtain the neutral plane height. In the case of a compartment fire this is simply:

$$\dot{m}_o = \dot{m}_i + \dot{m}_f$$

where:

$\dot{m}_o$ - mass flow out of doorway

$\dot{m}_i$ - mass flow into doorway

$\dot{m}_f$ - fuel volatilization rate

and:

$$\dot{m}_o = 1563 C_o W_d \int_{z_n}^{z_d} \left[\frac{1}{T_d(z')} \int_{z_n}^{z'} \left(\frac{1}{T_\infty} - \frac{1}{T_i(z'')} \right) dz'' \right]^{1/2} dz'$$

$$\dot{m}_i = 1563 C_i W_d \int_{0}^{z_n} \left[\frac{1}{T_d(z')} \int_{z'}^{z_n} \left(\frac{1}{T_\infty} - \frac{1}{T_i(z'')} \right) dz'' \right]^{1/2} dz'$$

where:

C_o and C_i - orifice coefficients for outflow and inflow

W_d - door width

z_n - neutral plane height

z_d - door height

T_∞ - temperature of ambient air

The temperatures measured on thermocouple rake in the compartment were related to a corresponding velocity profile through Bernouilli's equation, where the temperatures determined a corresponding pressure difference between the compartment and the surroundings. The height at which this velocity is zero is the neutral plane. These temperatures were used in the integration of modified Bernouilli's equations for velocity, which determined the mass flow into and out of the doorway. The equation for inflow was integrated from the floor of the compartment to the neutral plane height and the outflow equation was integrated from the neutral plane height to the top of the door. This required that the neutral plan height be determined iteratively.

The second thermocouple rake in the compartment door was used to determine a temperature profile in the doorway and find an inflection point in that profile. This inflection point was set as the interface height between the upper and lower compartment layers. Also, the interface height was the starting point for an iterative routine that solved the above mass balance equation for the neutral plane height. The neutral plane height was then substituted back into the equations for the mass inflow and outflow in the doorway.

Vita

Christopher A. McKay

Education:

1997 Bachelor of Science in Mechanical Engineering, Virginia Polytechnic Institute and State University, Blacksburg, VA

1992 Culpeper County High School, Culpeper, VA

Professional:

1999 – present Research Scientist, Battelle Memorial Institute, Stafford, VA

1997 Engineering Intern, Rochester Corporation, Culpeper, VA

Publications:

Wieczorek, C.J., Vandsburger, U., McKay, C., Sathyamoorthy, S., Lattimer, B., 1999, "The Applicability of Correlations Between the Species Formation and the Global Equivalence Ratio in a ½Scaled ISO Compartment with Nongaseous Fuel," Proceedings, Sixth (6^{th}) International Symposium, International Association for Fire Safety Science (IAFSS), Poitiers, France.

Wieczorek, C.J., Vandsburger, U., McKay, C., Lattimer, B., 1998, "Species Formation using Liquid n-hexane Fires in a Scaled ISO Compartment," NIST BFRL Annual Conference on Fire Research.